

Anja Irene Langås
Helene Sæle Tveit
Solveig Hegstad Sæternes

Greenhouse Gas Emission and Energy Production from a Ground- Mounted Solar Park

Bachelor's thesis in Engineering, Renewable Energy
Supervisor: Engin Söylemez

May 2023

Anja Irene Langås
Helene Sæle Tveit
Solveig Hegstad Sæternes

Greenhouse Gas Emission and Energy Production from a Ground-Mounted Solar Park

Bachelor's thesis in Engineering, Renewable Energy
Supervisor: Engin Söylemez
May 2023

Norwegian University of Science and Technology
Faculty of Engineering
Department of Energy and Process Engineering





Faculty of Engineering
Department of Energy and
Process Engineering

Bachelor thesis

Project title: Greenhouse Gas Emission and Energy Production from a Ground-Mounted Solar Park	Date received: 21.11.2022
	Submission date: 22.05.2023
	Number of pages / appendix: 103 / 17
Project title (Norwegian): Klimagassutslipp og energiproduksjon fra en bakkemontert solpark	Internal supervisor: Engin Söylemez
Project participants: Anja Irene Langås Helene Sæle Tveit Solveig Hegstad Sæternes	Project number: BIFOREN23-16
	Contact person: Beate Nesje
External organization: ANEO	

Fritt tilgjengelig:

Tilgjengelig etter avtale med oppdragsgiver:

Rapporten frigitt etter:

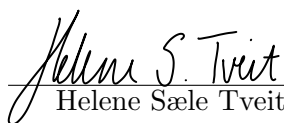
Preface

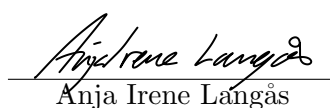
This bachelor thesis is written as a part of the Bachelor program Renewable Energy Engineering at the Norwegian University of Science and Technology (NTNU) in Trondheim, Norway. The thesis is the final part of the study program, and is written in collaboration with Aneo. The purpose is to utilize acquired knowledge and experiences from the program to identify, formulate and solve a relevant problem within the renewable energy field.

The main objective of the thesis is to investigate the climate- and environmental effect of an installed ground-mounted solar energy park based on several simulations, calculations and analyses. All group members have contributed to the thesis and the work load have been distributed evenly between the members. This thesis has contributed to an increased understanding of important aspects regarding sustainable design of a ground-mounted solar park using different software tools.

We would like to thank our internal supervisor, Engin Söylemez at NTNU for frequent support and assistance throughout the project. We would also like to thank our two external supervisors, Beate Nesje and Anders Teigmoen from Aneo for the support, ideas and professional guidance regarding the thesis and simulations, as well as feedback during the whole process. In addition we want to extend our gratitude to Lisa Åsgård from the Norwegian Environment Agency for contributing with information and advice, and for being accessible to answer all our questions.

Trondheim, 22. May 2023


Helene Sæle Tveit


Anja Irene Langås


Solveig Hegstad Sæternes

Abstract

In light of climate change, there is a need for a transition from fossil energy sources to renewable energy such as solar energy. In a world where sustainable development is essential, it becomes more important to address the total climate and environmental impacts of solar energy. The environmental consequences related to ground-mounted solar parks are mainly determined by their location, natural values and land-use, as well as the solar panels. As a result, it will be necessary to take these factors into consideration when designing and installing sustainable ground-mounted solar parks in the future.

The purpose of this bachelor thesis is to find the optimal distance between the solar panels in a solar park with regard to greenhouse gas emissions and energy production. The main focus is on six different cases with a pitch of 8 and 15 meters for three different types of land-use changes. The land-use changes are low site productivity forest, high site productivity forest and constructed area that are turned into an area for a ground-mounted solar park.

An LCA was conducted in order to estimate the greenhouse gas emission from the life cycle of the solar panels. The global warming potential was calculated for the production, transport, mounting and recycling of the PV panel. The carbon footprint from land-use change was determined based on a tool in Microsoft Office Excel from the Norwegian Environment Agency. To simulate the energy production, the solar park was simulated in PVsyst software for the various cases with different area types and pitches. In order to find the optimal design for the solar park, a ratio was calculated with results from total greenhouse gas emissions and energy production for the different cases.

The results from the LCA analysis indicate that the total greenhouse gas emission during the life cycle for one panel is 582.61 kg CO₂-eq. The production phase of the panels accounted for the largest share of emissions. This is because the production phase consists of several energy-intensive processes in China where fossil energy sources are commonly used. The total emissions for land-used change over 30 years were 12 648.7 ton CO₂-eq, 13 546.3 ton CO₂-eq, and 0 ton CO₂-eq for low site productivity forest, high site productivity forest and constructed area respectively.

The simulation results in PVsyst indicate that the solar park installed on constructed area with a pitch of 8 meters injects most energy to the grid, with a yearly contribution of 34 050 MWh. This is because this case has the highest albedo values and more panels that can produce energy, despite more shading loss. From all the simulations, it was evident that bifacial PV panels increased the energy production as they can collect solar irradiance from both sides. In addition, lower temperatures during the winter reduced losses in the system and increased the performance of the PV system.

When looking at the ratio between emissions and production for the six cases, the best case is constructed area with a pitch of 15 meters. This case had the lowest ratio of 35.3034 kg CO₂-eq/MWh. For the area types of low site productivity and high site productivity forest, a distance of 9 meters gives the lowest ratio of 52.1935 kg CO₂-eq/MWh and 53.2148 kg CO₂-eq/MWh respectively. The worst case is for high site productivity forest with a pitch of 15 meters. From an environmental and sustainable perspective, this indicates that it is preferable to install future solar parks in constructed or already developed areas to reduce greenhouse gas emissions.

Sammendrag

I lys av klimaendringene er det behov for en rask omstilling og overgang fra fossile energikilder til fornybar energi som solenergi. I en verden hvor bærekraftig utvikling er essensielt, blir det viktig å adressere den totale klima- og miljøpåvirkningen av solparker. Miljøpåvirkningen knyttet til bakkemonterte solparker bestemmes hovedsakelig av dens lokasjon, naturverdier og arealbruk, samt solpanelene. Som et resultat av dette vil det være nødvendig å ta disse faktorene i betraktning ved utforming og installasjon av bærekraftige bakkemonterte solparker i fremtiden.

Hensikten med denne bacheloroppgaven er å finne optimal avstand mellom solpanelene i en solpark i forhold til klimagassutslipp og energiproduksjon. Det blir hovedsakelig sett på produksjon og utslipp fra seks ulike caser fordelt på tre ulike typer arealbruksendringer. Disse arealbruksendringene er lavbonitetsskog, høybonitetsskog og konstruert område som blir gjort om til et utbygd område for en bakkemontert solpark.

En LCA analyse ble gjennomført for å finne utslippene gjennom livsløpet til et solpanel. Det ble sett på globalt oppvarmingspotensial i forbindelse med produksjon, transport, montering og resirkulering av panelet. Utslippene i forbindelse med arealbruksendringer ble beregnet med utgangspunkt i et verktøy i Microsoft Office Excel utviklet av Miljødirektoratet. For å simulere energiproduksjonen ble solparken simulert i programmet PVsyst for de ulike casene med forskjellige type areal og avstander mellom panelene. For å finne optimalt design for solparken ble det regnet ut et forholdstall med resultater fra totalt klimagassutslipp og energiproduksjon for ulike case.

Resultatene fra LCA analysen viser at utslippet gjennom livsløpet til et panel er 582.61 kg CO₂-ekv. Totalt sett stod produksjonen av panelene for den største andelen av klimagassutslippene. Årsaken til dette er at produksjonen består av flere energikrevende prosesser i Kina som er kjent for å benytte fossile energikilder. Beregningene av arealbruksendringene gav et totalt utslipp for 30 år på lavbonitetsskog, høybonitetsskog og konstruert område på henholdsvis 12 648.7 tonn CO₂-ekv, 13 546.3 tonn CO₂-ekv og 0 tonn CO₂-ekv.

Simuleringene i PVsyst viser at konstruert område med en avstand på 8 meter mellom panelene gir høyest produksjon, hvor det totalt blir det sendt 34 050 MWh årlig til strømmettet. Årsaken til dette er at denne simuleringen har høyest albedoverdier og flere paneler installert i solparken, til tross for høyt skyggetap. For alle simuleringene er det også tydelig at tosidige solpaneler øker energiproduksjonen ettersom de kan samle inn solinnstråling fra begge sider. I tillegg viser resultatene at lave temperaturer i vintermånedene gir redusert tap i systemet for denne perioden og økte ytelsen til PV systemet.

Forholdstallet mellom utslipp og produksjon er best for casen med avstand 15 meter og konstruert område, med en verdi på 35.3034 kg CO₂-eq/MWh. For arealtypen lavbonitet- og høybonitet skog gir en avstand på 9 meter det laveste forholdstallet på henholdsvis 52.1935 kg CO₂-eq/MWh og 53.2148 kg CO₂-eq/MWh. Den minst klimavennlige casen er ved høybonitetsskog hvor det er 15 meters avstand mellom panelene. Dette indikerer at det vil være mest miljøvennlig å installere fremtidens solparker på konstruert mark eller allerede utbygde områder med tanke på klimagassutslipp og energiproduksjon.

Contents

Preface	i
Abstract	ii
Sammendrag	iii
List of terms	vi
1 Introduction	1
1.1 Motivation	1
1.2 Background	2
1.3 Problem Definition and Objective	5
1.4 Structure of the Thesis	6
2 Theory	7
2.1 Meteorology	7
2.2 Panel Orientation	10
2.3 Photovoltaic Systems	11
2.4 Design of PV Systems	14
2.5 Losses in a PV System	17
2.6 Bifacial and Monofacial PV Modules	18
2.7 Production of Solar Panels	20
2.8 Land-Use Change	21
2.9 Area and Energy	26
3 Methodology	27
3.1 Case Study	27
3.2 Life Cycle Assessment	27
3.3 Land-Use Change	37
3.4 PVSyst	39
3.5 Ratio between Production and Emission	47
4 Results	49
4.1 Life Cycle Impact Assessment	49
4.2 Land-Use Change	53
4.3 PV Production	54
4.4 Ratio between Production and Emission	62
5 Discussion	65
5.1 Life Cycle Interpretation	65
5.2 Land-Use Change	68
5.3 PV Production	71
5.4 Ratio between Production and Emissions	77
6 Further Work	79
7 Conclusion	80
A JA-solar 550 Wp Panel	I
B Inventory List	III

C Emissions from Recycling	XI
D Land-Use Change Calculations	XII
E Snow Cover Calculations	XIII
E.1 Snow Data from the Norwegian Climate Service Center	XIII
E.2 MATLAB-script	XIV
F Ratio between Production and Emission Calculations	XVI

List of Symbols

Symbols	Unit	Description
A	m ²	Area
a ₁	MWh/year	The yearly energy production
ALB	-	ground reactance factor or albedo
E ₂	ton CO ₂ -eq/hectare/year	Emission factor for the first year of the transition
E ₃	ton CO ₂ -eq/hectare/year	Emission factor for the next 19 years of the transition
E ₄	ton CO ₂ -eq/hectare/year	Emission factor for the area 20 years
E _{area}	kg CO ₂ -eq	Emission from land-use change
E _{PV}	kg CO ₂ -eq	Emission from production and mounting of PV panels
G	W/m ²	Total global horizontal radiation
G _B	W/m ²	Direct horizontal radiation
G _{Bt}	W/m ²	Direct tilted radiation
G _D	W/m ²	Diffuse horizontal radiation
G _{Dt}	W/m ²	Diffuse tilted radiation
G _{Gt}	W/m ²	Ground reflected radiation
G _t	W	Solar radiation
I	A	Current
I _{max}	A	Current at maximum power
I _{SC}	A	Short-circuit current
k	kg CO ₂ -eq	The annual degradation
n	years	Production period
P	W	Electric power
P _{in}	W	Power from solar radiation
P _{max}	W	Maximum power
P _{nom}	-	DC:AC ratio
P _{tot}	MWh/30 years	Production from 30 years
U	W/(m ² K)	Th value of thermal losses
U _c	W/(m ² K)	The constant loss factor
U _v	W/(m ² K)/m/s	The wind loss factor
s _n	MWh	The total energy production included degradation
T _{Amb}	°C	Ambient temperature
v	m/s	Wind velocity
V	V	Voltage
V _{max}	V	Voltage at maximum power
V _{OC}	V	Open-circuit voltage
z	°	Azimuth angle
α	°	altitude angle
β	°	Surface angle
η _{max}	%	Efficiency
φ	°	Zenith angle

List of Abbreviations

Abbreviations

AC	Alternating current
AMI	Air mass index
AR5	Area resource map in the scale of 1:5000
DC	Direct current
DiffHor	Horizontal diffuse irradiation
CdTe	Cadmium telluride
CIGS	Copper indium gallium diselenide
C-Si	Crystalline silicon
CH ₄	Methane
CO ₂	Carbon dioxide
CO ₂ -eq	CO ₂ equivalents
E _{Array}	Effective energy at the output of the array
E _{Grid}	Energy injected into grid
EU	Europe
EVA	Ethyl vinyl acetate
GlobEff	Effective Global, corr. for IAM and shadings
GlobHor	Global horizontal irradiation
GWP	Global warming potential
HV	High voltage
IEA PVPS	International Energy Agency's Photovoltaic Power Systems Programme
IPCC	Intergovernmental Panel on Climate Change
ISO	International Standards Organization
IT	Insulated Terra
LCA	Life cycle assessment
LCI	Life cycle inventory
LCIA	Life cycle impact assessment
MG-Si	metallurgical grade silicon
MPP	Maximum power point
MPPT	Maximum power point tracking
MV	Medium voltage
MWac	Megawatts alternating current
MWp	c Mega watt peak
N ₂ O	Nitrous oxide
NIBIO	Norwegian Institute of Bioeconomy Research
NIR2022	National Inventory Report from 2022
PET	Polyethylene terephthalate
PP	Polypropylene
PR	Performance ratio
PV	Photovoltaic
PVF	Polyvinyl fluoride
SG-Si	Solare grade silicon
Si	Silicon
STC	Standard Test Conditions
T _{Amb}	Ambient Temperature
UN	United Nations
UV	Ultraviolet
V712	Vegdirektoratet's manual about impact analysis

List of Terms / Dictionary

English	Norwegian	Definition
Albedo	-	A measure for the light or radiation reflected from a surface
Bog	Myr	Wet area with organic soil
CO ₂ equivalents	CO ₂ ekvivalenter	A metric measure used to compare emission from various greenhouse gases based on their GWP
Constructed area	Konstruert område	An area that is highly impacted by humans and very little biologically productive
Decare	Dekar	1000 m ²
Emission factor	Utslippsfaktor	A value
Irradiance	Solinnstråling	the rate of solar power in the form of electromagnetic radiation falling on a surface per unit area
Norwegian Environment Agency	Miljødirektoratet	A Norwegian government agency under the Ministry of Climate and Environment
Land-use change	Arealbruksendring	Areas change from one area category to another
Photovoltaic	Fotovoltaisk	Conversion of light into electricity using semiconducting materials
Pitch	-	Distance between solar panels
Settlement	Utbygd areal	Area type with buildings and areas that can be classified as technical interventions and surrounding developed area
Site productivity	Bonitet	Capacity of wood production in forest

List of Figures

1.1	Sustainable Development Goal 7, 13 and 15. [58]	2
1.2	The different steps in a LCA. [52]	3
1.3	Total energy supply (TES) by energy source for China, year 1990-2021. [30]	4
1.4	Total energy supply (TES) by energy source for Europe, year 1990-2020. [32]	4
2.1	Direct radiation on horizontal and tilted surface. [39]	8
2.2	Daily sun path across the sky from sunrise to sunset. [39]	9
2.3	The change in performance with variation in tilt and azimuth angle. [37]	10
2.4	Variation of tilt of solar panel for different seasons. [37]	10
2.5	The I-V curve for a PV panel. [37]	12
2.6	The I-V curve influenced by (a) increased irradiation and (b) increased cell temperature. [39]	13
2.7	The decrease in a PV panels efficiency over 25 years. [37]	14
2.8	Two solar cells connected in (a) parallel and (b) series. [39]	15
2.9	A PV system with modules, strings, arrays and inverter. [19]	15
2.10	A PV system connected to distribution network. [65]	16
2.11	Reflected, diffuse and direct irradiance received on a bifacial solar panel. [50]	18
2.12	Components of (a) monofacial and (b) bifacial module. [44]	19
2.13	Supply chain of silicon-based PV electricity production. [25]	21
2.14	Forest	23
3.1	System boundary for the LCA.	30
3.2	Maps of the chosen area in Halden.	40
3.3	Horizon in PVsyst for the chosen location in Halden.	40
3.4	Orientation parameters in PVsyst.	41
3.5	Design the array display, for a pitch at 8 meters.	42
3.6	3D-scene	43
3.7	Ohmic losses	44
3.8	Different 3D-scene designs	47
3.9	The JA PV panels degradation over 30 years. [36]	48
4.1	Flow chart for production of 1 m ² PV panel.	50
4.2	An overview of where the emissions come from during the production of the PV panel.	50
4.3	Flow chart for transport by ship from Nanjing to Halden.	51
4.4	Flow chart for 1 m ² open ground construction.	51
4.5	Flow chart for 1 kg takeback and recycling of c-Si module.	52
4.6	Flow chart for 1 kg takeback and recycling of c-Si module.	52
4.7	Flow chart for 1 kg takeback and recycling of c-Si module.	52
4.8	Flow chart for 1 kg takeback and recycling of c-Si module.	53
4.9	Normalized production per installed kWp.	56
4.10	Performance ratio (PR)	56
4.11	Loss diagram for forests	58
4.12	Normalized production per installed kWp.	59
4.13	Performance ratio (PR)	60
4.14	Loss diagram for constructed area.	61
4.15	Production and emissions [kg CO ₂ -ekv/MWh]	63
D.1	Land use change calculations in Excel	XII

D.2	Land use change calculations in Excel with formulas	XII
F.1	Ratio between Production and Emission calculations in Excel	XVI
F.2	Ratio between Production and Emission calculations in Excel with formulas . . .	XVII

List of Tables

2.1	Albedo values for different surfaces. [16]	7
2.2	Site productivity [62]	22
2.3	Emission factors for land degradation (NIR2022). [47]	24
2.4	Emission factors from the V712 handbook and the newer emission factors from NIR2022.	25
3.1	Illustration of the different cases.	27
3.2	Inventory list for the production of 1 m ² PV panels.	33
3.3	Inventory list for the transport of all the PV panels to Halden in Norway.	34
3.4	Inventory list for 1 the mounting of 1 m ² PV panel.	35
3.5	Inventory list for the treatment of 1 kg c-Si PV module.	36
3.6	Inventory list for 1 kg glass cullets recovered from c-Si PV module treatment.	36
3.7	Inventory list for 1 kg aluminum scrap recovered from c-Si PV module treatment.	36
3.8	Inventory list for 1 kg copper scrap recovered from c-Si PV module treatment.	37
3.9	Parameters for JA-solars 550 Wp panel.	37
3.10	Inputs in the Excel spreadsheet for calculating emissions for land-use change from forest with low or high site productivity to settlement.	38
3.11	Emission factors used in the Excel spreadsheet. [54]	39
3.12	Geographical parameters for the chosen location in Halden.	39
3.13	Average amount of snow cover in Halden. 0 = No snow, 1 = Mostly bare ground, 2 = Equal amount snow cover and bare ground, 3 = Mostly snow-covered ground, 4 = Snow-covered ground. [43]	45
3.14	Albedo values	46
4.1	What the colors in Figure 4.2 indicate.	51
4.2	CO ₂ emissions for the various processes and the total emission for one PV panel, excluded the transport from China to Halden.	53
4.3	Emission and absorption for a land-use change from forest of low site productivity to settlement.	54
4.4	Emission and absorption from a land-use change from forest of high site productivity to settlement.	54
4.5	Emission and absorption from land-use change from a constructed area to settlement.	54
4.6	Simulation results related to PV array and inverter.	54
4.7	The main results for forests simulations for pitch of 8 and 15 meters.	55
4.8	The main results for constructed area simulations for pitch of 8 and 15 meters.	59
4.9	Number of panels and production from PVsyst for the pitches between 8-15 meters.	62
4.10	The ratio between emission and production for the six cases A-F. The values are given in kg CO ₂ per MWh.	62
4.11	Production and total emission over the panels lifetime.	63
4.12	kg CO ₂ -eq per MWh energy production.	64

1 Introduction

This introduction chapter presents the motivation and background for the thesis, along with the project definition and objectives. Finally, the structure and the different chapters of the thesis are presented.

1.1 Motivation

The United Nations (UN) Intergovernmental Panel on Climate Change (IPCC) are evident in their official climate reports. The world is approaching crucial levels of global warming that will result in irreversible impacts. The recent UN climate report from April 2023 indicates that greenhouse gas emissions over the last decade have reached the highest level in human history. It is crucial to address climate change as well as environmental degradation and work toward a more sustainable future. In 2015, the UN member states adopted the UN Sustainable Development Goals and the Paris Agreement which represents a global framework for sustainable development, and the aim to limit global temperature rise to 1.5°C [82, 13]. To achieve these goals, every country must take rapid and bold climate action and reduce their greenhouse gas emissions. One important and essential contributor to reaching these goals is the development of renewable energy technologies. [84]

In May 2022, the European Commission adopted an EU solar energy strategy as a part of their REPowerEU plan to transit towards clean energy and reduce the EU's dependence on imported fossil fuels [22]. The strategy aims to install 320 GW of new solar photovoltaic capacity by 2025, which is more than doubling compared to 2020, and almost 600 GW by 2030 [15]. To contribute to the green shift in Europe, The Norwegian government has presented ambitions to increase solar energy production by 5 to 10 TWh within 2030, which represents an increase of 3 300% over 7 years. [80, 81, 92].

In 2021, solar energy had the second largest generation growth of all renewable technologies, after wind, increasing all of 22% from the year before. Solar energy is modular, renewable, flexible with regard to location, as well as cheap. It is considered a clean and renewable energy source, as there are no emissions from producing energy by this technology, and there exists an indefinite amount of solar radiance [24]. In addition, during the last decade, there have been great improvements in solar panels' efficiency, and the cost of solar power has decreased by 82%, as manufacturing, especially in China, has increased [39, 14].

In Norway, solar energy is less utilized compared to other countries in Europe. However, it is the energy source with the largest growth. In 2022, only 0.1% of the power generation in Norway was solar energy. As of today, Norwegian solar installations mainly have taken place on roofs and facades of both private and public buildings. No big-scale ground-mounted solar parks are installed in Norway. In order to reach the government goals set for increasing solar energy production, the installation of ground-mounted solar parks will play a key role in this transition. It is considered the easiest way to develop more renewable power, as it requires little maintenance, can be installed in a wide variety of places and it rarely causes conflicts and interference with nature. [63, 39, 88, 49]

In a world where sustainable development is essential, it becomes more important to address the total climate and environmental impacts of solar energy. The environmental consequences related to ground-mounted solar power parks are mostly determined by their location, natural values and land-use, as well as the consequences of solar panels. As a result, it will be necessary to take these aspects into consideration when designing and installing sustainable ground-mounted parks for the future. [23]

1.2 Background

In 1987, the UN Commission launched the Brundtland Report *Our Common Future* [21], which stated the critical global environmental issues. The report presented sustainable development as a part of a new green transition and strategy for a better future, and was defined as "the development that meets the needs of the present without compromising the ability of future generations to meet their own needs" [21]. To achieve this, the international society must focus on the environmental, social and economic conditions that are inextricably linked [83]. Traditional business development and focus on profit must be replaced by new business strategies where economic, social and environmental sustainability are in focus [21, 41].

Based on this, the UN adopted the Sustainable Development Goals as a shared global agenda and tool for sustainable development. In total, there are 17 goals and 169 targets that aim to eradicate poverty, combat inequality and injustice, protect the planet, and ensure peace and justice for all people. Member states consider the UN Sustainable Development Goals (SDG) as the primary instrument for creating a sustainable world. [58]



Figure 1.1: Sustainable Development Goal 7, 13 and 15. [58]

In relation to the sustainable development of ground-mounted solar parks, the SDGs 7, 13 and 15 are relevant, presented in Figure 1.1. Goal 7, clean energy for all, is fundamental as solar energy is a renewable source of energy that can help reduce greenhouse gas emissions and combat climate change. This can also contribute to reach Goal 13, climate Action. Goal 15, life on land, highlights sustainable forest management, the integration of ecosystems and biodiversity into planning processes and accounting, and other related issues. Every year, 10 million hectares of forest are destroyed. This has a huge impact on biodiversity, and in the coming decades, around 40 000 species will be at risk of extinction. [57]

Another outcome of deforestation and land degradation is greenhouse gas emissions. Non-developed areas can contain large carbon stocks, and development of the area may entail considerable greenhouse gas emissions and reduce potential future carbon storage in the area. Emissions of carbon dioxide due to changes in land-use mainly come from the cutting down of forests and instead using the land for agriculture or settlements, urbanization, roads etc. When large areas of forests are cut down, the land often turns into less productive grasslands with

considerably less capacity of storing CO₂. The biggest emissions are linked to development on areas of bog and forest of high site productivity. [86]

In order to address the total environmental impact of an installed ground-mounted solar park, the greenhouse gas emissions of the solar panels must be assessed from a life-cycle perspective in addition to the land-use change aspect. As seen in Figure 1.2, this includes raw material extraction, manufacturing, transportation and use, as well as disposal or recycling at the end of the lifetime. A life cycle assessment (LCA) is a common method used to evaluate and analyze the environmental impacts of a product, service, or activity. [2, 23]

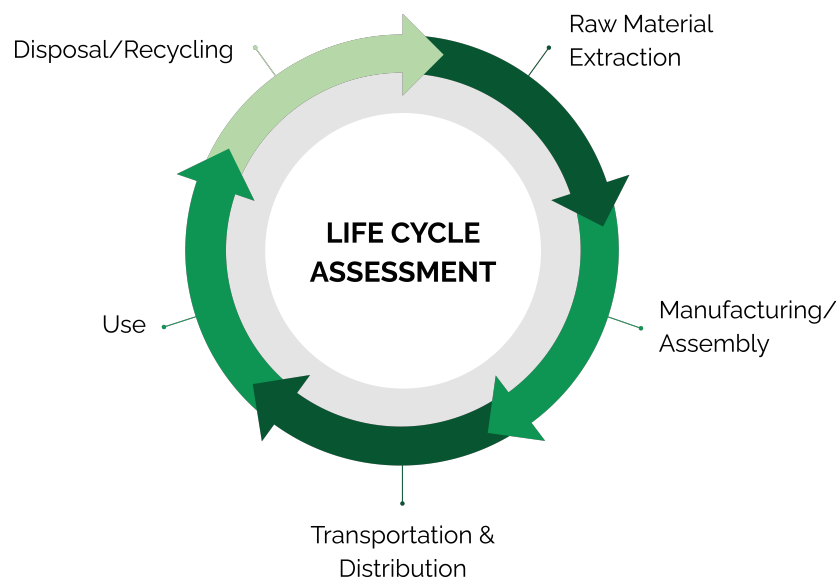


Figure 1.2: The different steps in a LCA. [52]

In recent years, several LCAs and Environmental Product Declarations (EPD) have been published for solar panels and their components within the Norwegian market. All these publications indicate that the production phase contributes the most to greenhouse gas emissions from a life cycle perspective for a solar energy park. The production phase includes the manufacture of the materials, which constitutes a significant part of the emissions, as well as the production of the solar panels and materials included in the construction. Concrete and steel are commonly used, and count for large amounts of greenhouse gas emissions in the material production. In connection with this, the location of the production and its energy mix has a great impact on the amount of emissions. China is a leading global manufacturer of PV panels today and is known for an energy mix of fossil fuels where coal and oil constitute a large amount, as seen in Figure 1.3 [30]. [23, 31]

1 INTRODUCTION

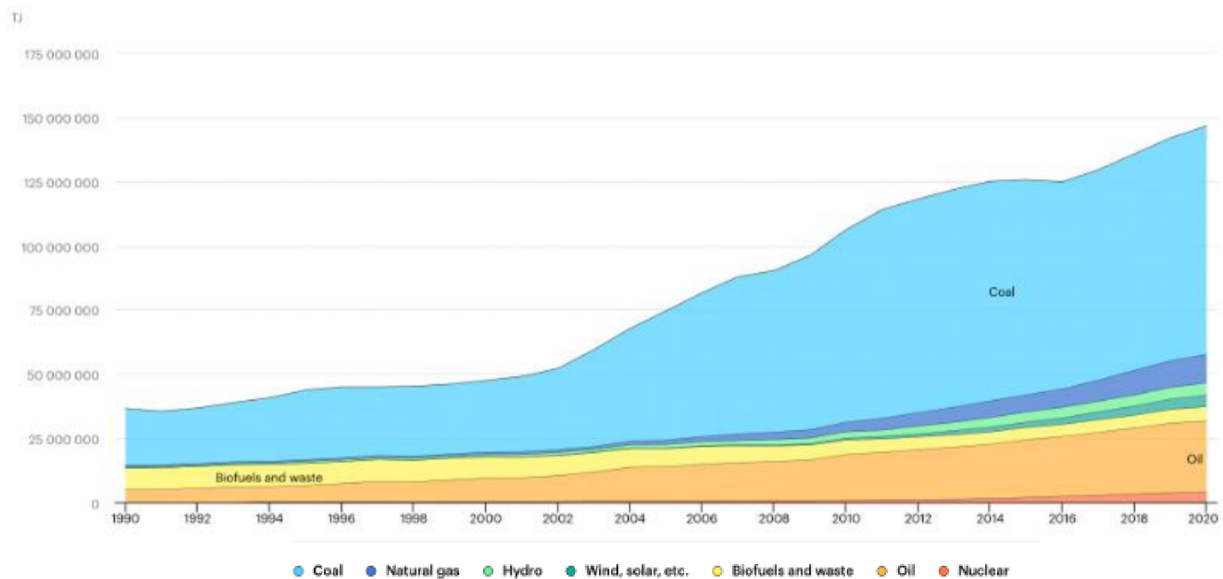


Figure 1.3: Total energy supply (TES) by energy source for China, year 1990-2021. [30]

In contrast, the energy mix in Europe consists of a more wide span of energy sources as seen in Figure 1.4. Still, fossil fuels such as coal and oil contribute with a large amount, but it is decreasing. In light of the REPowerEU strategy, as well as the SDGs and Paris Agreement, it can be assumed that it will continue to decrease, and that renewable energy will constitute more of the future energy mix in Europe. [32]

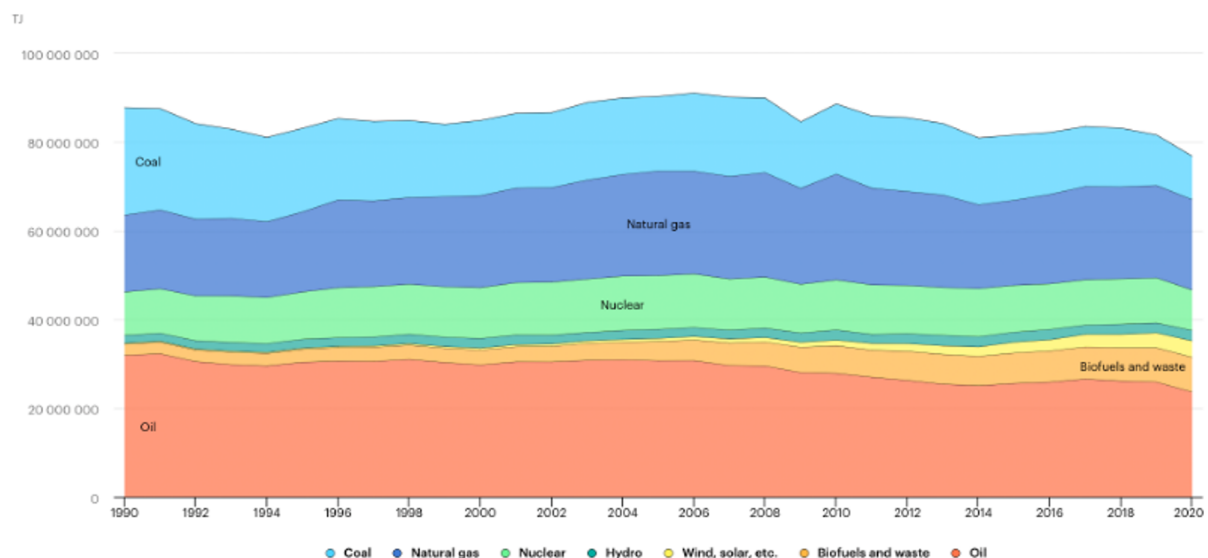


Figure 1.4: Total energy supply (TES) by energy source for Europe, year 1990-2020. [32]

In addition to the production phase, the emissions related to transport are dependent on the location for production and the PV system. The EPD publications indicate that these emissions are significantly lower than the emissions from production. For the operation and maintenance phase, as well as the end of life, the emissions depend on factors and assumptions related to how and how often the solar panels are maintained, along with how and where they are disposed or recycled. [23]

From a national perspective, Norwegian companies play a key role in the global green transition in the solar energy industry. Several companies within broad disciplines participate along many parts of the solar energy industry value chain. Unlike the majority of European countries, the Norwegian industry supplies both materials and components to the global solar industry market. The most important ones are related to the production and export of silicon materials, which are essential in solar cells for solar energy production. This Norwegian production sequence is known for having technological and environmental advantages. [9, 49]

According to Sintef, the world's most environmentally friendly silicon production for solar cells is in Norway. In addition, Norwegian companies study the possibilities to produce other environment-friendly products within the solar industry. With higher focus and support related to sustainable production in for example the EU, Norway will be an important contributor in creating and implementing a more sustainable life cycle for the solar industry today and in the future. [9, 49]

1.3 Problem Definition and Objective

This bachelor thesis is given by Aneo. Aneo is a new renewable company established by TrønderEnergi and HitecVision in September 2022. They are focusing on renewable energy production, electrification and energy efficiency in the Nordic region. Aneo contributes in the green transition by developing, producing and distributing renewable energy such as solar, hydro and wind power. Within solar energy production, Aneo aims to assess solar energy production from a ground-mounted solar park in relation to sustainability. [5, 6]

The main objective of the thesis is to investigate the climate- and environmental effect of an installed ground-mounted solar energy park. The thesis intends to calculate CO₂ emissions and energy production of ground-mounted solar power, looking at what type of area is used and the distance between solar panels. The goal is to find the ratio between production and greenhouse gas emission, and the ideal combination of pitch and area type.

The CO₂ emissions for all the PV panels installed in the solar park will be calculated through an LCA. The LCA is a cradle-to-grave study, conducted in the software program SimaPro. The program is used to analyze the impacts and emissions of a monocrystalline bifacial solar panel. In addition to the emissions related to the solar panel itself, the greenhouse gas emissions from the location and land-use change are taken into consideration. The park is chosen to be located in Halden in the southeast part of Norway. The type of area for the chosen location will have an impact on the total emission-related results. Therefore, the thesis will look at two relevant type of areas; forest and constructed area. In addition, both forest with high site productivity and low site productivity will be analyzed. The emissions from land-use change will be calculated in a Microsoft Office Excel spreadsheet from the Norwegian Environment Agency.

To estimate and calculate the energy production generated from the solar park, the simulation software called PVsyst will be used. Several simulations for different distances between each row of solar panels, called pitch, will be done. The goal is to find the ratio between production and greenhouse gas emissions, and the ideal combination of pitch in a specific area type.

It should be noted that the assessments, calculations and simulations done in this thesis represent the current situation, and because of the rapid development of solar energy, updated documents and research should be examined and taken into account.

1.4 Structure of the Thesis

Chapter 2 - *Theory* contains the theoretical framework and concepts related to meteorology, photovoltaics and their production and construction, as well as design of photovoltaics systems. Along with a presentation of land-use change with area classifications, carbon storage and emissions from land-use change.

Chapter 3 - *Methodology* explains the different cases relevant for the thesis, and the data collection and treatment process. The method for the LCA in SimaPro is presented, along with the simulations in PVsyst and calculations based on the spreadsheet from The Norwegian Environment Agency.

Chapter 4 - *Results* presents the results from the LCA, land-use change calculations and simulations from PVsyst for all the cases. In addition, the ratios between solar energy production and greenhouse gas emissions are presented.

Chapter 5 - *Discussion* discuss the results, as well as the chosen methods, assumptions and relevant topics.

Chapter 6 - *Further Work* suggests aspects and actions of the thesis that could improve the thesis or that is left uncovered in the thesis, and may be interesting to study further.

Chapter 7 - *Conclusion* summarizes the main results.

2 Theory

The theory chapter presents the theoretical framework for this thesis. The first part is an introduction to meteorology, photovoltaic systems and panels. Secondly, the production of panels is described before the theory related to land-use change is outlined.

2.1 Meteorology

In this section, relevant and fundamental theories related to meteorological aspects such as albedo, solar irradiance and sun path will be presented.

2.1.1 Albedo

The albedo value represents the earth's surface's ability to reflect light compared to the total incoming sunlight. Generally, dark colors absorb more light energy, while light colors reflect most of the incoming light [17]. The values vary between 0 and 1, where 0 means a "perfect absorber" that absorbs all the incoming sunlight. Examples of surfaces with low albedo value are ocean, forests and some types of urban surfaces, such as asphalt. When the albedo is 1, the surface is a "perfect reflector" that reflects all the solar energy. Surfaces with high albedo values are sand, snow, and some urban surfaces such as concrete. Albedo values for different surfaces are presented in Table 2.1. [16]

Table 2.1: Albedo values for different surfaces. [16]

Type of surface	Albedo values
Urban situation	0.14 - 0.22
Grass	0.15 - 0.25
Fresh grass	0.26
Fresh snow	0.82
Wet snow	0.55 - 0.75
Dry asphalt	0.09 - 0.15
Wet asphalt	0.18
Concrete	0.25 - 0.35
Red tiles	0.33
Aluminum	0.85
New galvanised steel	0.35
Very dirty galvanised steel	0.08

2.1.2 Solar Irradiance

Irradiance is the rate of solar power in the form of electromagnetic radiation falling on a surface per unit area. It is measured in the SI unit W/m^2 . Solar irradiation is the integration of the solar irradiance over a given time interval, with the SI units J/m^2 or Wh/m^2 . [39]

Direct or beam horizontal radiation (G_B) is electromagnetic radiation per unit area that moves through the atmosphere in a direct path from the sun to the earth's surface. A large part of the solar radiation is scattered by molecules in the atmosphere, reflected back to space, and absorbed by the atmosphere. This atmospheric interaction is a part of the total sun rays and will be scattered or non-directional. As a result, this radiation enters the earth's surface from the entire sky vault. This is called diffuse radiation (G_D). Global horizontal radiation (G) is

the total amount of direct and diffusion received on a horizontal surface. This can be found by using Equation 2.1. [39]

$$G = G_B + G_D \quad (2.1)$$

Where:

G	= Total global horizontal radiation	$[\text{W}/\text{m}^2]$
G_B	= Direct horizontal radiation	$[\text{W}/\text{m}^2]$
G_D	= Diffuse horizontal radiation	$[\text{W}/\text{m}^2]$

Solar panels are usually installed and designed with an angle relative to the surface in order to increase the amount of solar radiation and reduce losses related to reflection. The total amount of radiation on a tilted surface at a given location and time depends on the orientation and slope of the surface. The difference between direct radiation and direct tilted radiation is illustrated in Figure 2.1, where β represents the surface tilt angle. The other angles will be presented in Section 2.1.3.

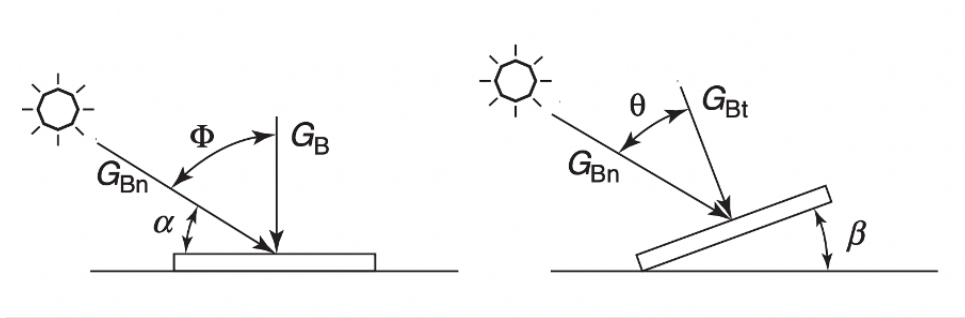


Figure 2.1: Direct radiation on horizontal and tilted surface. [39]

The total diffuse (G_{Dt}), direct radiation (G_{Dt}) and ground reflected (G_{Gt}) solar radiation at a given area on a tilted surface is called global tilted radiation (G_t), given by Equation 2.2. [39]

$$G_t = G_{Dt} + G_{Dt} + G_{Gt} \quad (2.2)$$

Where:

G_t	= Global titled radiation	$[\text{W}/\text{m}^2]$
G_{Dt}	= Direct titled radiation	$[\text{W}/\text{m}^2]$
G_{Dt}	= Diffuse tilted radiation	$[\text{W}/\text{m}^2]$
G_{Gt}	= Ground reflected radiation	$[\text{W}/\text{m}^2]$

The ground-reflected radiation on a tilted surface can be found by using Equation 2.3 [39].

$$G_{Gt} = G \cdot 0.5 \cdot ALB \quad (2.3)$$

Where:

G_{Gt}	= Direct titled radiation	[W/m ²]
G	= Total global horizontal radiation	[W/m ²]
ALB	= Ground reflectance factor or albedo	[-]

2.1.3 Sun Path

The sun path across the sky varies throughout the year. The path is relevant in order to calculate the solar radiation on surfaces as well as the correct orientation and placement of solar panels. The daily sun path across the sky from sunrise in the east to sunset in the west is illustrated in Figure 2.2. The solar altitude angle, α , defines the angle between the horizontal plane and the sun's rays. This angle is related to the solar zenith angle, ϕ . The zenith is an angular measurement between the sun's rays and the vertical plane. This angle is the same as the incidence angle, ϕ for a horizontal plane. [39]

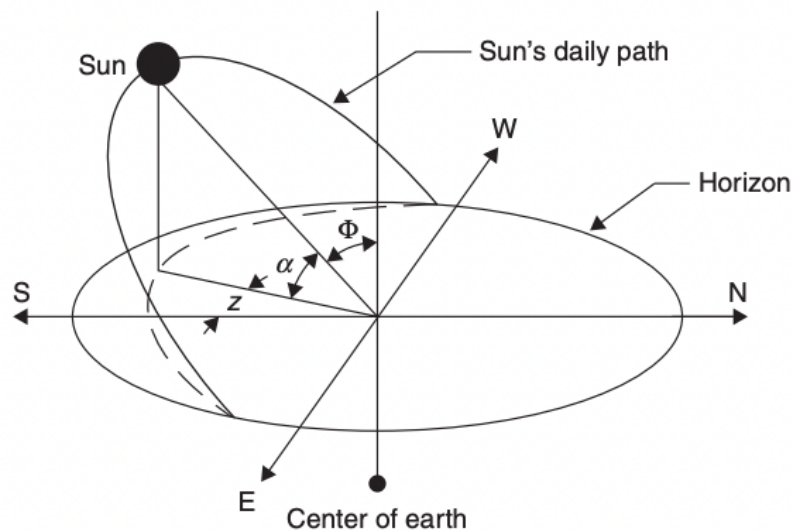


Figure 2.2: Daily sun path across the sky from sunrise to sunset. [39]

The azimuth angle, z , represents the angle along the horizon. This is the angle of the sun's ray in relation to the horizontal plane from south for the Northern Hemisphere or from north for the Southern Hemisphere. At solar noon the sun is exactly on the meridian, with the north-south line, and the azimuth angle is 0° . The tilt angle that impacts the performance of a solar system in the Northern Hemisphere depends on the azimuth angle, as shown in Figure 2.3. [39, 37]

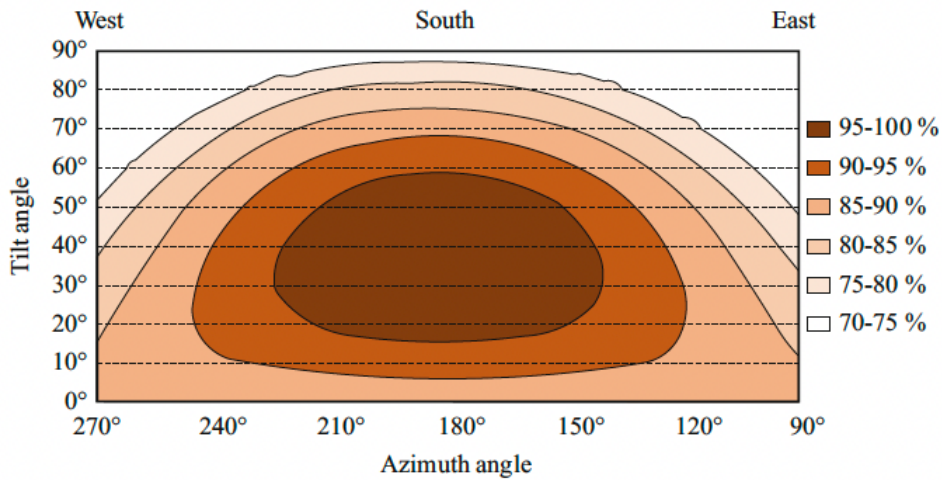


Figure 2.3: The change in performance with variation in tilt and azimuth angle. [37]

2.2 Panel Orientation

The amount of solar radiation reaching the Earth varies with the time of the day, the season of the year and site location. Sites around the equator have the highest amount of solar radiation as it falls directly on the surface. The direct solar radiation decreases when the latitude from the equator increases. The optimal solar panel orientation is to reach the geographic or true north in the Southern Hemisphere or the south in the Northern Hemisphere. In order to obtain maximum output, PV modules are tilted at the same angle as the geographical latitude for a given location. The angle is low near the equator and increases the closer it is to the poles. The tilt angle can vary by using a tracker changing the angle according to the sun's daily path to increase the radiation on the PV panel surface. [37]

The tilt of the PV panel also depends on the terrain and base where it is installed. For ground-mounted solar panels, the tilt angle is based on the latitude of the location. When panels are installed on a sloped surface, the module tilt should be adjusted and follow the specific angle of the inclined roof. The different seasons during a year also have an impact on the tilt angle. Due to the lower altitude of sunlight in winter compared to the summer season, the panels are more tilted during winter than in summer time, as shown in Figure 2.4. [37]

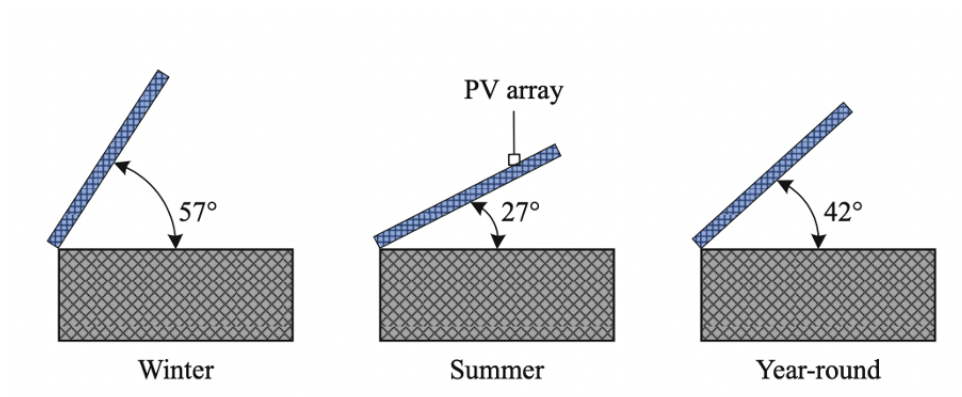


Figure 2.4: Variation of tilt of solar panel for different seasons. [37]

2.3 Photovoltaic Systems

The term 'photovoltaic' (PV) is composed of the two words photo, which means light, and voltaic, meaning electricity. PV technology refers to the hardware device that converts sunlight directly into electricity. The technology has had a great improvement related to efficiency during the last decade. This technological development, the good availability of solar radiation, and minimal maintenance are all factors making PV systems more valuable than other energy sources on the market today. In addition, the system requires minimal maintenance and has a long life as the system does not have any moving parts. [39, 37]

2.3.1 Semiconductors

The core of PV technology is a cell semiconductor material. This material can conduct electricity better than an insulator, but not as well as conductor materials. When a semiconductor material is exposed to photons of sunlight, it absorbs the light's energy and transfers it to electrons. This energy causes a flow of electrons through the material as an electrical current. The total amount of produced energy depends on the band gap. The band gap of PV semiconductors indicates which wavelengths of the light spectrum the specific material can absorb. When the band gap matches the wavelength of light that strikes the surface of a PV cell, all the light energy can effectively be used. [39, 20]

There are several semiconductor materials with different atomic structures used in PV cells. The most commonly used semiconductor material for PV panels are often silicon, which accounts for about 80% of the PV market today. Silicon cells are made of silicon atoms that can be connected in a monocrystalline or a polycrystalline structure. Monocrystalline silicon cells have a single continuous crystal lattice structure that converts light into electric energy more efficiently. Their high efficiency is typically around 14-15%, while the premium one is over 20%. A disadvantage of this cell type is a manufacturing process known as complicated and expensive. Polycrystalline or polycrystalline cells are made of several monocrystalline silicon grains. This cell is cheaper as the manufacturing process required is more simple, but it is less efficient. The efficiency is about 13-15% for one panel, and for premium panels it is up to 17%. These modules are expected to be operative for at least 25 years. [39, 20]

Thin-film photovoltaic is another known semiconductor material used in PV cells. There are two main types of thin-film materials called cadmium telluride (CdTe) and copper indium gallium diselenide (CIGS). CdTe is known for its low-cost manufacturing process and high tolerance to heat, but its efficiency is not as high as silicon. The efficiency is about 10-11%. CIGS cells have a moderate efficiency of 10-13%, low manufacturing costs, and are lightweight. Other solar technologies, such as perovskite and organic PV cells, are under development. [39, 20]

2.3.2 The I-V Curve

An essential characteristic of PV cells is the I-V curve. This curve illustrates the relationship between the voltage and current produced by a PV panel under the Standard Test Conditions (STC). Under STC the irradiance is 1000 W/m^2 , the air mass index (AMI) is 1.5 and the cell temperature is 25°C . Figure 2.4 illustrates the I-V curve with the short-circuit current (I_{SC}) and the open-circuit voltage (V_{OC}) at STC. [37]

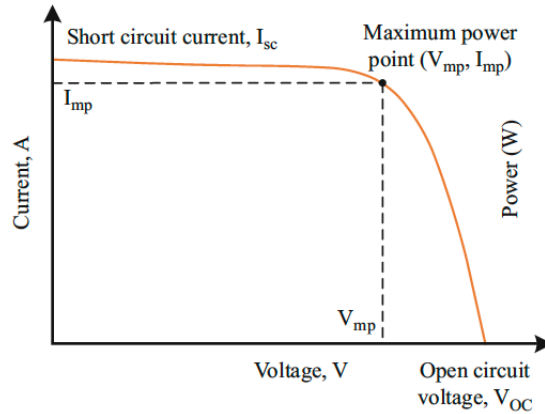


Figure 2.5: The I-V curve for a PV panel. [37]

The V_{OC} voltage value represents a solar cell connected to an infinite-resistance load, where the current is zero. This V_{OC} value is the maximum voltage that a PV module can produce, and occurs when the PV cell circuit is open. I_{SC} represents the maximum current, as seen in Figure 2.4. In this case, the voltage across the cell is zero. Between the short-circuit and open-circuit value, a current and voltage will arise and generate electric power. Power is obtained by Equation 2.4. [37]

$$P = V \cdot I \tag{2.4}$$

Where:

P = Electric power	[W]
V = Voltage	[V]
I = Current	[A]

At one point on the I-V curve, the PV module generates the maximum possible power, called the maximum power point (MPP). At this critical MPP point, the current is known as I_{mp} and the voltage V_{mp} . Under real conditions, the cell temperature and irradiance can vary. Changes in these two parameters will influence the PV cell characteristics as shown in Figure 2.6. An increase in solar irradiance will increase the current and cause small changes in voltage. As a result, this will increase the power. When the cell temperature grows, the voltage becomes lower. However, the increase in current is small, and the power output will decrease. [37, 39]

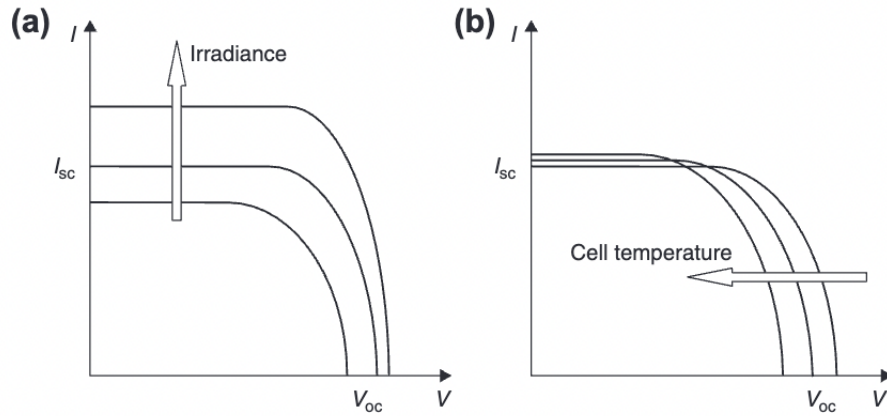


Figure 2.6: The I-V curve influenced by (a) increased irradiance and (b) increased cell temperature. [39]

2.3.3 Efficiency and Performance Ratio

The efficiency factor of a PV cell or panel represents the share of solar radiation that can be converted into useful electrical energy. The efficiency is commonly reported under STC conditions. Efficiency can be calculated by dividing the maximum electrical power output with the incident light power, as seen in Equation 2.5. [39]

$$\eta_{\max} = \frac{P_{\max}}{P_{In}} = \frac{I_{\max} \cdot V_{\max}}{A \cdot G_t} \quad (2.5)$$

Where:

η_{\max}	= Efficiency	[%]
P_{\max}	= Maximum power	[W]
P_{in}	= Power from solar radiation	[W]
I_{\max}	= Current at maximum power	[A]
V_{\max}	= Voltage at maximum power	[V]
A	= Area	[m ²]
G_t	= Solar radiation	[W]

The performance ratio (PR) indicates the performance of a PV system. As seen in Equation 2.6, the performance ratio is the ratio of the system yield, with respect to potential yield under STC conditions. The ratio is independent of location and is influenced by factors such as solar insolation, the efficiency of components in the PV system, the size of the inverters relative to the PV array, and the utilization factor of the system. [39, 69]

$$\text{Performance ratio} = \frac{\text{System yield}}{\text{Potential yield}} \quad (2.6)$$

Where:

Performance ratio	[-]
System yield	[kWh]
Potential yield	[kWh]

During the PV panels operating lifespan, the efficiency and performance are expected to decrease due to use and operation. Figure 2.7 illustrates how the efficiency can drop over a period of 25 years. [37]

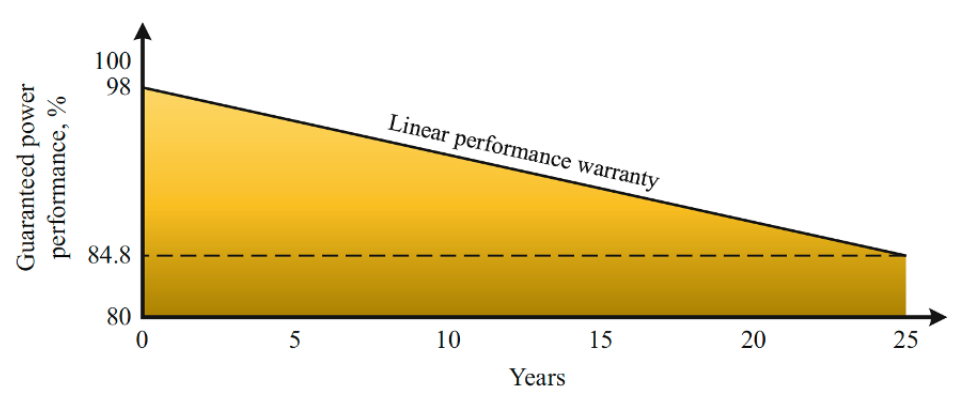


Figure 2.7: The decrease in a PV panels efficiency over 25 years. [37]

2.4 Design of PV Systems

PV systems are usually installed as stand-alone or grid-connected systems. Stand-alone PV systems are independent of the electricity grid, and are commonly used at locations where there is limited or no access to an electric network. Normally the produced energy is stored in batteries to increase the availability. A grid-connected system is connected to the local grid. For this system, generated energy can be used directly to meet the load or be sold to an electricity supply company. When the system is not able to provide the required energy, power can be supplied back from the network by payment. [39]

2.4.1 Components of a PV System

Depending on how the PV system is designed, there are different components and applications integrated in a specific system. Generally, the main component of a PV system is the PV panel, also called a PV module. One panel consists of many PV cells which convert solar irradiance into DC energy by the photovoltaic effect. PV systems can be dimensioned and developed as any virtual size. The systems are modular, and more panels can be added both in height and length to increase the total electrical output. One module mounted with the short side to the ground is called portrait orientation. Several portrait modules can be installed within a given row length to increase the power output [48]. Modules or cells can be connected in series to

increase the voltage and be interconnected in parallel to increase the current to the grid, as seen in Figure 2.8. [39]

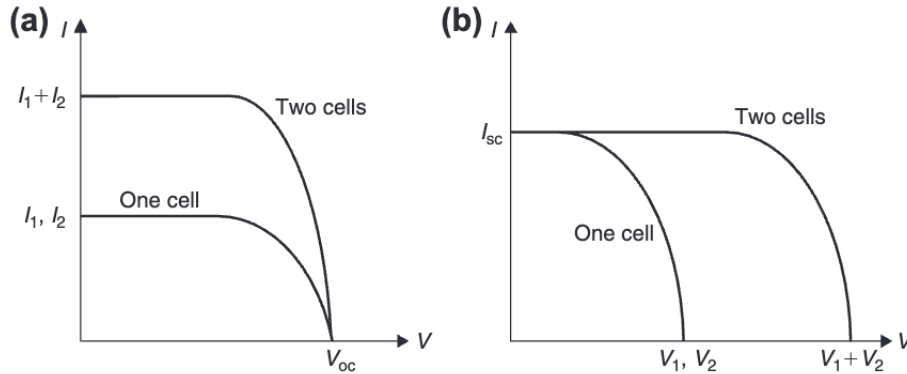


Figure 2.8: Two solar cells connected in (a) parallel and (b) series. [39]

Figure 2.9 illustrates a PV system with modules, arrays, strings and inverter. Modules can be wired in series to create a string, and they can be connected in either series or parallel, or a combination of both, to design an array. As the panels produce DC, there is a need to convert it to AC electricity in order to reach a frequency and voltage that is suitable for the connected utility distribution grid by an inverter. Inverters have several maximum power point tracking (MPPT) inputs that can be connected to an array of solar panels. [37, 39, 76]

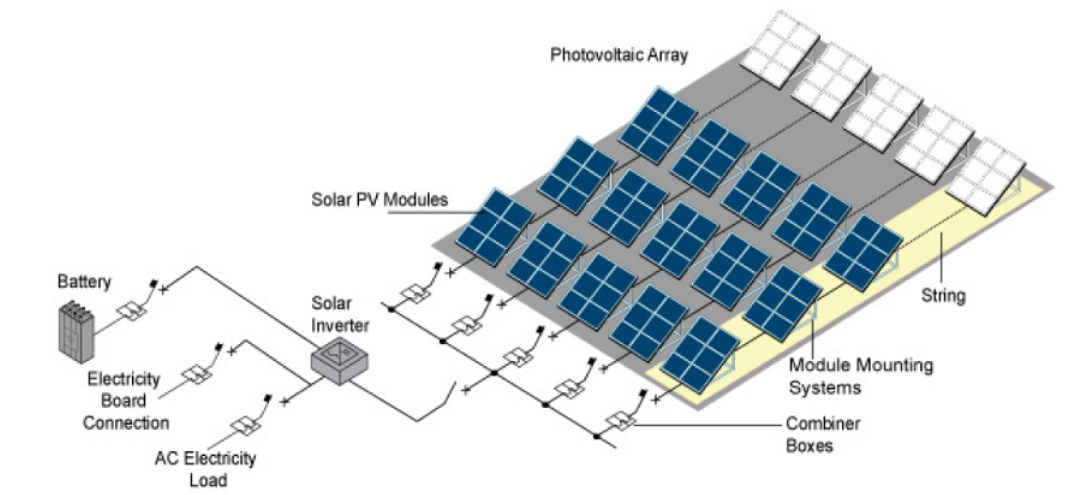


Figure 2.9: A PV system with modules, strings, arrays and inverter. [19]

2.4.2 Power from PV to Grid

The inverter needs to match the total PV power generated from the solar park. A widely-used indicator when sizing the inverter is the Pnom ratio, also named the DC:AC ratio. This is defined as the ratio between the PV array's nominal power under STC conditions and the inverters' nominal power, as seen in Equation 2.7. This value usually lies between 1.25 and 1.30, but it can vary with respect to the different systems. [70]

$$P_{nom} = \frac{\text{PV array nominal power}}{\text{Inverter nominal power}} \quad (2.7)$$

Where:

P_{nom}	[-]
PV array nominal power	[kWp]
Inverter nominal power	[kWp]

The inverter also needs to be designed for the connected grid. There are Norwegian and international laws, standards and regulations that must be taken into consideration when designing a PV system connected to grid. They are set based on desired energy and efficiency transmission from the energy producer system to the consumer where safety, losses and dimensioning are taken into account. The Norwegian power grid can be divided into three categories as seen in Figure 2.10. These are transmission networks (normally 420 and 300 kV), regional networks (normally 132 and 66 kV) and distribution networks. Distributions networks can be divided into low-voltage and high-voltage grid systems. Within low-voltage systems the most common type in Norway is the IT (Insulated Terra) network, which has a voltage of $\pm 10\%$ 230 V [18]. As a result, 207 V is the minimum and 253 V is the maximum voltage for IT grids. [40, 91, 65]

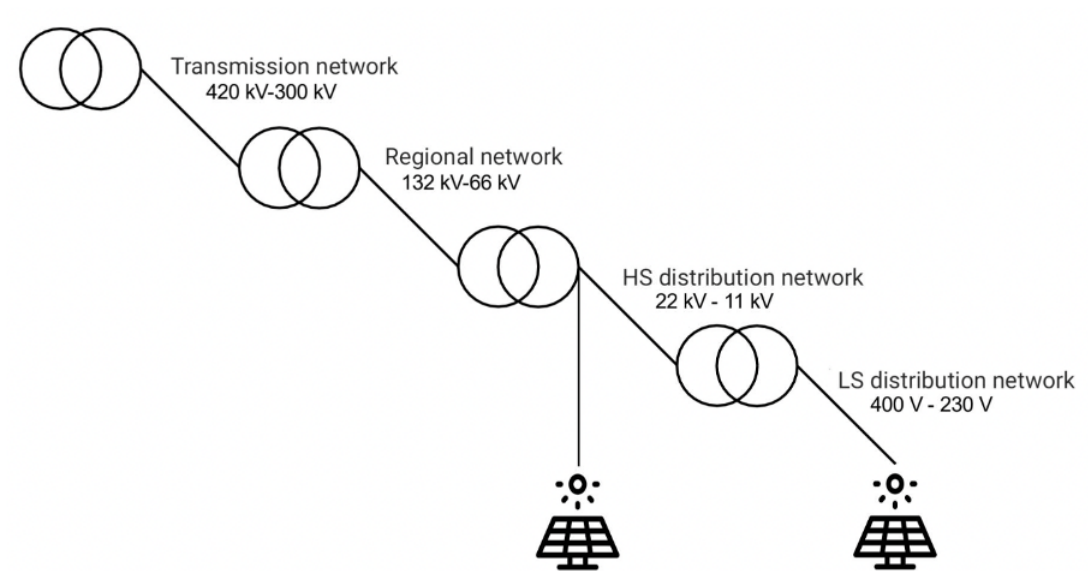


Figure 2.10: A PV system connected to distribution network. [65]

2.5 Losses in a PV System

In a PV system there are different types of energy losses that affect the generated power output. The losses presented in this subsection are based on information from the simulation program PVsyst. Some of the different losses are array loss, direct current (DC) wiring losses, alternating current (AC) wiring losses, AC losses in transformers and system losses. [46, 79]

Array losses are losses related to the power generated by the PV modules linked to its nominal power presented by the manufacturer specifically for STC conditions. Array losses are often connected to the solar irradiance, temperature, conduction, mismatches in the solar panels, as well as the thermal loss factor [71]. The thermal loss factor is connected to thermal parameters that influence the electrical performance of a PV system and can potentially give a thermal loss. This loss is mainly dependent on the energy balance between ambient temperature and the cell temperature due to incident irradiance. The thermal loss factor or balance is given by Equation 2.8. For free-standing ground-mounting systems where the air circulates all around the collectors, U_c is 29 W/(m²K) and U_v is 0 W/(m²K)/ m/s. [46, 72, 79]

$$U = U_c + U_v \cdot v \quad (2.8)$$

Where:

U	= The value of thermal losses	[W/(m ² K)]
U_c	= The constant loss factor	[W/(m ² K)]
U_v	= The wind loss factor	[W/(m ² K)/m/s]
v	= Wind velocity	[m/s]

There are also losses related to incoming irradiance for the rear side of a bifacial panel. This is called the view factor. The view factor represents the ratio between solar irradiance reflected from the ground that reaches the backside of the bifacial panel, and the irradiance lost and reflected back to the sky. [75]

Wiring losses are connected to the resistance of the wires in an electric circuit. This type of energy loss is separated into DC wiring losses and AC wiring losses. DC wiring losses are related to wiring and interconnection from the PV modules and strings in a PV system. This loss can be calculated by summing all the resistances in series and doing a circuit analysis to find the voltage drop that occurs when the current flow through the resistors. The AC wiring losses represent the impedance, also called resistance, between the inverter output and a potential medium voltage (MV) transformer or injection point. The AC wiring losses can be calculated based on a loss fraction, under STC conditions or P_{nom} and the chosen wire section in PVsyst. Based on today's industrial practice and PVsyst, the average DC and AC wiring losses for ground-mounted PV systems are normally less than or equal to 2% for a string inverter and are 0.8% with the central inverter. [46, 79]

AC losses in the transformer apply in the same way as AC wiring losses, mentioned above. This type of loss depends on the chosen MV/HV external transformer with its amount and the properties of the MV/HV line up to injection. This line can be either an overhead transmission line or an underground cable, dimensioned according to voltage, current capacity and length

of line. For a standard MV transformer, the losses for an aluminum winding transformer are considered 1.1%, and 0.9% for a Copper winding transformer. The losses for a standard high voltage (HV) transformer are 0.5%. [46, 79]

In order to optimize the efficiency and energy output of PV systems, it is desirable to maximize the amount of modules in a given area. As a result, many PV modules are usually installed in several portraits in height, and in multiple rows facing the true south. Consequently, this produces a shading loss as the panel's shade for the incoming radiation in the back rows. The losses can be minimized by estimating the possibility of shading by the front rows to the second one and further the subsequent rows. The maximum shading is at local solar noon during the day. [39, 7, 79]

2.6 Bifacial and Monofacial PV Modules

The market share of bifacial photovoltaic modules is increasing compared to monofacial PV technologies because of their new panel design. Bifacial PV panels have the ability to convert solar irradiance from both the front and back side of the panel, as shown in Figure 2.11. This enables the PV module to utilize the irradiance in a greater extent compared to traditional monofacial PV-modules with opaque backsheets. This bifacial technology transition has the potential to increase the solar power production per area. Potentially the energy yield of PV power can be improved up to 25 to 30%. [89]

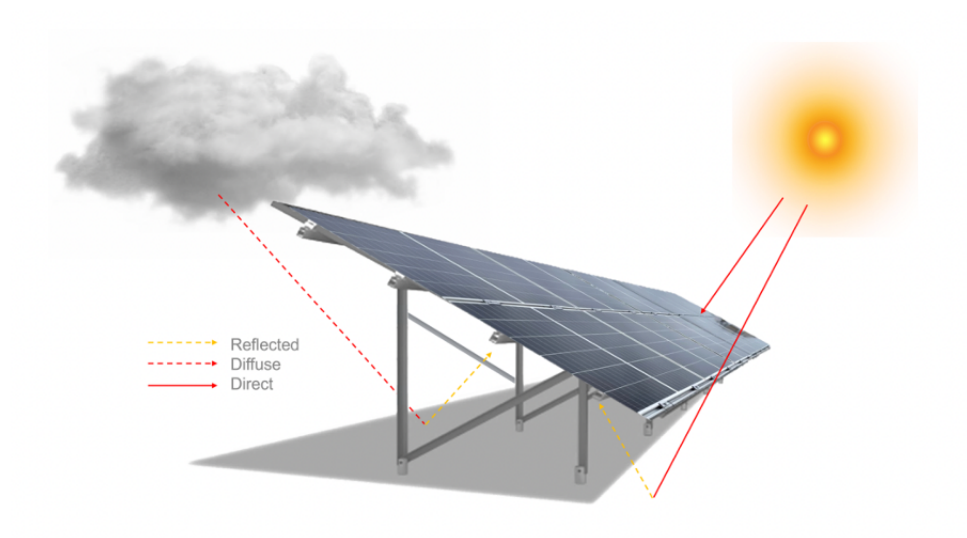


Figure 2.11: Reflected, diffuse and direct irradiance received on a bifacial solar panel. [50]

2.6.1 PV Module Construction

PV modules are designed and constructed for outdoor and environmental conditions such as tropic, arctic, marine and deserts [39]. The construction of a standard PV module includes frame, front tempered glass, encapsulant layers, solar cells, rear tempered glass, backsheets and junction box, as shown in Figure 2.12 [37].

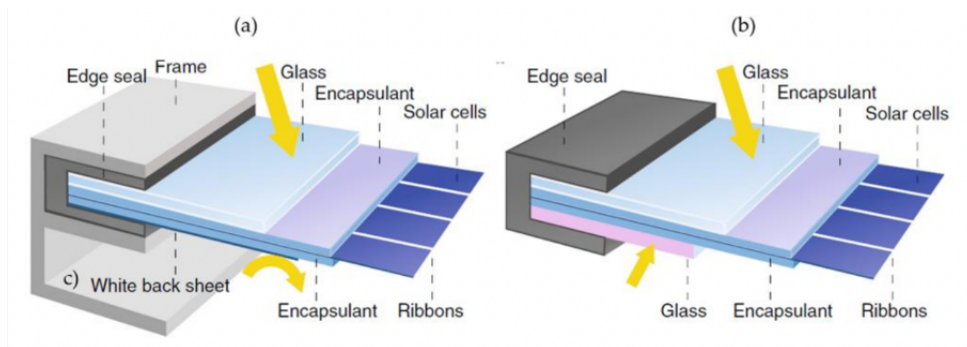


Figure 2.12: Components of (a) monofacial and (b) bifacial module. [44]

Glass is the top layer of a standard solar module. It protects the module against water, humidity and dirt, and ensures mechanical stability and rigidity. The module glass is usually true clear low iron glass that is anti-reflective which reduces reflection and enables a higher efficiency factor. The glass is made of strong transparent tempered glass to provide safety to the solar panel. The glass layers must be regularly cleaned to prevent dirt and soil, which reduces the photons ability to reach the cell with the silicon wafer. This causes loss called soiling losses. For a bifacial module, the glass covers both the top and rear side of the PV cell, as seen in Figure 2.12. [37, 67]

The frame attaches the module together and ensures robustness. It is typically made of aluminum due to the metal's strength and corrosion resistance. According to the fulfillment of security related to the operation and maintenance of the solar module, all the panels are connected electrically before they are grounded. The electrical flow through the PV modules is collected into a junction box placed on the top rear side of the module. [37]

In the middle of the PV module, there is an array of many solar cells converting sunlight to electricity. As mentioned in Chapter 2.3.1, there are different solar cell types. The choice of the cell has a big impact on the efficiency module output. The solar cell is protected from dirt and water by an encapsulant transparent material layer both on the top and rear side. Ethyl vinyl acetate (EVA) is the most common encapsulant material today. It is a thermal resistive material that tolerates high temperatures. This encapsulant material layer is important related to ensure long durability and module performance. [37, 67]

A traditional monofacial PV panel has a backsheet as the rear layer. It protects the panel against moisture and provides mechanical protection and electrical isolation. The backsheet material can be made of various types of plastics including PP, PET and PVF which gives different levels of protection, thermal stability and long term ultraviolet (UV) resistance. [90]

When installing PV panels, there are ranges of different possibilities. Some possibilities are flat roof installation, slated roof installations, facade installations and installed on open ground. Solar parks, which are not on buildings, uses open-ground mounting installations. Profiles are typically piled into the ground to form the foundation of open ground systems. In situations where piled profiles cannot be used, concrete foundations are used instead. When the foundation is in place the rest of the system is mounted and the panels are fixed. The materials used in open ground mounting systems are mostly zinc coated steel, stainless steel and aluminum. Ground-mounted PV systems are usually protected by a fence because of the risk of high voltage access and the insurance. [38]

2.7 Production of Solar Panels

The total production process of manufacturing monocrystalline PV panels is shown in Figure 2.13. The process starts with the production of metallurgical grade silicon (MG-Si) [25]. Silicon can be extracted from sand, quartz, and rocks that consist of silicon dioxide, SiO_2 . The silicon dioxide must be converted to silicon (Si) and is done by Equation 2.9. [8]



It is important that the silicon have a small amount of contaminants in order to be useful in PV applications. The first step in the converting process is to generate MG-Si. In this process, quartz is fed into an electric furnace, where it reacts with a carbon-based reduction agent. Some examples of reduction agents are coal, coke, charcoal, or wood chips. This process is an energy-intensive process. Today, China is the biggest producer of MG-Si with a specific production of $4.5 \cdot 10^6$ metric tons. Russia has the second largest production with a specific production of $6 \cdot 10^5$ metric tons MG-Si [28]. The produced MG-Si has normally a silicon purity of 98- 99%. [8]

As the silicon used in PV panels requires solar grade silicon (SG-Si) with a purity of 99.9999% (six nines pure) the MG-Si needs to be further purified. The most common purification method is the Simens process where MG-Si is chemically purified to SG-Si by thermal decomposition of trichlorosilane gas. As for the MG-Si process, SG-Si is also a very energy-demanding process. [8]

Then the purified silicon is melted together at a very high temperature before it enters a cooling process where large crystals of silicon are created. The next step is a solidification of the monocrystalline silicon where SG-Si is put in quart crucibles before it is melted in a furnace and cooled down. When the SG-Si is cold, it is cast into ingot blocks. The ingot is then sliced into thin dics, also called wafers. Then a metal conductor and layer of chosen chemical elements are added to the surface of the wafer. The chemical element can be a combination of boron and phosphorous. Then a PV cell is produced and can be collected together in order to create a Monocrystalline PV panel. A large share of the cells used to manufacture panels in Europe and America are imported from Asia Pacific and China, while the cells used in production in Asia Pacific and China are domestically produced. [25, 8, 51]

The next step is the production of solar grade silicon, single- and multi-crystalline silicon, single- and multi-crystalline silicon wafer, the PV cells and finally the PV panel. A large share of the cells used to manufacture panels in Europe and America are imported from Asia Pacific and China, while the cells used in production in Asia Pacific and China are domestically produced. The supply chain of silicon-based PV electricity production is shown in Figure 2.13. [25]

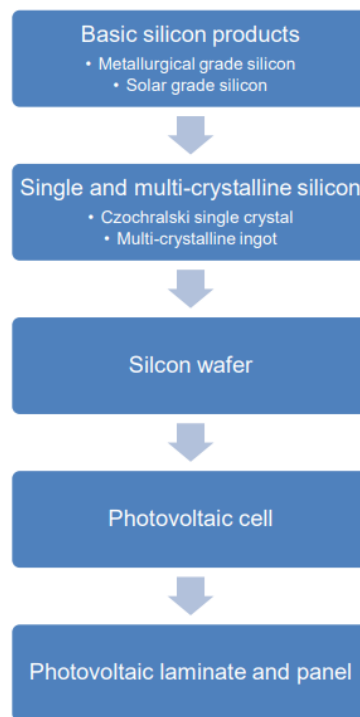


Figure 2.13: Supply chain of silicon-based PV electricity production. [25]

2.7.1 PV Module Recycling

The industry for the recycling of PV panels is growing, but still new. Researchers are exploring how to commercialize recycling to recover most of the components of PV panels economically. Solar panels and other components of solar power systems can be recycled in the glass, metal, and electronics industries. In this process, frames and junction boxes are typically removed before crushing, shredding, and milling are performed. The materials recovered from these processes, such as glass, aluminum, and copper, may be recycled, while the others, including silicon solar cells, may be incinerated. [94]

2.8 Land-Use Change

Half of man-made CO₂ emissions are absorbed by the sea and vegetation on land. Land-use change in these natural reservoirs and sinks of CO₂ will have a considerable impact on climate change in the future. The amount of emission from land-use change will vary depending on the type of area and several other factors, like the soil and vegetation. This section will mostly focus on land-use change from forest to settlement. [12]

2.8.1 Area Classifications

The AR5 classification system is a tool for systematic mapping and classification of land resources, focusing on the production potential for agriculture and forestry. It is the national classification system for utilization of land in Norway. First, it categorizes land area into type of area, and then the area is further classified based on site productivity, tree species and soil conditions, depending on the area type. AR5 is an abbreviation for area resource map in 1:5 000 scale. [61]

The area type forest is defined as an area with at least 6 trees per decaire which are or can become 5 meters in height, and are evenly divided throughout the area [61]. Forest is classified based on both tree species, site productivity and soil condition. Tree species have six characteristics: coniferous forest, mixed forest, deciduous forest, non-forested, not registered and not relevant. [3]

Site productivity is the area's capacity to produce wood. This property has seven characterizations: very high, high, medium, low, impediment, not registered and not relevant [3]. Corresponding production capacities per decaire and year are presented in Table 2.2.

Table 2.2: Site productivity [62]

Site productivity	Production capacity per decaire and year
Very high	$>1.0 \text{ m}^3$
High	$0.5 - 1.0 \text{ m}^3$
Medium	$0.3 - 0.5 \text{ m}^3$
Low	$0.1 - 0.3 \text{ m}^3$
Impediment	$<0.1 \text{ m}^3$

The last characterization for a forest is the soil condition. First after an area is classified as a forest, and has been given values for tree species and site productivity, the soil condition is to be decided. The area type forest may have the soil conditions organic soil and mineral soil. Organic soils are formed from sedimentation when organic matter is deposited more quickly than it can be decomposed. Mineral soils are formed from the weathering of rocks, and consist primarily of inorganic material. [27, 3]

The area type settlement includes buildings and areas that can be classified as technical interventions and surrounding developed area. This includes buildings, gardens, roads, parks, log landings, parking lots and gravel pits. A constructed area is an area where the soil is highly impacted by humans and very little biologically productive. Examples are quarry, gravel pits, and enclosures with gravel. Permanent construction areas can also be classified as constructed areas. Constructed areas fall under the area category settlements. [3]

2.8.2 Forest as a Carbon Storage

Forest play an important part in the carbon cycle. Trees pull carbon out of the atmosphere through the process of photosynthesis, bind it as sugar, and release oxygen. About 50% of tree trunks are made of carbon, which is sequestered in the forest until the tree decomposes and CO_2 is released back in the atmosphere. [10]

The amount and speed of carbon capture and storage depends on the age of the trees and the number of trees in the stand. Forests that are in their early stages of growth contain many trees and are highly effective at sequestering carbon. Due to their rapid growth, young trees can absorb carbon at a significant rate. There is high competition for light, resources and growing space. Not every sapling become large trees, but little carbon is released when they die and decompose. As the forest matures it will grow and store more carbon. Figure 2.14a shows a new-growth forest. [10]

Established or mature forests consist of "middle-aged trees", which are medium to large in size, healthy and with a large root system. Middle-aged trees have a slower growth rate compared to younger trees, but they have a greater capacity to sequester and store carbon. When large trees die, they are promptly replaced by younger trees seizing the opportunity to occupy the new space. As few trees are dying compared to those that are growing, the overall net productivity remains positive, leading to an increase in carbon capture. [10]

The carbon cycle within old-growth forests is relatively stable, or less dynamic. Large trees dominate and by shading impede the growth of small saplings, resulting in a low rate of recruitment of young trees and near-zero net productivity. Carbon is still well stored within the large trees, slowly decomposing logs, thick layers of leaf litter, and soil. Even though the large trees capture the same amount of carbon as middle-aged trees, the rate of carbon sequestration is a lot slower than in younger forests, due to the fewer number of trees in an old growth stand. Figure 2.14b shows a old-growth forest. [10]



(a) *New growth forest* [56]



(b) *Old growth forest* [11]

Figure 2.14: Forest

The main absorption of CO_2 takes place in the trees, but this is not where the largest carbon storage is found. The trees, with trunk, twigs and bark, account for approximately 10% of the forest's carbon stock. More than 60% of the forest ecosystem's carbon stocks are in the forest soil. The amount of stored carbon will vary depending on local factors such as local geology, soil type, and vegetation. Some soil types can bind up larger amounts of carbon than other soil types. Soils containing more organic material have a greater capacity to sequester carbon, as organic material itself is stored carbon and it has the ability to easily bind loose carbon molecules. Moreover, soils that are frozen for a significant part of the year or have shallow groundwater can also store large quantities of carbon, as decomposition processes are slower in these environments. [12, 10]

Other than CO_2 , methane (CH_4) and nitrous oxide (N_2O) are important greenhouse gases listed in the Kyoto protocol that require emission reduction. These greenhouse gases are also influenced by the management of Norwegian forests. Dead trees emit CH_4 and N_2O as well as CO_2 . However, the absorption of CO_2 is higher than the emission of CO_2 , CH_4 and N_2O , and forests will have net absorption, meaning the carbon storage in forest will increase over time. [86]

In addition to forest, bogs are a type of area that serve as huge carbon sinks. Bog is a type of wetland, meaning areas that are flooded and filled with water for part of the year, and also have drier periods where the water recedes or dries up. Plants that die in the bog sink into

the water and form deep layers of peat, and the bog can sequester these organic matters for thousands of years. According to the Norwegian Institute of Bioeconomy Research (NIBIO), the total amount of carbon in bogs worldwide is roughly the same as in the atmosphere. Norwegian bogs, covering around 5% of Norway’s land area, store at least 950 million tons of carbon. This is equivalent to approximately 3 500 million tons of CO₂, or Norway’s annual greenhouse gas emission for 66 years. [53, 60]

2.8.3 Emission from Land-Use Change

Land-use change is a considerable source for greenhouse gas emissions, and the largest cause for loss of biodiversity. Especially change from carbon-rich areas such as forest, bog, cropland and pasture to settlement is a large cause for emissions. Also change from forest and bog, which are very carbon-rich, to less carbon-rich areas such as cropland and pasture, causes emissions. Land-use change can also cause absorption of greenhouse gases, for example reforestation and change from settlement to other area categories (e.g. removal of roads to restore original area). According to numbers from the Norwegian Environment Agency, land-use change causes around 1.9 million ton CO₂-equivalents every year (2022). [47]

The various area categories have a corresponding emission factor that is used to calculate the emissions from land-use change of that specific area type. Table 2.3 shows the emission factors per decare for change from forest of high, medium and low site productivity and bog to settlement. The emission factors include decomposition of living biomass, dead organic matter and soil as a result of land-use change, as well as lost absorption for 75 years. The emission factors in Table 2.3 are based on the National Inventory Report for greenhouse gas emissions by the Norwegian Environment Agency from 2022.

Table 2.3: Emission factors for land degradation (NIR2022). [47]

Type of area		Emission factor [ton CO ₂ -eqv/decar]	
		Area with mineral soil	Area with organic soil
Forest	Low site productivity	60	169
	Medium site productivity	71	182
	High site productivity	84	194
Bog		-	337

Table 2.3 shows that areas with organic soil have significantly higher emission factors than areas with mineral soil. Bog, which consists only of organic soil, have a very high emission factor, even compared to forest with organic soil. There are some uncertainties when it comes to emission factors, especially for soil, as collecting soil samples is expensive and it often takes a long time before changes in soil carbon are seen [96]. However, it is clear that drainage of bog will have significantly higher emissions from the soil compared to forest. If the bog is already drained, the difference between organic and mineral soil will lessen. [47]

Emissions from land-use change will depend on the type of area affected and how they are affected. The greenhouse gas account for the land-use sector is based on the methodology of the UN climate panel, where one reports the annual man-made emissions and absorption from the six land-use categories forest, cultivated land, pasture, water and bog, settlement and other open land, as well as changes in carbon stocks in wood products. In addition, the emissions

and absorption that occur when transitioning between the various area categories are reported. When a forest is built down and the area changes from forest to settlement, there will be reported an emission both from the trees that are cut down and from the carbon sequestered in the soil. When calculating emissions from areas and land-use changes, the general formula used is shown in Equation 2.10. [96]

$$\text{Emission} = \text{Size of area} \cdot \text{Emission factor} \cdot \text{Years} \quad (2.10)$$

Where

Emission	[CO ₂ -eq]
Size of area	[hectare]
Emission factor	[ton CO ₂ -eq/hectare/year]
Years	[year]

The emission factors used in land-use change the last years are from the V712 handbook (2018), but the Norwegian Environment Agency has recently updated these emission factors in National Inventory Report from 2022 (NIR2022). Some of the emission factors from V712 and NIR2022 are presented in Table 2.4. The change in emission factors for forests are very small. The biggest change is in the emission factor for bog, which has increased from 201.9 to 337. [47]

Table 2.4: Emission factors from the V712 handbook and the newer emission factors from NIR2022.

	V712	NIR2022
Forest	Low site productivity	60.4
	Medium site productivity	68.7
	High site productivity	80.3
Bog	201.9	337.0

The first year of the transition phase will have the largest emissions, as removal of biomass have a lot of instant emission. Emission from the soil is calculated over 20 years, since it is assumed that the amount of carbon in the soil is stabilised 20 years after the land-use change. One can look at separate emission factors for the first year of the transition phase and the next 19 years. To estimate emissions for a longer period than the transition phase of 20 years, there is a separate emission factor for the area after 20 years. Because the emissions from the soil have stabilised, the emissions will be a lot smaller after 20 years. [54]

When estimating the total absorption and emission from a land-use change, the loss of absorption from if the land-use change had not happened is also included in the calculations. This value is also found with Equation 2.10, using a separate emission factor for the area if there is no land-use change and the area is left alone. This emission factor is the same for all years of the transition phase, and can be multiplied by any number of years one want to look at. A difference between the emission factors from the V712 handbook and NIR2022 is that V712 only looks at 20 years, while the factors from NIR2022 calculates lost emission from a period of 75 years. [54]

2.9 Area and Energy

Development of renewable energy generation and the power grid requires a considerable amount of area. Ground-mounted solar power is making its way into the Norwegian power system. These power parks can be everything from a few dozens decare to several square kilometers in area size. Solar power parks are often planned in forest areas, and in those cases the forest must be cut down. In some cases, the area is planned to be used as pasture as well, and thus a land-use change from forest to infield pasture. In these cases, there might be a considerable carbon loss from the forest and soil, as well as lost future carbon absorption, compared to the greenhouse gas emissions from other renewable power generation. The total climate benefit can still be high, even when the solar park is placed in forest areas. Solar parks can also be built on abandoned farmland or other already developed areas. Building in these areas would have less greenhouse gas emission compared to building in forest. [47]

Wind turbines are often placed on ridges and hills with good wind conditions and relatively poor soil. The turbines with foundations and roads can therefore cause large greenhouse gas emission from land-use change. The road network constitutes to around 80-90% of the utilized area in a wind farm, and the roads are therefore the land-use that most often come in conflict with carbon-rich soils. However, in many cases the roads can be placed relatively freely in the terrain, and the most carbon-rich areas can be avoided where it is possible. [47]

Norway's potential for water power is already mostly developed or protected, and many new power stations with big regulation reservoirs are unlikely. Nevertheless, there is still a relatively big potential for smaller hydro power plants, as well as extensions of already existing power plants. Development of water power can lead to greenhouse gas emissions by damming of new area or if the roads are built on carbon-rich areas. [47]

The Norwegian Environment Agency have recently analyzed the possibilities for emission cuts in land-based industry, energy supply and the petroleum sector. In their report from 2022 [26] it is estimated that 24 TWh new renewable energy is needed towards 2030 for these sectors. 1 TWh wind power corresponds to a planned area of around 35 km². Within this area, the direct interventions (before revegetation) amount to approximately 1.6 km². 1 TWh ground-mounted solar power is roughly estimated to use an area of 10 km². The amount of area required for water power varies, and depends on if for example regulating reservoirs are a part of the equation. For solar and wind power to cover the power demand of 24 TWh alone, it would require a land-use of 100 - 150 km². Development to this extent by 2030 would be challenging based on the time needed for licence processing and execution of the project. [47]

Ground-mounted solar power in areas with forest stands out as the renewable production with the largest greenhouse gas emission. At the same time, it will be demanding to achieve all the power production needed to reach the climate goals, and solar parks can rapidly prove large volumes of new energy by 2030. If additional limitations are placed on land-use compared to today's licence practice, this can have huge consequences for the realistic production potential and therefore also the climate goals for other sectors than land-use. [47]

3 Methodology

This chapter explains the different cases relevant to the thesis. In addition, the methodology for the LCA, land-use change calculations and simulations in PVsyst will be outlined. Lastly, the method for assembling the data from all calculations to find the ratio between emission and production is described. All assumptions done in the thesis are also presented in this chapter.

3.1 Case Study

In the following section, the six different cases will be described and presented. The cases are given by Aneo. To better understand the cases, Table 3.1 presents and visualizes the main parameters and data for each case. All six cases have some values and data in common. These values are the area for each case, which is shaped as a rectangle and covers 300 000 m². It is located in a relatively flat area in Halden in the southeast part of Norway and has a solar radiation of 950-1100 kWh/kWp. The bifacial solar panel JA-solar 550 Wp and the Huawei 160 kW inverter are used in all six cases, the panel is presented in Appendix A.

Table 3.1: Illustration of the different cases.

Type of area	Pitch	
	8 meter	15 meter
Constructed area	A	B
Forest with low site productivity	C	D
Forest with high site productivity	E	F

As seen in Table 3.1, all six cases are given a letter to assure clarity throughout the thesis. Case A and B examine constructed areas with a pitch of 8 meters and 15 meters respectively. For Case C and D the type of area is forest with low site productivity, where C considers a pitch of 8 meters and D 15 meters. The last type of area is forest with high site productivity. Within this area, Case E involves a pitch of 8 meters and Case F has 15 meters.

In addition to the presented six cases, which are the main focus of the thesis, a supplement was made. Further six simulations were done in order to find the optimal pitch by looking at CO₂ emissions and energy production within the different types of area. The pitch varies from 8 to 15 meters, with one meter in between. The method used to find these results are based on the same principles and methodology as for the presented six cases above. These simulations will only be outlined in the sections where the ratio between the production and emissions is presented and analyzed.

3.2 Life Cycle Assessment

This LCA follows the International Standards Organization (ISO) standards 14040 and 14044. The 14040 standard cover principles and framework for an LCA study, and 14044 represents requirements and guidelines for the analysis. In addition, both standards describe the limitations, reporting, critical view and relationship between the different parts of an LCA. The parts are goal and scope, the life cycle inventory phase (LCI), the life cycle impact assessment phase (LCIA) and the interpretation phase. [34, 33]

The analysis is a cradle-to-grave study that considers the total impact for each step of the PV panels life cycle, from raw material extraction and the process through manufacturing, transportation, product use, and finally disposal or recycling [2]. Only the impact of the solar panel is calculated. Other PV system components such as inverters, wirings, and transformers are excluded from the analysis. Within every life cycle step, the total CO₂ emissions will be calculated and analyzed. The PV panel used in this study is JA-solar 550 Wp. This panel has mono-crystalline cells and is bifacial with glass on both the rear and back sides.

3.2.1 SimaPro

SimaPro 9.4.0.2 Multi user was utilized in this thesis for data collection and calculations of impact for the solar panels. SimaPro is an LCA software utilized by companies, consultancies and universities all over the world. The software builds complex models from a life cycle perspective, and can be used to determine the environmental impact of products and services through all life cycle stages, from extraction of raw materials to manufacturing, distribution, use, and disposal. [85]

There are several inbuilt models in SimaPro. One of the most used methodologies in SimaPro is the IMPACT2002+ method, which looks at 15 midpoint categories. Another methodology is the IPCC 2013 GWP100 methodology and its successor IPCC 2021 GWP100. The method is developed by a wide range of researchers on climate change and experts from IPCC within climate assessment. For Global warming potential (GWP) there is implemented different time horizons such as 20 years, 100 years and 500 years. They are based on the energy absorbed by a gas over the time horizons. The GWP100 is recommended as a default [66]. The method used in this LCA is IPCC 2013 GWP100. [95, 66, 29, 93]

3.2.2 Goal and Scope

The first part of the LCA, according to the ISO 14040 and 14044 standards, is to define the goal and scope for the study [35]. Referring to the SDG goals, the Paris Agreement and the IPCC climate reports outlined in Section 1, there is a high demand related to the production of sustainable energy, such as solar power. Although solar panels produce clean energy, the production process and transport requires energy and resources, which can cause emissions and other negative climate- and environmental impacts. Based on this the main goal of this study is to calculate the CO₂ emissions of one bifacial monocrystalline PV panel from raw materials to recycling. As the analysis will present the emissions for the life cycle process, it will be interesting to examine the process or material that contributes the most CO₂ emission in the production chain, and how these can be reduced.

The intended audience of this LCA study is mainly the project contributor Aneo. As the thesis will be published online, the results from the analysis are also available to the public. The analysis can give an indication of what should be prioritized in future PV panel development and production. In addition, it is important to clarify the fact that the main focus of the analysis is not the science behind PV production itself.

Within the scope part of the analysis the functional unit, impact category and system boundary will be outlined. The functional unit is one of the key elements in an LCA study and is used as a reference unit when the inputs and outputs of the analysis are calculated. It describes a quantity of a product or a product system on the basis of the performance it delivers in its

end-use application. The functional unit in this LCA is 1 m² and 1 kg of ground-mounted PV panel. 1 m² is the functional unit for the production and mounting of the PV panels, while 1 kg is the functional unit for the recycling of the panels. Considering the active area and mass of the PV panels vary based on the pitch, these functional units will be useful for a comparison of the results.

The impact category indicates which type of environmental impacts the analysis will focus on. The endpoint impact category used in this LCA is climate change. This endpoint impact category includes the midpoint category global warming. These categories are chosen because they look at greenhouse gas emission, which is the focus of this thesis. Additionally, non-renewable energy is used in transportation and parts of production. These factors are highly dependent on the energy mix in the specific country. Transportation and production of PV panels contribute to greenhouse gas emissions, thereby global warming.

According to ISO 14040, the system boundary specifies which unit processes are included in the study [34]. All processes that could have an impact on the environment and emissions should be included. The system boundary for this LCA is cradle-to-grave. This was chosen based on available information, and in order to give a correct overview and measure of the total CO₂ emissions generated for the PV panels. Emissions related to the operation step including maintenance (cleaning) of the PV panels are not included in this analysis. Sources indicate that this part of the life cycle does not emit CO₂ emissions [87]. The system boundary is shown in Figure 3.1 and include all the inputs and outputs in the PV panels life cycle, from raw material acquisition and pre-processing to end-of-life treatment.

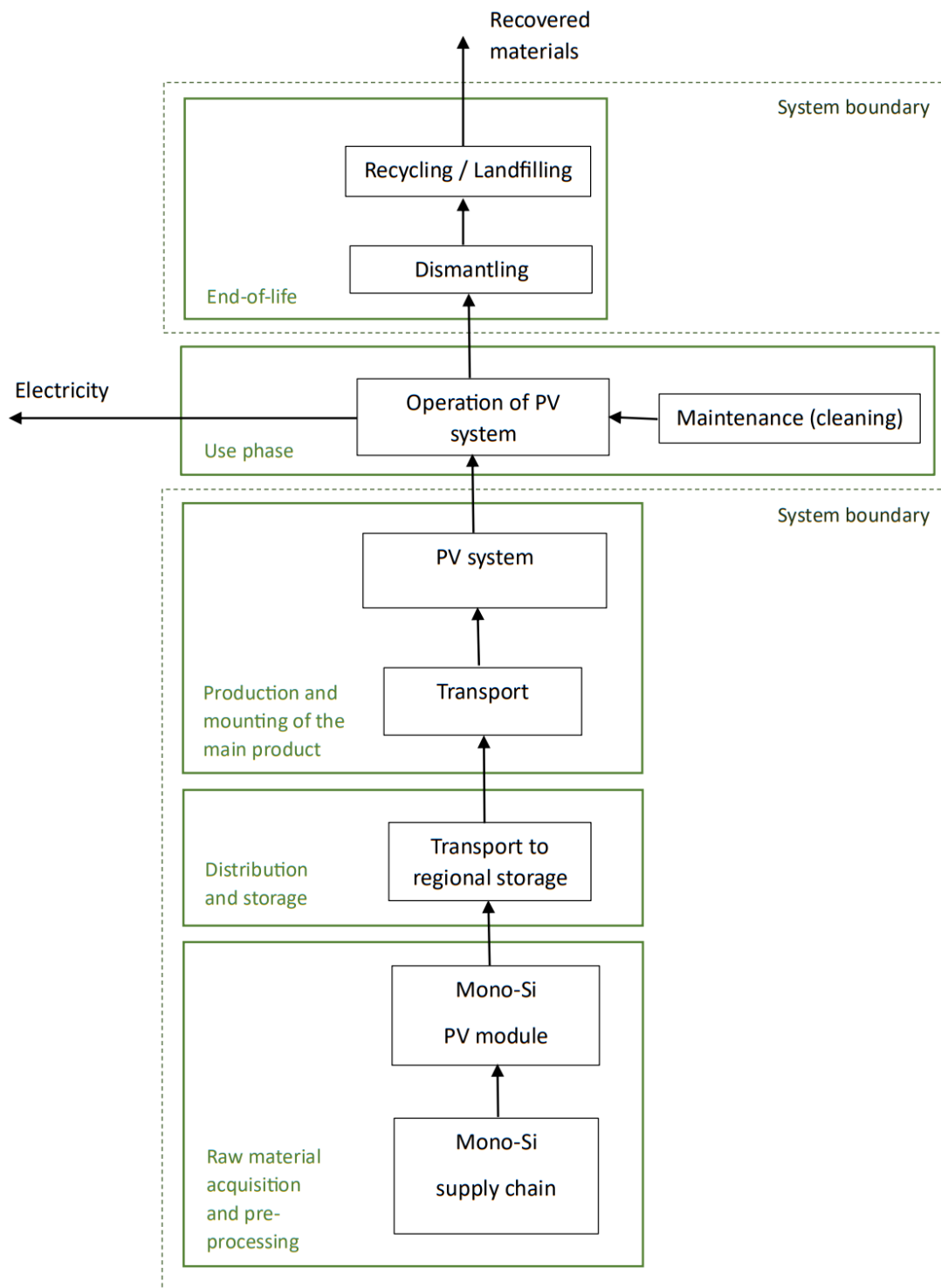


Figure 3.1: System boundary for the LCA.

3.2.3 Life Cycle Inventory

The life cycle inventory is the second phase in an LCA study, and is described in ISO 14040. In this phase a compilation and quantification of inputs and outputs of the PV panel is outlined. This includes transportation, materials and energy which all are relevant steps in order to produce a PV panel. This section begins with a description of the assumptions for the analysis, before the inventory lists are presented. [34]

In order to complete the LCA calculations in SimaPro, several assumptions were made. The PV panel used in this analysis is JA-solar 550 Wp. A more detailed datasheet with information and technical specifications of the panel is presented in Appendix A. In total there are 144 mono-crystalline cells collected into a bifacial panel with double glass.

Assumptions related to the analysis of the production of the monocrystalline PV panel are:

- The PV panels are produced in China, as JA-Solar have many of their production sites there.
- The backsheet in monofacial PV panels can be replaced by glass or a transparent backsheet to get a bifacial PV panel [45].
- The materials in the backsheet are included for the first time in the inventory list for the production of the PV panel.

Today's globalization and international society have resulted in a great global flow of raw materials and resources. The flow is often controlled by politics and economics. More specifically, where it is suitable and economically beneficial for raw material extraction and production. This also applies to the production of PV panels. As a result, transport is an important factor that must be included in the LCA analysis in order to give a correct result. The different assumptions made for transport for the whole system boundary are listed below:

- All transport needed within the processes of producing the PV panel, the mounting of the PV panel and the recycling of the PV panel is included in the inventory lists.
- All transport between countries will take place by ship.
- It only takes one ship to transport all the panels. The transport is the same regardless of the number of panels.
- The materials recovered in treatment of used PV panels are transported by ship to the recycling site.

Assumptions regarding the mounting of the PV panels are:

- The mounting process is similar in Norway and Switzerland, at Mont Soleil.
- The system has a concrete foundation and the structure is made of steel.

Assumptions concerning the recycling of PV panels are:

- The panels are treated in a first generation recycling process.
- The materials are glass cullets, aluminum scrap and copper scrap recovered from c-Si module treatment.

The inventory list for this LCA study is based on a report by The International Energy Agency's Photovoltaic Power Systems Programme (IEA PVPS). The report is called *Life Cycle Inventories and Life Cycle Assessment of Photovoltaic Systems* [25], and was released in 2020. This report is a part of IEAs task 12, PV Sustainability Activities, and gives the latest life cycle inventories among PV LCA experts in North America, Europe, Asia and Australia. In the report, there are life cycle inventories for mono- and multicrystalline silicon, CdTe, CIGS and perovskite silicon tandem solar cells. The report covers manufacturing in Europe, China, North America, Asia and the Pacific. This report was chosen as it gives the latest life cycle inventories. The lack of an inventory list for bifacial panels is made up for by the fact that the back of the monofacial panel can be replaced with glass like the front of the panel [45]. [25]

The inventory list was based on the inventory list for monocrystalline silicon, ground-mount PV mounting systems and end-of-life treatment of crystalline silicon (c-Si) PV modules in the IEA PVPS report. The inventory lists from the report includes product, materials, auxiliaries, energy, infrastructure, transport, disposal, resources and emissions for the various processes. The inventory lists from the report that are used in this thesis are presented in Appendix B.

Table 3.2 shows the inventory list for the production of 1 m² PV panels. This inventory list is similar to Table 19 in the IEA PVPS report. The only difference is the removal of the materials used in the backsheet. In addition, materials of one more front glass were added to the analysis in order to get a bifacial panel. A doubling of the glass makes up for the back side of the panel. The PV cell is called a Photovoltaic cell, single-Si. The production and processes leading up to this cell have the same inventory list as Table 6-10, 12 and 16 in the IEA PVPS report. The inventory lists for the panel and the cell include all needed transport. The panels are assumed produced in China, so the inventory lists from the report are the ones with production in China.

Table 3.2: Inventory list for the production of 1 m² PV panels.

	PV panel production in China	Amount	Unit
Product	Outputs photovoltaic panel, single-Si	1	m2
Materials	Inputs Photovoltaic cell, single-Si	9.35E-1	m2
	Aluminum alloy, AlMg3	2.13E+0	kg
	Copper	1.03E-1	kg
	Wire drawing	1.03E-1	kg
	Diode	2.81E-3	kg
	Silicone product	1.22E-1	kg
	Tin	1.29E-2	kg
	Lead	7.25E-4	kg
	Solar glass, low-iron	1.76E+1	kg
	Tempering, flat glass	1.76E+1	kg
	Glass fibre reinforced plastic, polyamide, injection moulding	2.95E-1	kg
Auxiliaries	Tap water	5.03E+0	kg
	Hydrogen fluoride	6.24E-2	kg
	1-propano	1.59E-2	kg
	Isopropano	1.47E-4	kg
	Potassium hydroxide	5.14E-2	kg
	Soap	1.16E-2	kg
	Corrugated board, mixed fibre	7.63E-1	kg
	EUR-flat pallet	5.00E-2	unit
Energy	Electricity, medium voltage	1.40E+1	kWh
	Diesel, burned in building machine	8.75E-3	MJ
Infrastructure	Photovoltaic panel factory	4.00E-6	unit
Transport	Transport, freight, lorry, fleet average	2.77E+0	tkm
	Transport, freight, rail	1.66E+1	tkm
Disposal	Municipal solid waste, 22.9% water, to municipal incineration	3.00E-2	kg
	Polyvinylfluoride, 0.2% water, to municipal incineration	4.29E-3	kg
	Plastics, mixture, 15.3% water, to municipal incineration	2.81E-2	kg
	Used mineral oil, 10% water, to hazardous waste incineration	1.61E-3	kg
Resources	Transformation, from pasture and meadow	4.72E+0	kg
	Transformation, to industrial area, built up	1.50E+0	kg
	Transformation, to industrial area, vegetation	3.22E+0	kg
	Sewage, from residence, to wastewater treatment, class 2	4.53E-3	m3
Emissions air	Heat, waste	5.03E+1	MJ
	NMVOC, non-methane volatile organic compounds, unspecified orgin	8.06E-3	kg
	Carbon dioxide, fossil	2.18E-2	kg
	Water, CN	5.03E-1	kg

Table 3.3 shows the inventory list for the transport of all the PV panels to Halden in Norway. The IEA PVS report uses transoceanic ships for the transoceanic transports, but these ships are obsolete in SimaPro. Because of this, container ships were chosen as they are the main ship type for commodities exported from China [4]. Transoceanic ships and container ships are both intended to transport large quantities. The distance from Nanjing, a port in China, to Halden is estimated to be 12 679 nautical miles by ship [64].

Table 3.3: Inventory list for the transport of all the PV panels to Halden in Norway.

Transport of the panels	Amount	Unit
Outputs		
Transport to Halden	1	unit
Inputs		
Transport, freight, sea, container ship	23481.506	tkm

Table 3.4 shows the inventory list for the mounting of 1 m² PV panel. This inventory list is the same as Table 36, Unit process LCI data of ground-mount PV mounting systems, in the IEA PVPS report. The mounting structure used in the IEA PVS report is based on the mounting structure at the Mont Soleil installation presented in another report from 2012 [38]. The data from this report has a functional unit of 1 m² and includes materials, packaging, and transport of mounting structures and disposal of packaging materials. In the report from 2012 it is stated that the amount of materials may vary depending on the panel size and location of the solar park. For example, larger panels will require less material per square meter. [38]

Table 3.4: Inventory list for 1 the mounting of 1 m² PV panel.

	Ground-mount PV mounting systems	Amount	Unit
	Outputs		
Product	Open ground construction	1	m2
Materials	Gravel, round	350	kg
	Zinc, primary	3	kg
	Inputs		
	Concrete, normal	2.05E-2	m3
	Reinforcing steel	3.95E+1	kg
	Steel, low-alloyed	2.51E+0	kg
	Particleboard, average glue mix, uncoated	9.98E-4	m3
	Roof tile	5.41E-1	kg
	Polyurethane, flexible foam	9.94E-2	kg
	Zinc coating	1.83E-1	m3
	Polyethylene, HDPE, granulate	4.17E-2	kg
	Acetone, liquid	4.57E-2	kg
	polyvinylchloride	1.11E-2	kg
	Bitumen	2.03E-2	kg
	Rock wool	1.92E-2	kg
	Flat glass, coated	7.21E-3	kg
	Acrylic binder	5.20E-3	kg
	Silicone product	4.79E-2	kg
Transport	Transport, freight, lorry 7.5-16 metric ton	9.45E+0	tkm
	Transport, freight, lorry 16-32 metric ton	2.95E+0	tkm
Disposal	Concrete, 5% water, to inert material landfill	4.87E+1	kg
	Building, reinforcement steel, to sorting plant	3.95E+1	kg
	Building, fibre board, to final disposa	6.79E-1	kg
	Building, polyurethane foam, to final disposal	9.94E-2	kg
	Building, polyethylene/polypropylene products, to final disposal	4.17E-2	kg
	Building, polyethylene/polypropylene products, to final disposal	1.11E-2	kg
	Building, polyvinylchloride products, to final disposal	1.11E-2	kg
	Building, mineral wool, to sorting plant	1.92E-2	kg
	Building, glass pane (in burnable frame), to sorting plant	7.21E-3	kg
	Resources	Transformation, from pasture and meadow	4.72E+0
	Transformation, to industrial area, built up	1.50E+0	m2
	Transformation, to industrial area, vegetation	3.22E+0	m2
	Occupation, industrial area, built up	4.50E+1	m2a
	Occupation, industrial area, vegetation	9.67E+1	m2a
Emission	Acetone	4.57E-2	kg

Table 3.5 shows the inventory list for the treatment of 1 kg used c-Si PV panel. Table 3.6 shows the inventory list for 1 kg glass cullets recovered from c-Si PV panel treatment. Table 3.7 shows the inventory list for 1 kg aluminum scrap recovered from c-Si PV panel treatment. Table 3.8 shows the inventory list for 1 kg copper scraps recovered from c-Si PV panel treatment. These four inventory lists are the same as Table 29 in the IEA PVPS report, and together they are the inventory for c-Si module recycling in Western Europe.

Table 3.5: Inventory list for the treatment of 1 kg c-Si PV module.

	Treatment of used c-Si PV modules	Amount	Unit
Product	Outputs Treatment, c-Si PV module	1	kg
Technosphere	Inputs Electricity, medium voltage, production ENTSO	5.56E-2	kWh
	Diesel, burned in building machine	3.24E-2	MJ
	Disposal, plastics, mixture, 15.3% water, to municipal incineration	7.34E-2	kg
	Disposal, plastics, mixture, 15.3% water, to sanitary landfill	1.28E-2	kg
	Transport, freight, lorry 3.5-7.5 metric ton, EURO 5	5.00E-2	tkm
	Transport, freight, lorry, fleet average	2.00E-1	tkm

Table 3.6: Inventory list for 1 kg glass cullets recovered from c-Si PV module treatment.

	Recovered glass cullets	Amount	Unit
Product	Outputs Glass cullets, recovered from c-Si PV module treatment	1	kg
Technosphere	treatment Electricity, medium voltage, production ENTSO	4.05E-3	kWh
	Diesel, burned in building machine	2.36E-3	MJ
	Disposal, plastics, mixture, 15.3% water, to municipal incineration	5.34E-3	kg
	Disposal, plastics, mixture, 15.3% water, to sanitary landfill	9.33E-4	kg
	Transport, freight, lorry 3.5-7.5 metric ton, EURO 5	3.64E-3	tkm
	Transport, freight, lorry, fleet average	3.64E-3	tkm

Table 3.7: Inventory list for 1 kg aluminum scrap recovered from c-Si PV module treatment.

	Recovered aluminum scrap	Amount	Unit
Product	Outputs aluminum scrap, recovered from c-Si PV module treatment	1	kg
Technosphere	treatment Electricity, medium voltage, production ENTSO	1.42E-1	kWh
	Diesel, burned in building machine	8.25E-2	MJ
	Disposal, plastics, mixture, 15.3% water, to municipal incineration	1.87E-1	kg
	Disposal, plastics, mixture, 15.3% water, to sanitary landfill	3.26E-2	kg
	Transport, freight, lorry 3.5-7.5 metric ton, EURO 5	1.27E-1	tkm
	Transport, freight, lorry, fleet average	2 5.09E-1	tkm

Table 3.8: Inventory list for 1 kg copper scrap recovered from c-Si PV module treatment.

	Recovered copper scrap	Amount	Unit
Product	Outputs		
	Copper scrap, recovered from c-Si PV module treatment	1	kg
Technosphere	treatment		
	Electricity, medium voltage, production ENTSO	8.09E-1	kWh
	Diesel, burned in building machine	4.71E-1	MJ
	Disposal, plastics, mixture, 15.3% water, to municipal incineration	1.07E+0	kg
	Disposal, plastics, mixture, 15.3% water, to sanitary landfill	1.87E-1	kg
	Transport, freight, lorry 3.5-7.5 metric ton, EURO 5	7.27E-1	tkm
	Transport, freight, lorry, fleet average	2.91E+0	tkm

Table 3.5, 3.6, 3.7 and 3.8 have four separate values for the same recycling process. In order to calculate the total amount of the CO₂-equivalents from the used PV panels, all the values were adopted to fit one panel, then added together. This was done based on the total amount of the recovered materials used in one panel, and the emissions from the recovery of these materials. The calculations are shown in Appendix C. The parameters of the PV panel used in the calculations are presented in Table 3.9 [36]. The other values used for these calculations are from the IEA PVPS report. They are the total amount of aluminum per m², the total amount of copper per m² and the total amount of glass per m².

Table 3.9: Parameters for JA-solars 550 Wp panel.

Parameters JA-solar 550 Wp	
Length [m]	2.278
Width [m]	1.134
Mass [kg]	31.8

3.3 Land-Use Change

The Norwegian Environment Agency has published a spreadsheet in Microsoft Excel that can be used to calculate emissions from land-use change. This spreadsheet has been used as recommended by an expert from the Norwegian Environment Agency. The agency is a governmental organization part of the Ministry of Climate and the Environment, and works towards several environmental aspects such as reducing greenhouse gas emissions and pollution, as well as managing Norwegian nature [55]. They have recently made a new and updated spreadsheet to estimate greenhouse gas emissions from land-use change, but this spreadsheet is still for consultation. As the biggest change is in emission factors for bog and organic soil, and emission factors for forest with mineral soil remains more or less the same, it was decided that for this thesis it would be acceptable to use the older version. However, it should be noted that if one is looking at land-use change for bog or organic soil, the Excel spreadsheet used for this thesis is outdated.

All inputs used in the calculations in the spreadsheet in Excel are presented in Table 3.10. These inputs apply for calculating emissions for land-use change from forest with high or low site productivity to settlement. Coniferous forest was chosen as this is the dominant tree species around Halden [59]. Mineral soil was chosen as this is the soil type usually used if the specific area is not determined. When the area is determined, the soil type of the area can be found in NIBIO’s map with area information, called *Kilden* [59].

Table 3.10: Inputs in the Excel spreadsheet for calculating emissions for land-use change from forest with low or high site productivity to settlement.

Inputs	
Municipality	Halden
Number of area categories	1
Area category before change	Forest
Size of area (decar)	300
Tree species	Coniferous forest
Site productivity	High / low
Soil	Mineral soil
Area category after change	Settlement

The Excel spreadsheet looks at area change over 20 years. As the lifespan of the solar park is assumed to be 30 years, the results from the Excel spreadsheet have been adapted to 30 years. The emission and absorption if there is no land-use change is divided by 20 years, and then multiplied with 30 years to get the correct value. The soil is assumed settlement 20 years after the change, so the same method can not be used for the value for emission if there is a land-use change. Instead, a separate emission factor for the area after the transition phase of 20 years is used to calculate the emission for the last ten operational years of the solar park. This emission factor is much lower, as the emissions from the soil are assumed to stabilize after 20 years. The value from the ten last years was then added to the value for 20 years, which could be extracted from the Excel spreadsheet.

All emission factors used in the calculations in the Excel spreadsheet for land-use change from forest to settlement are presented in Table 3.11. Positive emission factors indicate there is an emission, and negative emission factors mean there is an absorption. The calculations are based on Equation 2.10, presented in Chapter 2.8.3. With the adaption to 30 years, Equation 3.1 is used. The calculations are attached in Appendix D.

$$\text{Emission} = \text{Size} \cdot (E_2 \cdot 1 \text{ year} + E_3 \cdot 19 \text{ years} + E_4 \cdot 10 \text{ years}) \quad (3.1)$$

Where:

Size = Size of area	[hectare]
E_2 = Emission factor for the first year of the transition	[ton CO ₂ -eq/hectare/year]
E_3 = Emission factor for the next 19 years of the transition	[ton CO ₂ -eq/hectare/year]
E_4 = Emission factor for the area after 20 years	[ton CO ₂ -eq/hectare/year]

Table 3.11: Emission factors used in the Excel spreadsheet. [54]

Emission factors <i>[ton CO₂-eq/hectare/year]</i>		
Change from forest to settlement	Low site productivity	High site productivity
If there is no change in the area (E_1)	-3.3	-3.7
For the first year of the transition (E_2)	39.78	57.66
Per year for the next 19 years of transition (E_3)	14.19	14.19
For the area after the transition phase (E_4)	1.33	1.33

In Cases A and B, where the solar park is built on a constructed area, it is not possible to calculate emissions from land-use change, as a constructed area is classified as settlement and therefore there is no change according to the classifications [54]. Because of this, all emissions are assumed to be zero in these cases.

3.4 PVsyst

The simulation program, Pvsyst student version 7.3.3, was used to get simulation data and estimate the solar energy production for the different cases with respect to pitch and the albedo value for the three types of area. This software tool was chosen based on recommendations and preferences from the managing directors at Aneo.

PVsyst is one of the leading software tools for studying, sizing, simulation and data analysis of PV systems. The software offers different solar energy tools, meteorological data sources and PV system components databases related to design and simulations for both grid-connected and stand-alone PV systems [68, 78]. The total time interval for the simulations was set to one year of solar energy production.

3.4.1 Geographical Site

The geographical site for all the simulations was a location near Halden in the southeast part of Norway. Close to Halden, it was chosen a flat and open area with solar radiation of approximately 950-1100 kWh/kWp, in accordance to Aneo's requirements. In order to find a relatively flat area, Norgeskart was used. Figure 3.2 shows the chosen area of 300 000 m² west of the main center in Halden. The coordinates for this area are presented in Table 3.12. This specific location is only used in PVsyst. For the rest of the thesis, an unspecified location close to Halden is used.

Table 3.12: Geographical parameters for the chosen location in Halden.

Geographical information	Value
Latitude [°]	59
Longitude [°]	11
Altitude [m]	48

Meteonorm, version 8.1, is a software providing solar data based on a total of 8 325 different weather stations located around the world. This Meteonorm database is available in PVsyst, and was used to collect data needed to simulate the PV production for all cases. As a result, all the cases will be simulated based on the same weather and solar conditions. This was done in

3 METHODOLOGY

order to make it possible to compare the results for the different cases. The coordinates for the geographical site location from Norgeskart were used to define the site location in PVsyst.

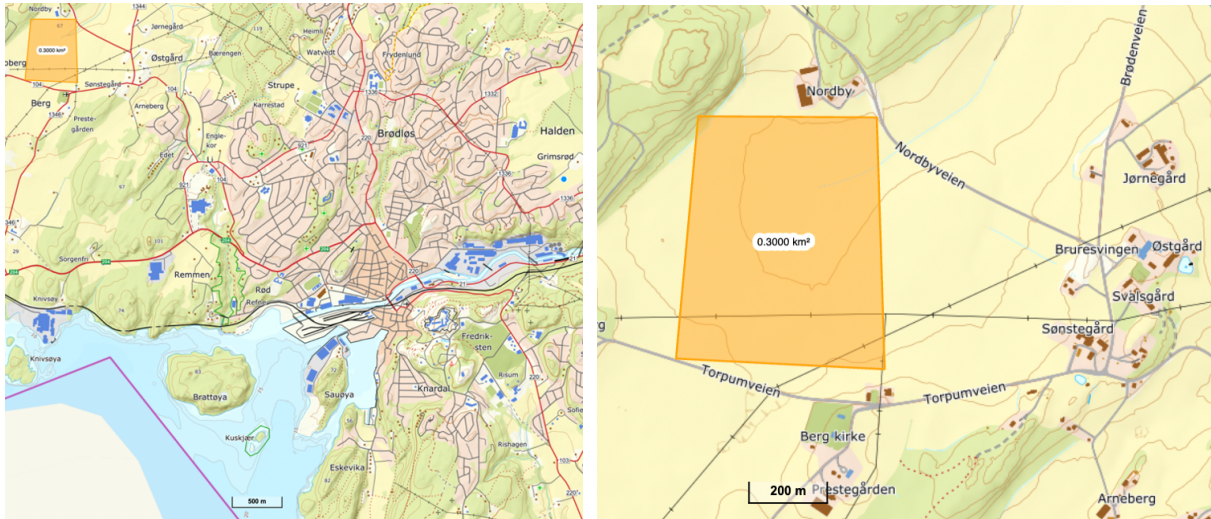


Figure 3.2: Maps of the chosen area in Halden.

The coordinates were also used to load the horizon for this location into PVsyst. The horizon and the sun height for the chosen location are shown in Figure 3.3. The red line shows the horizon facing south. The yellow shows the sun height at different hours of the day in the various months. The horizon is the same for all cases as the solar park is located at the same site in Halden.

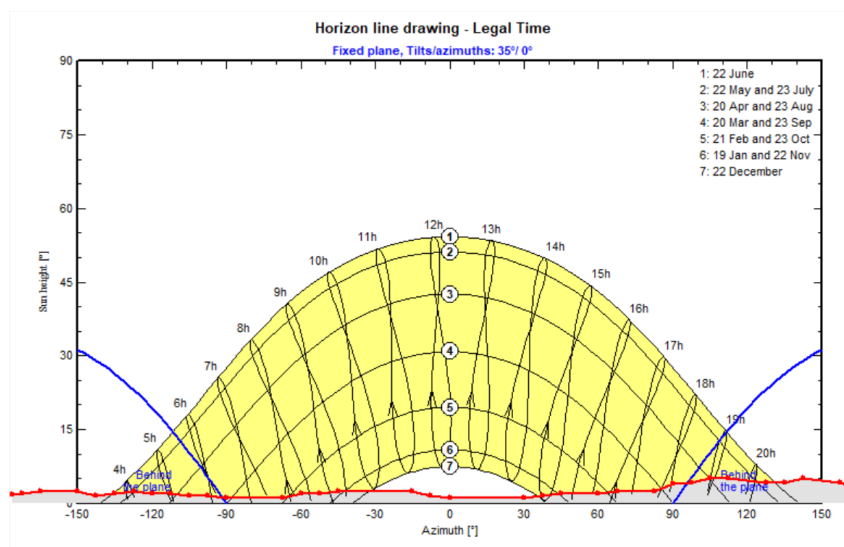


Figure 3.3: Horizon in PVsyst for the chosen location in Halden.

3.4.2 Orientation

Once the location and site were registered and selected, the first step in the actual design was to select the orientation of the PV system. PVsyst has three main categories within field types, with several underlying specific alternatives. They are fixed orientation planes, one-axis tracking planes and two-axis tracking planes. Within fixed orientation planes, fixed tilt plane was selected

as the field type. This setting was set as it was chosen to study a fixed system where there is no tracking system where the tilt can be adjusted or rotated with respect to for example season, time of the day and the sun's ray in order to optimize the solar energy production. In addition, a fixed tilt plane simulation was preferred by Aneo.

The tilt angle was set to 35° and the azimuth angle to 0° . The angle of the panels were decided based on preferences and recommendations by Aneo. Generally, the selected angles for solar panels in PV systems are able to produce maximal energy when the sun is at its highest in the Northern Hemisphere. Higher tilt also reduces the chance of snow setting on the panels. The optimization setting was set with respect to yearly irradiation yield as this gives the optimal energy production throughout the whole year. Figure 3.4 shows all the chosen parameters in the orientation section in PVsyst.

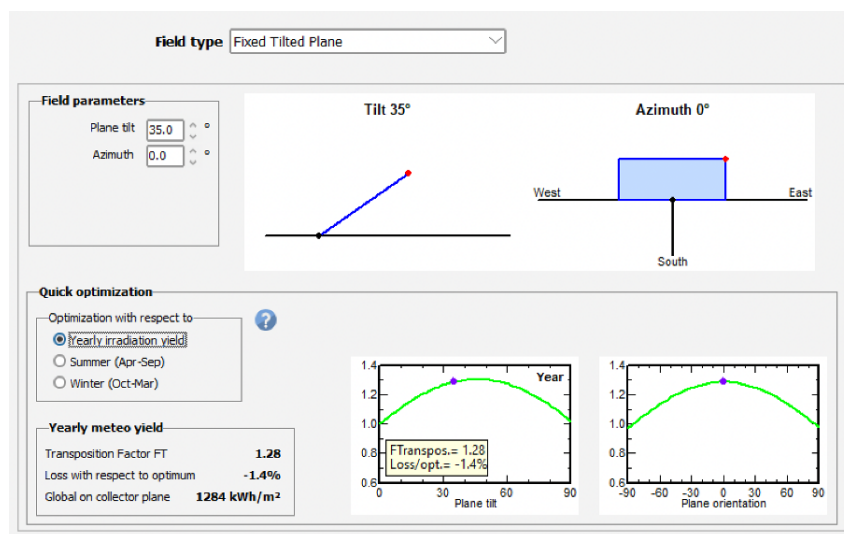


Figure 3.4: Orientation parameters in PVsyst.

3.4.3 System

Setting the system parameters includes defining the PV panel and the inverters, as well as designing the array. The PV panel set in system was the bifacial module JA-solar 550 Wp. The bifacial feature of this panel was included by using unlimited sheds in the 2D-model, and by setting the albedo values. Unlimited sheds was chosen as this is a common setting used for regular big PV systems with a single orientation, identical pitch between sheds, and without taking into consideration the sheds extremities. These factors are representative for the different cases studied in the thesis. The albedo values used in the calculation will be presented in Section 3.4.6. [74]

The inverter used for the system was Huawei Technologies 160 KW, 600-1 500 V, selected by Aneo. Inverters have several MPPT-inputs that can be connected to one array of PV panels. This is relevant for the simulated cases in PVsyst. Therefore, the normal multi-MPPT-feature function was used for the inverter. Each array is homogeneous, which means that the same PV panels are used for all simulations with the same amount of modules in series. This results in an MPPT-input that has identical electrical requirements, which is normal for the majority of multi-MPPT devices. The system was completed when the overload loss was at 0.5% and the Pnom ratio was around 1.4, given by Aneo. These values changes by the number of MPPT-inputs, modules in series and number of strings. [76]

To design the array, modules in series and number of strings had to be decided, as shown in Figure 3.5a. Modules in series was set to 27. The selected inverter was capable of withstanding 1 500 V at -10°C . This voltage value is relevant as it reaches its maximum possible voltage when the cell temperature is -10°C . The default is set to -10°C for most European countries and is also the coldest design point used by Aneo. For Case C and E there were in total 27 panels in series that gave a voltage of 1 473 V to the inverter shown in Figure 3.5b. This fits well as the inverter has a capacity of 1 500 V. In order to find the number of strings, the total number of modules in the 3D-model is divided by the amount of modules in the series. The 3D-model will be further presented in Section 3.4.4 about near shadings. [73]

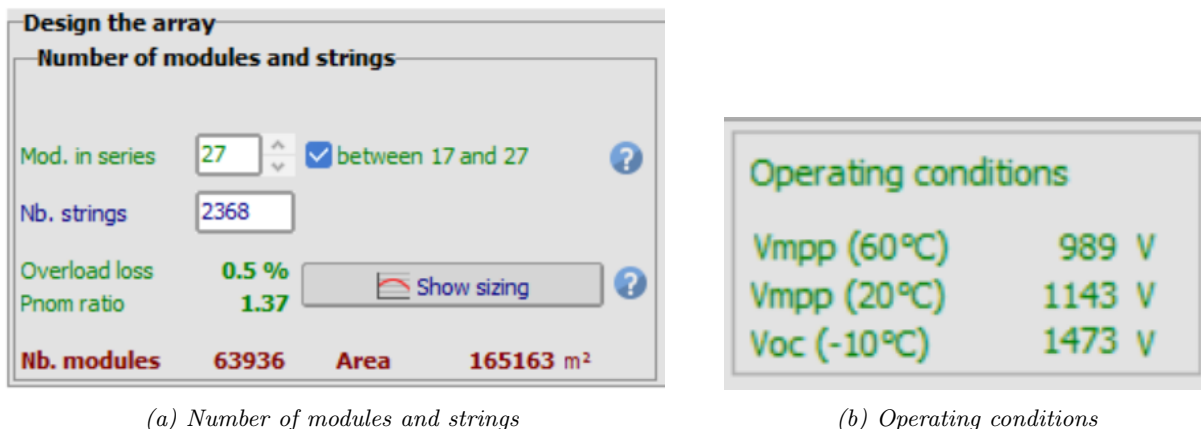


Figure 3.5: Design the array display, for a pitch at 8 meters.

3.4.4 Near Shadings

Near shadings in PVsyst ensures that the simulations include the shading factors produced by near objects, which produce visible shades on the PV panels. Examples of such objects could be other PV panels nearby, buildings and growing trees and plants. One way to include some of these factors was to design a 3D-scene of the solar park. However, only the shades from the panels were taken into account. [77]

As part of the 3D-scene design, the first step was to define a 300 000 m² zone, which would be filled with tables. This zone is the total area of the studied solar park. Various parameters had to be defined before the zone could be filled with panels. These are parameters such as the distance from the ground, the orientation values presented in Section 3.4.2, and the pitch between panels, which varies with the different cases presented in Section 3.1.

One table consists of two PV panels in height and 27 panels in length. These are the same as the PV panel set in System, presented in Section 3.4.3. There are two panels in height as this is the industry standard given by Aneo. 27 panels in length come from the number of modules in series in System. The tables consist of two strings of modules. Figure 3.6a shows one table and Figure 3.6b shows the zone filled with these tables.

When the 3D-scene was completed, the electrical shading for the whole year had to be taken into account. This was done by using the electrical shading loss according to module strings in the simulation. This mode considers electrical effects produced as the PV panels are connected in series in strings. As a result, this will give an upper limit for electrical effects when estimating the shading losses. Based on the system geometry and by-pass diode recovery the electrical effect was set to 70%, as it usually is between 60 to 80%. A higher electrical effect is needed for regular shading patterns. [79]

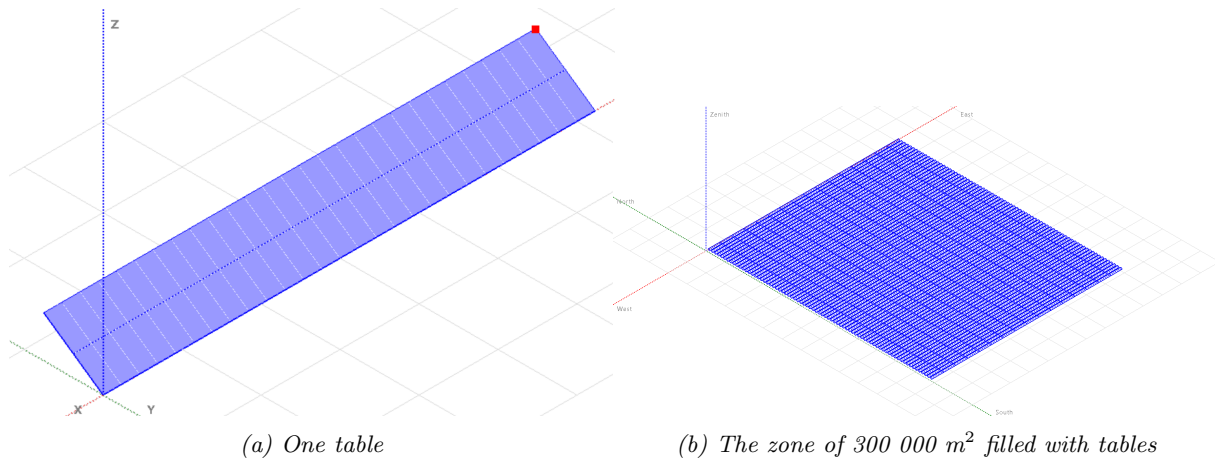


Figure 3.6: 3D-scene

3.4.5 Detailed Losses

To include the different losses in the simulation, the losses had to be specified. The first one was the thermal parameter. The modules were set as free-mounted with air circulation to resemble reality as much as possible. The thermal parameter is calculated by the thermal balance, also called the heat loss factor. The balance gives the operating temperature, used when modeling the PV panels. In addition to calculating the loss factor, the wind loss factor, U_v , was set to 0 W/(m²K)/ m/s as this is recommended by the simulation program, PVsyst, because the wind speed is often not well estimated in the meta database and may not give representative values for reality. Additionally, the constant loss factor, U_c , was set to 29 W/(m²K) according to PVsyst measurements on several free-standing ground-mounting systems where there is free air circulation. [79]

A number of factors had to be considered to include ohmic losses. Figure 3.7 shows the various settings for the ohmic losses, Figure 3.7a shows the setting for medium voltage transformers and Figure 3.7b shows the settings for high voltage transformers.

DC circuit: ohmic losses for the array
 Specified by:
 Global wiring resistance 0.5373 mΩ Calculated
 Loss fraction at STC 1.50 % Default ?
 Voltage Drop across series diode 0.7 V Default

AC losses after the inverter
AC Wire loss Inverter to transfo (per inverter)
 Uses AC circuit ohmic loss
 per inverter Whole system ?
 Length Inverter to Transformer 200.0 m Wire section 50 mm² ?
 Loss fraction at PNom 1.88 %
 Pnom: Pac = 160.0 kW, Vac = 800 V Tri, I = 115.5 A
 Voltage drop at PNom 15.0 V (1.88%)
 Copper Alu
 Uses one or several MV transformers
 Uses a HV transformer

Medium Voltage line
 MV line voltage 22.0 kV
 Length MV Transfo to injection 200 m Wire section 700 mm² ?
 Loss fraction at PNom 0.03 %
 Pnom: Pac = 25710 kW, Vac = 22.0 kV Tri, I = 675 A
 Voltage drop at PNom 6.3 V (0.03%)
 Copper Alu

Medium and High voltage transformers
 MV Transformer(s), full system ?
 Number of MV transfos 1 night disconnect
Generic values
 Reference Pac(PNom) 25.71 MW
 Iron loss (constant value) 0.13 % 32.85 kW default
 Copper (resistive) loss 0.74 % at PNom default
 Transfo equivalent resistance 3 x 0.19 mΩ
Transformer from Datasheets
 Uses datasheets data
 Nominal power N/A MVA
 Iron losses (no load loss) N/A MVA
 Copper (resistive) loss at PNom N/A MVA
 Global loss at PNom N/A MVA
 Global efficiency at PNom N/A %

(a) Medium voltage transformer settings

AC losses after the inverter
AC Wire loss Inverter to transfo (per inverter)
 Uses AC circuit ohmic loss
 per inverter Whole system ?
 Length Inverter to Transformer 200.0 m Wire section 50 mm² ?
 Loss fraction at PNom 1.88 %
 Pnom: Pac = 160.0 kW, Vac = 800 V Tri, I = 115.5 A
 Voltage drop at PNom 15.0 V (1.88%)
 Copper Alu
 Uses one or several MV transformers
 Uses a HV transformer

High Voltage line from HV transfo to injection
 HV line = grid voltage 66 kV
 Length HV Transfo to injection 100 m Wire section 150 mm² ?
 Loss fraction at PNom 0.01 %
 Pnom: Pac = 25710 kW, Vac = 66 kV Tri, I = 225 A
 Voltage drop at PNom 5 V (0.01%)
 Copper Alu

Medium and High voltage transformers
 HV Transformer, full system ?
 Grid voltage 66 kV night disconnect
Generic values
 Reference Pac(PNom) 25.71 MW
 Iron loss (constant value) 0.10 % 25.70 kW
 Copper (resistive) loss 1.50 % at PNom
 Transfo equivalent resistance 3 x 282.4 mΩ
Transformer from Datasheets
 Nominal power 25.71 MVA
 Iron losses (no load loss) 0.0257 MVA 0.10%
 Copper (resistive) loss at PNom 0.3857 MVA 1.50%
 Global loss at PNom 0.4114 MVA 1.60%
 Global efficiency at PNom 98.40 %

(b) High voltage transformer settings

Figure 3.7: Ohmic losses

The wires with their ohmic resistances in the PV system induce losses. These losses are generated from the power from the PV panels to the terminals of the specific array. In the simulations a default global wiring loss fraction of 1.5% set with respect to the STC conditions, proposed by both PVsyst and Aneo.

In the simulations, the losses between the output of the inverter, the transformer and the injection point were taken into consideration. These losses were generated based on their wire length, loss fraction at Pnom as well as wire material and diameter. Additionally, generic values for the transformation were set. This includes losses related to the chosen MV/HV external transformer with its amount, the properties of the MV/HV lineup to the injection point. These settings are standard settings given by Aneo to make the simulation as close to a real case as possible. For this thesis, it was assumed one transformer for the entire system, one park transformer, and that the grid had the capacity to receive everything from the park.

The last loss set in PVsyst was soiling losses. Soiling can be dirt from industrial environments, trees and the soil. The Norwegian climate is known for being humid and having rainy periods. This reduces the soils impact on the energy production to the PV panels. However, this parameter can be used to involve the impact of snow covering the panels. Based on this, the yearly soiling losses factor was set to default and 3%. [79]

3.4.6 Albedo

In order to find the albedo values, the amount of snow in Halden had to be determined. The Norwegian Climate Service Center [42, 43] was used to estimate the average amount of snow cover in Halden. The date for average snow cover was only available for the years 2017-2022. Additionally, the average snow cover for each month was determined as shown in Figure 3.13. Appendix E shows the snow data from the Norwegian Climate Service center and the MATLAB-script used to find the monthly average.

Table 3.13: Average amount of snow cover in Halden. 0 = No snow, 1 = Mostly bare ground, 2 = Equal amount snow cover and bare ground, 3 = Mostly snow-covered ground, 4 = Snow-covered ground. [43]

Month	Snow cover
January	1
February	1.4
March	0.4
April	0
May	0
June	0
July	0
August	0
September	0
October	0
November	0
December	0.5

Once the monthly snow cover was estimated, the albedo values could be determined. Since albedo values change based on reflection from the surface, an assumption was made that high site productivity forest and low site productivity forest reflect light in the same way. This was assumed because in both cases the ground will be covered in vegetation with similar colors.

In order to make the albedo values resemble reality, different values were determined for each month, as the surface's ability to reflect light is highly connected to the type of surface and the season of the year. The Albedo values were set based on the amount of snow and Table 2.1 with Albedo values for different surfaces, presented in Section 2.1.1.

First, the albedo values for forests were estimated. February is the month with most snow, but still have mostly bare ground. The albedo value for February is the lowest albedo value for wet snow. The rest of the values for the forest are based on assumptions about the color and amount of grass. January have mostly bare ground, and because of this the value in January is the average between wet snow and fresh grass. March and December have little to no snow, but the snow is still reflecting light. Therefore the albedo value is a little higher than fresh grass, but lower than in January.

April and November have no snow, and it was assumed that these months have almost no grass, so the albedo value is the lowest value for grass. May and June are assumed to have fresh grass. July is assumed to have grass, therefore the albedo value is the middle for grass. August and September are assumed to have less fresh grass than July, but still have more grass than April. October is assumed to have more grass than November but less than September. Figure 3.14a shows the albedo values for the forest.

Constructed area without snow is assumed to have an albedo value of 0.25, the albedo for a darker concrete referred to Table 2.1. This assumption was made, as darker concrete is the type of surface that was seen to represent the constructed area the most. The albedo value of 0.25 is the same for every month, except for the winter months when snow appears. The albedo value for January is the average between wet snow and cement. The albedo values for February, March and December are based on the same assumptions as the forest, presented above. Figure 3.14b shows the albedo values for the constructed area used in the simulations in PVsyst.

Table 3.14: Albedo values

(a) Albedo values for low- and high site productivity

Month	Albedo value
January	0.405
February	0.55
March	0.3
April	0.15
May	0.26
June	0.26
July	0.225
August	0.2
September	0.2
October	0.175
November	0.15
December	0.3

(b) Albedo values for constructed area

Month	Albedo value
January	0.4
February	0.55
March	0.3
April	0.25
May	0.25
June	0.25
July	0.25
August	0.25
September	0.25
October	0.25
November	0.25
December	0.3

3.4.7 Simulations

Two projects were made in PVsyst, one for forest and one for constructed area, as different albedo values were estimated for forest and constructed area. Each project had eight variants for each pitch from 8 meters to 15 meters. These variants have similar settings, except the pitch between the modules and the values that were affected by the pitch, such as number of strings, nominal power, iron loss and copper loss. Figure 3.8 shows the different 3D-scene designs for a pitch of 8 meters and 15 meters. Once Orientation, System, Detailed losses, Horizon, Near shading and the general project settings were set, the simulations were simulated in PVsyst.

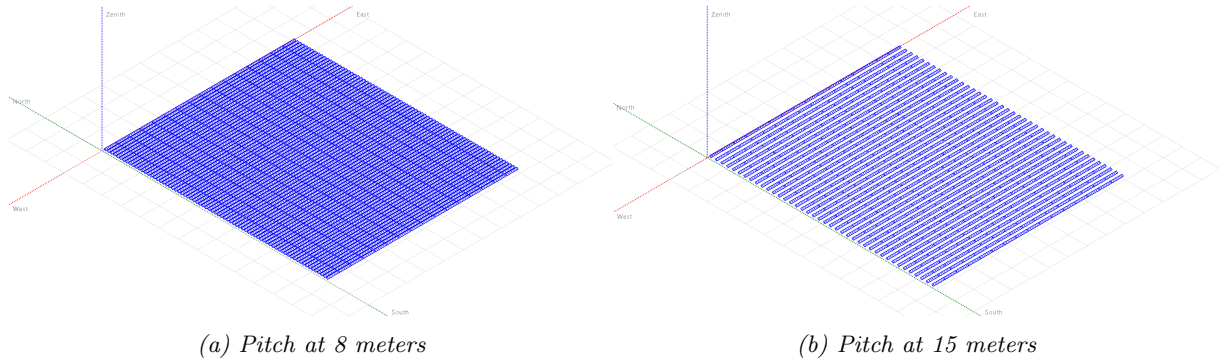


Figure 3.8: Different 3D-scene designs

3.5 Ratio between Production and Emission

In order to see the connection between the generated solar energy from the PV system, and the CO₂-equivalents related to land-use change and the life cycle of PV modules, different calculations have been done. The calculations for this section are attached in Appendix F.

To calculate the total CO₂-equivalents, the emissions from land-use change were added to the amount of CO₂-equivalents from the LCA. The values from the LCA were given as emission per quantity, so the emissions had to be converted to emissions per panel. This was done by using the area and the mass for one panel. Once the emissions were calculated for one panel, the number of panels obtained from the PVsyst simulation were used to get the exact CO₂-equivalents for the whole park. Then the emissions for the PV panels were added to the emissions from the different land-use changes.

$$\text{Emission and production ratio} = \frac{E_{PV} + E_{area}}{P_{tot}} \quad (3.2)$$

Where:

$$E_{PV} = \text{Emission from production and mounting of PV panels} \quad [\text{kg CO}_2\text{-eq}]$$

$$E_{area} = \text{Emission from land-use change} \quad [\text{kg CO}_2\text{-eq}]$$

$$P_{tot} = \text{Production from 30 years} \quad [\text{MWh}/30 \text{ years}]$$

Once the total emissions for each pitch were calculated, the ratio between emissions and production was calculated with Equation 3.2. Since the life expectancy of the solar panels are 30 years and the emissions from land-use change are calculated for 30 years, the value for production also had to be for 30 years to get the correct ratio. The JA-Solar PV panels have a 30-year linear power output warranty, with a 0.45% annual degradation over 30 years as seen in Figure 3.9 [36].

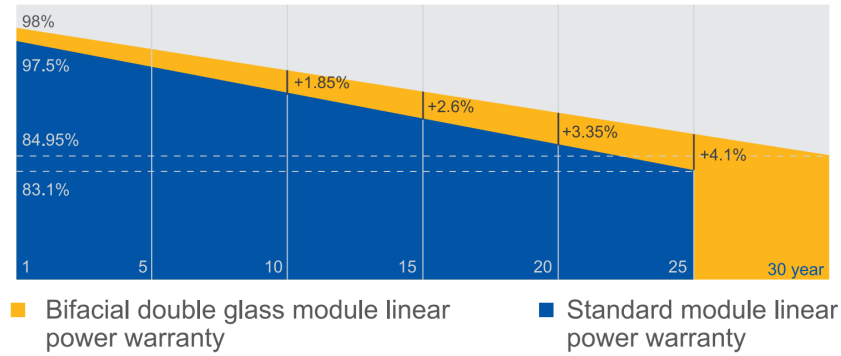


Figure 3.9: The JA PV panels degradation over 30 years. [36]

In order to take the annual degradation into account, the yearly production calculated in PVsyst was used in a geometric series, shown in Equation 3.3 [1]. k represents the value 99.55% as this is 100% subtracted from the annual degradation and 0.45%. This k value is constant in accordance with the manufacturer JA-Solar's official datasheet presented in Appendix A and Figure 3.9. In addition, the n value which represents the total period was set to 30 years and a_1 the yearly energy production.

$$\text{Given a geometric series } a_1 + ka_1 + k^2a_1 + \dots, s_n = \frac{a_1(k^n - 1)}{k - 1} \quad (3.3)$$

Where:

s_n	= The total energy production included degradation	[MWh]
a_1	= The yearly energy production	[MWh/year]
k	= The annual degradation	[kg CO ₂ -eq]
n	= Production period	[years]

4 Results

This chapter will cover the results and outcome of the LCA, land-use change calculations and the simulations in PVsyst for the six main cases. Additionally, solar production from all pitches between 8 to 15 meters will be outlined, as well as the calculations related to the connection between energy production and emissions.

4.1 Life Cycle Impact Assessment

The life cycle impact assessment is the third phase of an LCA, and is described in ISO 14040 [34]. In this phase, the results of the potential environmental impacts throughout the life cycle of the chosen solar panel are presented. The chosen method for the calculation was the IPCC 2013 GWP100 methodology in SimaPro. This is a methodology developed by the International Panel on Climate Change from the UN with a specific focus on global warming potential (GWP) with a time horizon of 100 years.

Figure 4.1 shows the flow chart for the production of 1 m² PV panel, and which processes contribute to the impacts of the total emission of kg CO₂-eq. The production of 1 m² PV panel releases 122 kg CO₂-eq. Most of the emissions come from the production of the PV cell, with the silicon production and the processes of making these cells. Besides the production of the PV cells, solar glass and electricity consumption accounted for a large part of the emissions. Electricity is required throughout many of the production processes and releases in total 51.48 kg CO₂-eq of producing 1 m² PV panel.

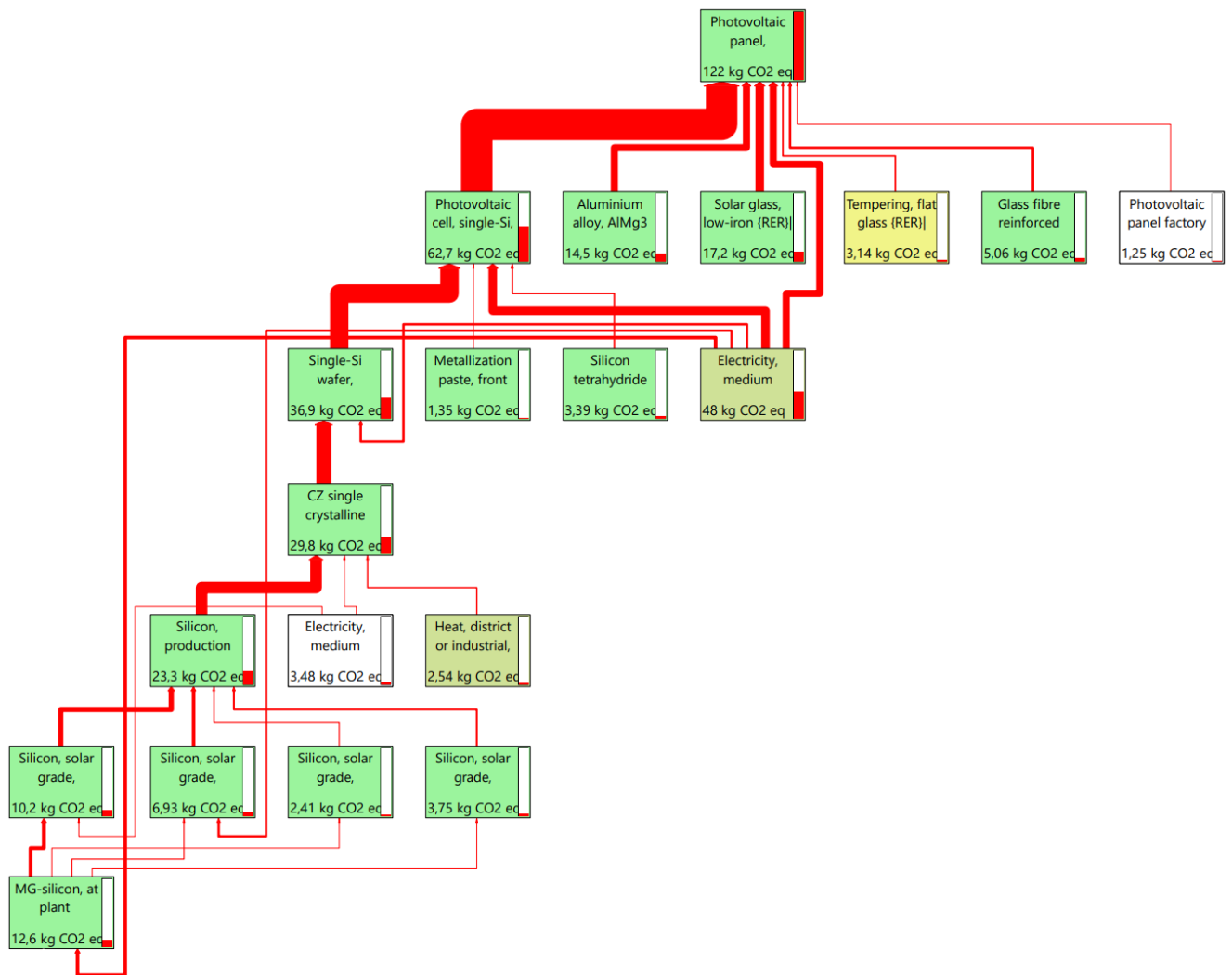


Figure 4.1: Flow chart for production of 1 m² PV panel.

Figure 4.2 gives an overview of where the emissions come from during the production of the PV panel. Table 4.1 shows what the colors in Figure 4.2 indicate. The green section in the figure shows the photovoltaic cell, the grey shows solar glass, the orange shows aluminum alloy and the yellow shows copper. These four categories account for the biggest part of the emissions, with 51.3%, 14.1%, 11.9% and 11.8% respectively.

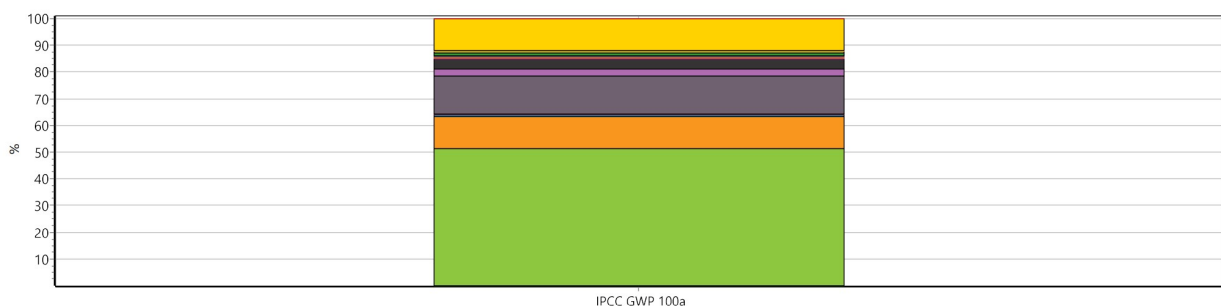


Figure 4.2: An overview of where the emissions come from during the production of the PV panel.

Table 4.1: What the colors in Figure 4.2 indicate.

Color	Category
Green	Photovoltaic panel
Orange	Aluminum alloy
Blue	Wire drawing, copper
Red	Silicone Product
Purple	Lead
Pink	Tempering, flat glass
Light Green	Photovoltaic cell
Yellow	Copper
Cyan	Diode
Red	Tin
Grey	Solar glass
Black	Glass fibre

Figure 4.3 shows the flow chart for the transport of the PV panels from Nanjing in China to Halden in Norway. The transport has emission of 220 kg CO₂-eq for all the panels installed in the PV park.

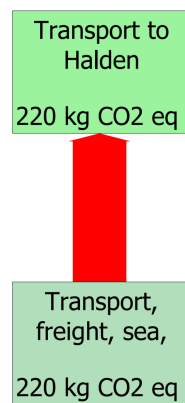


Figure 4.3: Flow chart for transport by ship from Nanjing to Halden.

Figure 4.4 illustrates the flow chart for 1 m² open ground construction. The mounting of 1 m² PV panel releases 91.9 kg CO₂-eq. Reinforcing steel contributes for the biggest part of the emissions with 78 kg CO₂-eq, this is 84.87% of the total emissions from the mounting. This is because the mounting structure used in the report requires 39.5 kg steel per m².

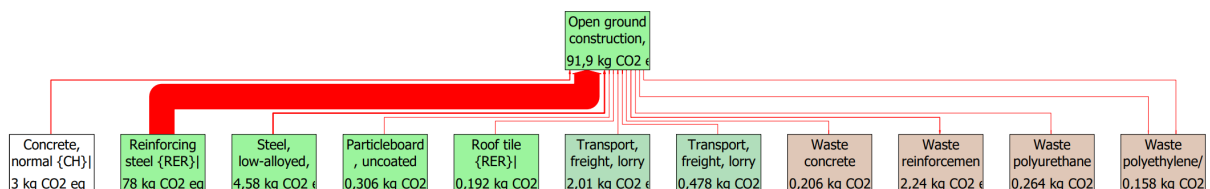


Figure 4.4: Flow chart for 1 m² open ground construction.

4 RESULTS

Figure 4.5, 4.6, 4.7 and 4.8 shows the flow charts for the treatment of used c-Si PV modules in a first generation recycling process. When combining the result from these four processes, the emissions from the recycling process of one C-Si panel is 30.05 kg CO₂-eq. The calculations for one c-Si panel in this section are shown in Appendix C. Figure 4.5 shows the flow chart for the treatment of 1 kg c-Si PV module. The treatment releases 0.459 kg CO₂-eq per 1 kg. The treatment of one panel will release 14.596 kg CO₂-eq.

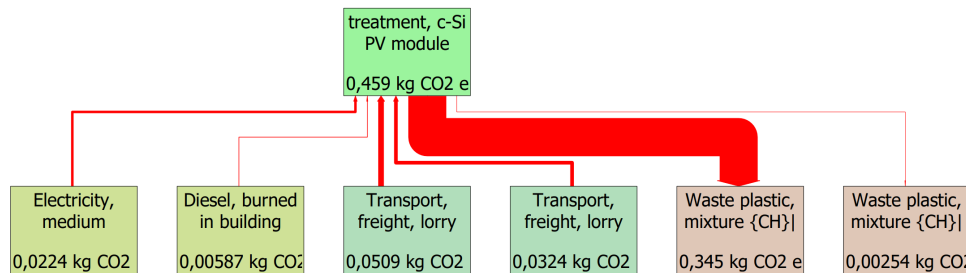


Figure 4.5: Flow chart for 1 kg takeback and recycling of c-Si module.

Figure 4.6 shows the flow chart for 1 kg glass cullets recovered from c-Si PV module. 1 kg glass cullets releases 0.158 kg CO₂-eq. The glass cullets from one c-Si PV module will release 14.383 kg CO₂-eq, and is calculated for glass on the front and the back of the module.

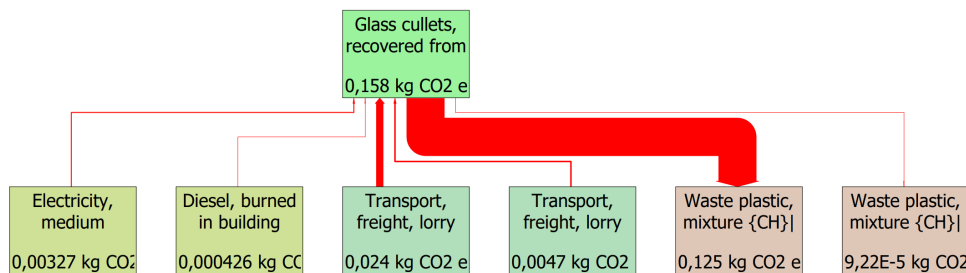


Figure 4.6: Flow chart for 1 kg takeback and recycling of c-Si module.

Figure 4.7 shows the flow chart for 1 kg aluminium scrap recovered c-Si PV module. 1 kg aluminium scrap releases 0.654 kg CO₂-eq. The aluminium from one c-Si PV module will release 0.078 kg CO₂-eq.

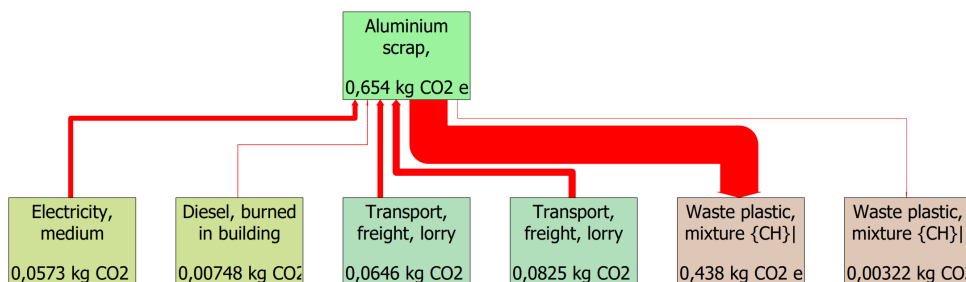


Figure 4.7: Flow chart for 1 kg takeback and recycling of c-Si module.

Figure 4.8 shows the flow chart for 1 kg copper scrap recovered from c-Si PV module. 1 kg copper scrap releases 3.74 kg CO₂-eq. The copper from one c-Si PV module will release 0.995 kg CO₂-eq.

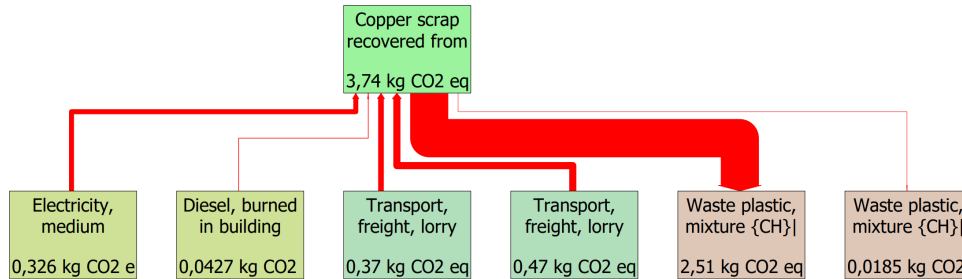


Figure 4.8: Flow chart for 1 kg takeback and recycling of c-Si module.

Table 4.2 shows the emissions associated with the production, mounting, transport and recycling of single-Si PV panels. Each process emits emissions based on a different quantity of the panel. The total emissions from one panel, excluding the transport from China to Halden, is 582.61 kg CO₂-eq.

Table 4.2: CO₂ emissions for the various processes and the total emission for one PV panel, excluded the transport from China to Halden.

Process	Quantity	kg CO ₂ -eq pr. quantity
Production	1 m ²	122
Mounting	1 m ²	91.9
Transport, China to halden	all panels	220
Recycling treatment	1 panel	30.05
Total excl. transport China to Halden	1 panel	582.61

4.2 Land-Use Change

This section presents the results from the land-use change calculations. Table 4.3, 4.4 and 4.5 shows emission and absorption from the area with and without a land-use change, and the total carbon footprint from a land-use change. All values are given in ton CO₂-equivalents. In this thesis, ton refers to a metric ton, which is equal to 1 000 kg. Positive numbers are emissions and negative numbers are absorption.

Table 4.3 and 4.4 shows that if there is no land-use change, the forest will have a considerable absorption of CO₂, and smaller emissions of CH₄ and N₂O. A land-use change causes emission of CO₂ and no change in CH₄ and N₂O. The total carbon footprint of a land-use change from forest with low site productivity to settlement is 12 648.7 ton CO₂-eq. A land-use change from forest with high site productivity to settlement causes an emission of 13 546.3 ton CO₂-eq. Table 4.5 shows that there are no absorption or emissions for the constructed area. A constructed area is already a settlement and there is no land-use change.

Table 4.3: Emission and absorption for a land-use change from forest of low site productivity to settlement.

Forest with low site productivity to settlement				
<i>[ton CO₂-eq]</i>				
	CO ₂	CH ₄	N ₂ O	Total
Emission/absorption without land-use change	-3 793.2	767.7	57.6	-2 967.9
Emission/absorption with land-use change	9 680.8	0.0	0.0	9 680.8
Total carbon footprint of the land-use change	13 474.0	-767.7	-57.6	12 648.7

Table 4.4: Emission and absorption from a land-use change from forest of high site productivity to settlement.

Forest with high site productivity to settlement				
<i>[ton CO₂-eq]</i>				
	CO ₂	CH ₄	N ₂ O	Total
Emission/absorption without land-use change	-4 154.6	767.7	57.6	-3 329.3
Emission/absorption with land-use change	10 217.0	0.0	0.0	10 217.0
Total carbon footprint of the land-use change	14 371.6	-767.7	-57.6	13 546.3

Table 4.5: Emission and absorption from land-use change from a constructed area to settlement.

Constructed area to settlement				
<i>[ton CO₂-eq]</i>				
	CO ₂	CH ₄	N ₂ O	Total
Emission/absorption without land-use change	0.0	0.0	0.0	0.0
Emission/absorption with land-use change	0.0	0.0	0.0	0.0
Total carbon footprint of the land-use change	0.0	0.0	0.0	0.0

4.3 PV Production

This section covers the outcome of the simulations done in the software PVsyst for all the six different cases presented in Section 3.1. As mentioned in Section 3.4.6, it is assumed that high site productivity and low site productivity forests have the same albedo values. As a result, the results for both high and low site productivity forests are collected into one simulation. More specifically, Case C and E represent the forests with a pitch of 8 meters while Case D and F examine the forests with 15 meters pitch. Table 4.6 presents the results related to PV panels and inverter characteristics from the simulations. These values are the same for the three different types of area.

Table 4.6: Simulation results related to PV array and inverter.

	Pitch of 8 meters	Pitch of 15 metes
PV array		
Numbers of modules	63 936	34 560
Module area [m ²]	165 163	89 277
System power [MWp]	35.16	19.01
Inverter		
Number of inverters	161	87
Total power [MWac]	25.7	13.9
Pnom ratio	1.37	1.37

4 RESULTS

As seen in Table 4.6 there are installed 63 936 modules and 161 inverters in total for Case A, C and E when the pitch is 8 meters. In addition, the module area is 165 163 m² for the same cases. This is almost twice the amount of modules, inverters and module area as for Case B, D and F when the pitch is 15 meters. For these cases, the number of modules is 34 560, the number of inverters is 87 and the module area is 89 277 m². The system power and total power are 35.16 MWp and 25.7 MWac (megawatts alternating current) respectively when the pitch is 8 meters, compared 19.01 MWp and 13.9 MWac for 15 meters pitch.

4.3.1 Forests

In this section, the simulation results from the energy production for forests will be described, before the losses illustrated in a loss diagram will be presented. These results are for Case C, D, E and F.

PV Production

The main monthly results from the simulations in PVsyst for forests for a pitch of 8 and 15 meters are shown in Table 4.7. The global horizontal irradiation, GlobHor, is highest in June with 173.5 kWh/m² when the ambient temperature, T_{Amb}, is 14.83°C, and lowest in December with 5.2 kWh/m² when T_{Amb} is 0.85°C.

The E_{Array} column in Table 4.7 represents the effective energy at the array output, and E_{Grid} presents the energy injected into the grid. These values are highest in June for both pitches. For Case C and E, E_{Array} is 5 505 MWh and E_{Grid} it is 5 221 MWh. For Case D and F, E_{Array} is 3 077 MWh and E_{grid} is 2 918 MWh. Lastly, the performance ratio (PR) is presented. This value is highest in April with 0.851 when the pitch is 8 meters, and in February with 0.924 for 15 meters.

Table 4.7: The main results for forests simulations for pitch of 8 and 15 meters.

				Pitch 8 meters				Pitch 15 meters			
	GlobHor [kWh/m ²]	DiffHor [kWh/m ²]	T _{Amb} [°C]	GlobEff [kWh/m ²]	E _{Array} [kWh]	E _{Grid} [kWh]	PR ratio	GlobEff [kWh/m ²]	E _{Array} {kWh}	E _{Grid} [kWh]	PR ratio
Jan	8.9	6.01	-0.85	10.3	314 643	261 018	0.347	16.0	270 345	238 664	0.588
Feb	25.3	16.60	-0.93	30.7	1 056 650	987 596	0.625	41.3	838 786	788 778	0.924
Mar	75.7	34.57	1.51	103.4	3 253 256	3 088 736	0.741	110.9	2 161 843	2 047 682	0.909
Apr	118.1	51.54	6.01	140.0	4 792 862	4 541 054	0.851	142.2	2 648 012	2 509 193	0.869
May	159.3	78.52	11.32	157.2	5 408 195	5 130 873	0.844	160.9	3 024 363	2 869 552	0.873
Jun	173.5	76.42	14.83	162.8	5 505 078	5 221 251	0.829	166.6	3 077 148	2 918 989	0.858
Jul	166.7	70.95	17.93	159.5	5 299 626	5 022 986	0.816	162.9	2 955 571	2 802 057	0.842
Aug	125.8	60.72	17.18	133.9	4 421 409	4 188 765	0.812	136.7	2 460 794	2 331 926	0.836
Sep	86.4	36.66	12.91	113.1	3 600 857	3 409 450	0.781	116.1	2 131 254	2 016 624	0.854
Oct	42.3	24.30	8.06	54.2	1 664 410	1 570 376	0.623	66.9	1 270 713	1 200 729	0.881
Nov	13.0	9.05	3.98	14.8	465 536	409 220	0.444	22.0	386 930	351 767	0.707
Des	5.2	4.25	0.85	5.1	156 480	106 227	0.263	7.3	129 387	101 566	0.465
Year	1 000.1	469.58	7.79	1 085.0	35 939 004	33 937 553	0.776	1 149.9	21 355 146	20 177 529	0.853

Figure 4.9 shows a monthly overview of the normalized production. The produced useful energy is illustrated with the color brown. The losses are presented in green and purple color. The collection losses are losses related to the level of PV-array losses, while the system losses are mainly losses associated with the inverter. As seen in Figure 4.9a and 4.9b, both the produced energy and losses are mainly the highest during the summer season for a pitch of 8 meters and 15 meters. In addition, the system losses are almost the same for all cases as it is 0.16 kWh/kWp/day for a pitch of 8 meters and 0.17 kWh/kWp/day for 15 meters.

4 RESULTS

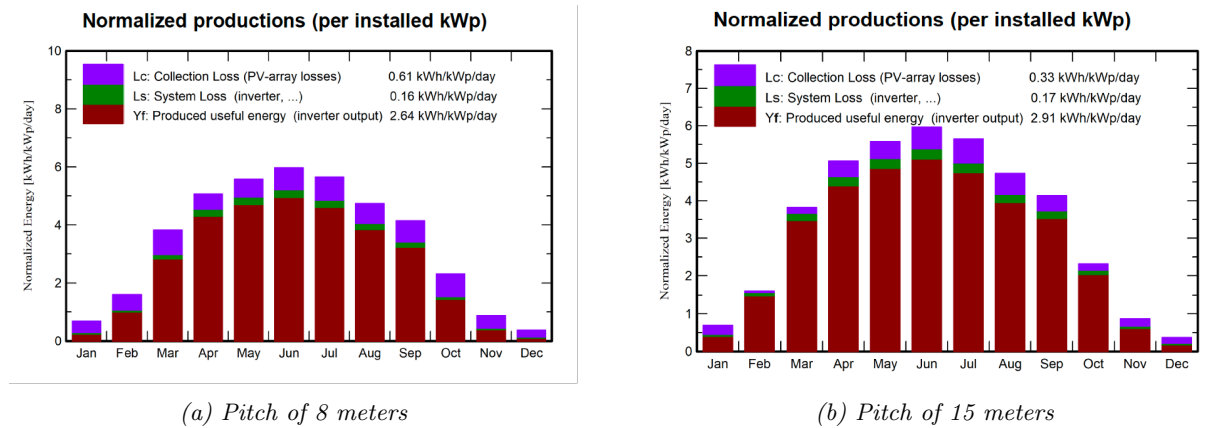


Figure 4.9: Normalized production per installed kWp.

Figure 4.10 presents the performance ratio for the forest simulations. The ratio is generally high during the spring, summer and autumn seasons and low in the winter season for all forest cases. For Case C and E, the peak is in April, as seen in Figure 4.10a. For Case D and F, the peak is in February, as shown in Figure 4.10b.

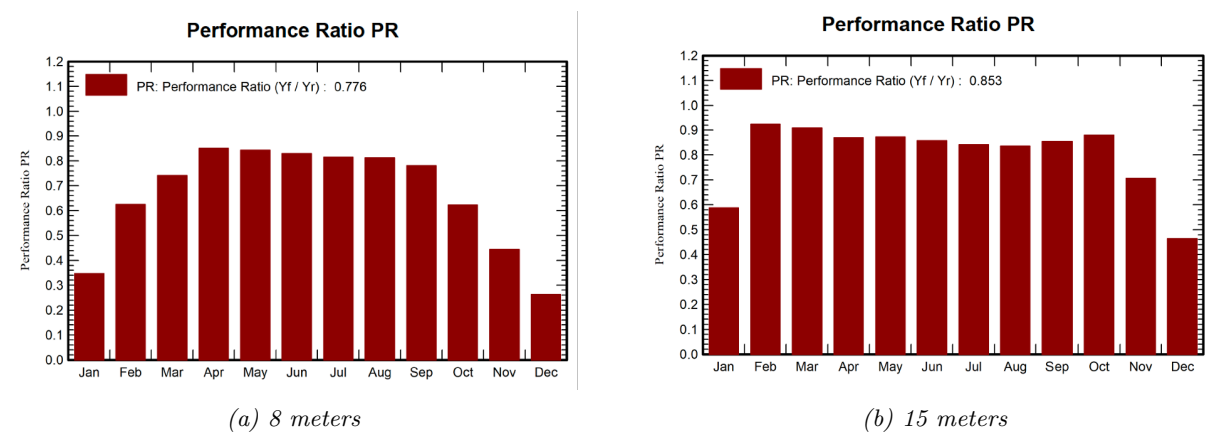


Figure 4.10: Performance ratio (PR)

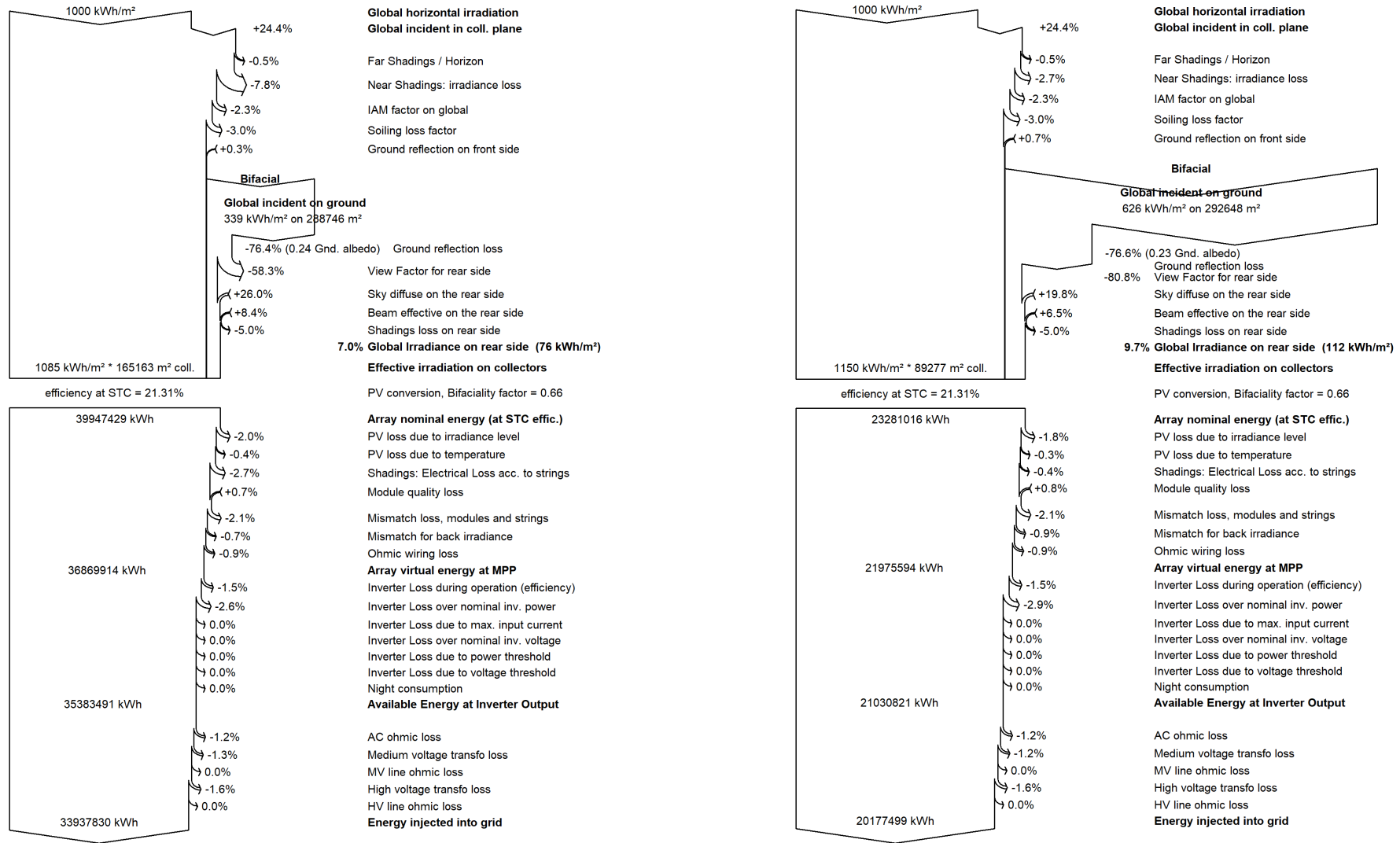
Loss Diagram

The losses for the simulated PV system are illustrated in a loss diagram in Figure 4.11 for both a pitch of 8 meters and 15 meters. The loss diagram starts with global horizontal irradiation of 1 000 kWh/m², then the global incident in collector plane value contributes with about 24% more irradiance. There are also irradiance losses related to near shadings. This loss is -7.8% for a pitch of 8 meters and -2.7% for a pitch of 15 meters. The soiling was set to -3% for all cases, as presented in Section 3.4.5.

The loss diagram indicates that the bifacial solar panels increase the amount of collected solar irradiance. As seen in Figure 4.11a the global incident on ground is 339 kWh/m² on 288 746 m² and 626 kWh/m² on 292 648 m² as shown in Figure 4.11b. There is also a ground reflection of -76% from the rear side. This loss is connected to the loss of irradiance due to the surface area's ability to reflect solar radiation. The ground reflection on the front side is 0.3% for a pitch of 8 meters and 0.7% for a pitch of 15 meters.

The view factor represents the ratio between solar irradiance reflected from the ground that reaches the backside of the bifacial panel, and the irradiance lost and reflected back to the sky. For Case C and E, the view factor is -58.3% and for Case D and F, it is -80.8%, as seen in Figure 4.11. The inverter losses during operation are about -1.5% and the inverter loss over nominal inverter power is -2.6% for a pitch of 8 meters, and -2.9% for a pitch of 15 meters.

There are also losses related to the transformer and its wiring. These losses are presented at the bottom of the loss diagrams in Figure 4.11a and 4.11b. The MV transformer loss is -1.3% for 8 meters and -1.2% for 15 meters. For all cases, the HV transformer loss is about -1.6% and the AC ohmic loss, from wiring up to the injection point is about -1.2%.



(a) Loss diagram - 8 meter forest

(b) Loss diagram - 15 meter forest

Figure 4.11: Loss diagram for forests

4.3.2 Constructed Area

This section presents the simulation results for the constructed area. The PV production will be described before losses will be presented. These results are for Case A and B.

PV Production

The main monthly results from the simulations in PVsyst for constructed area for a pitch of 8 and 15 meters are shown in Table 4.8. As the solar park is located in the same place in Halden for all cases the global horizon and diffuse irradiation and ambient temperature results are the same. They are presented in Section 4.3.1 for forest.

The E_{Array} column in Table 4.8 and E_{grid} are highest in June for both pitches. For Case A, E_{Array} is 5 496 MWh and E_{grid} it is 5 212 MWh. For Case B, E_{Array} is 3 070 MWh and E_{grid} is 2 912 MWh. Lastly, the performance ratio (PR) is presented. This value is highest in April with 0.854 when the pitch is 8 meters, and in February with 0.924 for 15 meters.

Table 4.8: The main results for constructed area simulations for pitch of 8 and 15 meters.

				Pitch 8 meters				Pitch 15 meters			
	GlobHor [kWh/m ²]	DiffHor [kWh/m ²]	T _{Amb} [°C]	GlobEff [kWh/m ²]	E _{Array} [kWh]	E _{Grid} [kWh]	PR ratio	GlobEff [kWh/m ²]	E _{Array} [kWh]	E _{Grid} [kWh]	PR ratio
Jan	8.9	6.01	-0.85	10.3	314 471	260 851	0.347	16.0	270 211	238 530	0.587
Feb	25.3	16.60	-0.93	30.7	1 056 655	987 600	0.625	41.3	838 788	788 775	0.924
Mar	75.7	34.57	1.51	103.4	3 253 256	3 088 731	0.741	110.9	2 161 845	2 047 680	0.909
Apr	118.1	51.54	6.01	140.3	4 844 855	4 590 165	0.854	142.8	2 692 747	2 551 300	0.878
May	159.3	78.52	11.32	157.1	5 399 702	5 122 853	0.843	160.8	3 017 838	2 863 394	0.872
Jun	173.5	76.42	14.83	162.8	5 496 128	5 212 776	0.829	166.5	3 070 342	2 912 553	0.856
Jul	166.7	70.95	17.93	159.6	5 320 731	5 042 992	0.817	163.2	2 971 645	2 817 284	0.844
Aug	125.8	60.72	17.18	134.1	4 451 608	4 217 436	0.814	137.1	2 484 978	2 354 890	0.841
Sep	86.4	36.66	12.91	113.2	3 615 755	3 423 612	0.781	116.3	2 148 318	2 032 706	0.858
Oct	42.3	24.30	8.06	54.3	1 676 278	1 581 957	0.625	67.0	1 286 763	1 215 952	0.888
Nov	13.0	9.05	3.98	14.9	471 567	415 118	0.449	22.1	391 920	356 610	0.713
Des	5.2	4.25	0.85	5.1	156 480	106 229	0.263	7.3	129 388	101 563	0.465
Year	1 000.1	469.58	7.79	1 085.7	36 057 486	34 050 320	0.777	1 151.3	21 464 786	20 281 236	0.856

Figure 4.12 presents the monthly normalized productions for constructed area. As seen in Figure 4.12a and 4.12b, both the produced energy and losses are mainly the highest during the summer season for a pitch of 8 meters and 15 meters. In addition, the system losses are almost the same for all cases as it is 0.16 kWh/kWp/day for a pitch of 8 meters and 0.17 kWh/kWp/day for 15 meters.

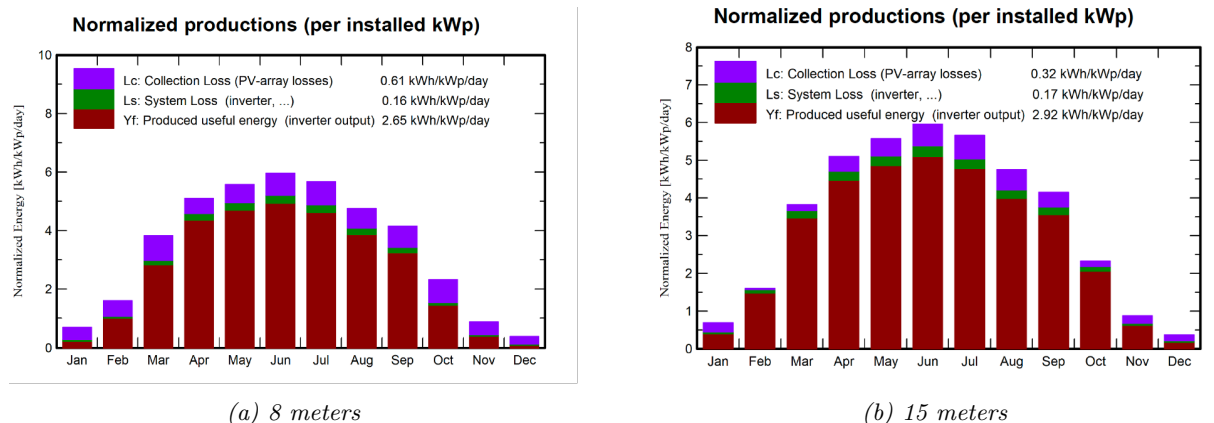


Figure 4.12: Normalized production per installed kWp.

Figure 4.13 presents the performance ratio for the constructed area simulations. The ratio is generally high during the spring, summer and autumn seasons and low in the winter season for all cases for constructed area. For Case A, the peak is in April as seen in Figure 4.13a, for Case B, the peak is in February, as shown in Figure 4.13b.

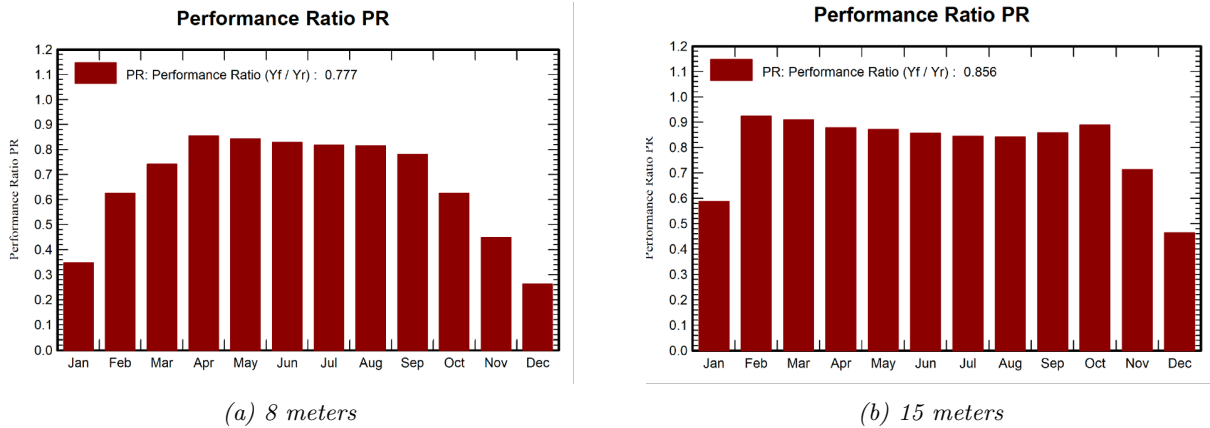


Figure 4.13: Performance ratio (PR)

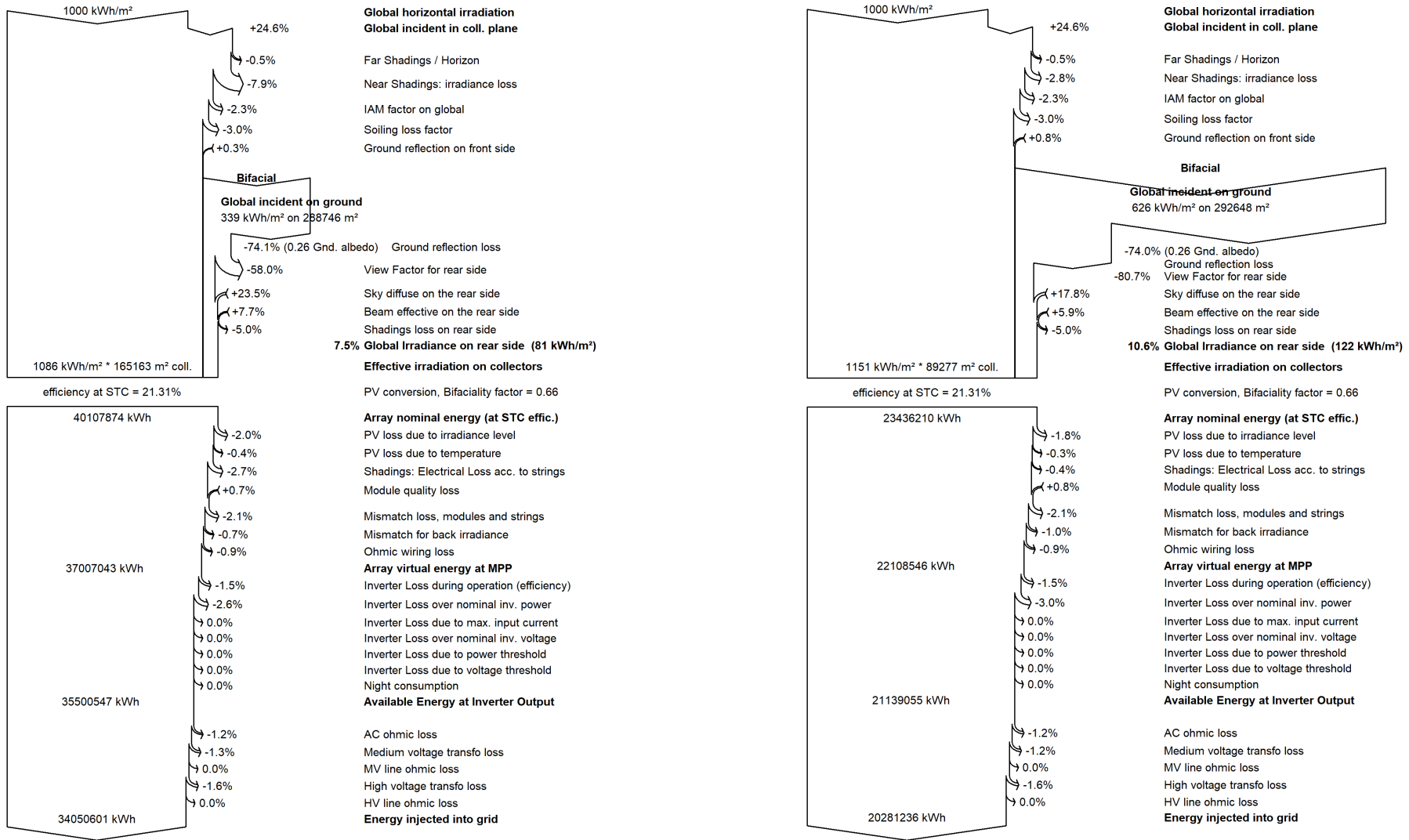
Loss Diagram

The losses for the simulated PV system are illustrated in a loss diagram in Figure 4.14 for both a pitch of 8 meters and 15 meters. As for the loss diagram for forests, these loss diagrams also start with global horizontal irradiation of 1 000 kWh/m², then the global incident in collector plane value contributes with about 24% more irradiance. There are also irradiance losses related to near shadings. This loss is -7.9% for a pitch of 8 meters and -2.8% for a pitch of 15 meters. The soiling was set to 3% for all cases, as presented in Section 3.4.5.

The loss diagram indicates that the bifacial solar panels increase the amount of collected solar irradiance. As seen in Figure 4.14a the global incident on ground is 339 kWh/m² on 288 746 m² and 626 kWh/m² on 292 648 m² as shown in Figure 4.14b. There is also a ground reflection of -74% from the rear side. The ground reflection on the front side is 0.3% for a pitch of 8 meters and 0.7% for a pitch of 15 meters. These values are similar to the cases for forest presented in Section 4.3.1.

The view factor represents the ratio between solar irradiance reflected from the ground that reaches the backside of the bifacial panel, and the irradiance lost and reflected back to the sky. For Case A the view factor is -58.0%, and for Case B it is -80.7%, as seen in Figure 4.14. The inverter losses during operation are about -1.5% and the inverter loss over nominal inverter power is -2.6% for a pitch of 8 meters, and -3% for a pitch of 15 meters.

There are also losses related to the transformer and its wiring. These losses are presented at the bottom of the loss diagrams in Figure 4.14a and 4.14b. The MV transformer loss is -1.3% for 8 meters and -1.2% for 15 meters. For all cases, the HV transformer loss is about -1.6% and the AC ohmic loss, from wiring up to the injection point is about -1.2%.



(a) 8 meters

(b) 15 meters

Figure 4.14: Loss diagram for constructed area.

4.3.3 Additional Pitches

Table 4.9 shows the number of panels and production per year for all the simulated pitches. The table shows the different productions for constructed area and forest.

Table 4.9: Number of panels and production from PV_{sys} for the pitches between 8-15 meters.

Pitch [m]	Number of panels	Production [MWh/år]	
		Constructed area	Forest
8	63 936	34 051	33 938
9	57 024	31 370	31 252
10	50 976	28 611	28 493
11	46 646	26 545	26 456
12	43 200	24 847	24 732
13	39 744	23 038	22 927
14	37 152	21 689	21 581
15	34 560	20 281	20 178

4.4 Ratio between Production and Emission

In this section, the results from the production and emissions are collected together. In addition to the results from the presented six cases, the results from the different pitches between 8 and 15 are presented.

The ratio between emission and production for the six cases A-F are presented in Table 4.10. The values are given in kg CO₂-eq per MWh. Case B, which is constructed area with a 15 meter pitch, has the lowest ratio, with 35.30 CO₂-eq/MWh. Case F, high site productivity forest with a pitch of 15 meters, has the highest ratio with 59.36 CO₂-eq/MWh.

Table 4.10: The ratio between emission and production for the six cases A-F. The values are given in kg CO₂ per MWh.

Ratio between emission and production [kg CO ₂ /MWh]		
Type of area	Pitch	
	8 meters	15 meters
Constructed area	38.90	35.30
Forest with low site productivity	52.28	57.77
Forest with high site productivity	53.22	59.36

In Figure 4.15, the ratio between production and CO₂ emission is illustrated. The light green line represents high site productivity forest, the dark green line low site productivity forest, and the brown line present the results for the constructed area.

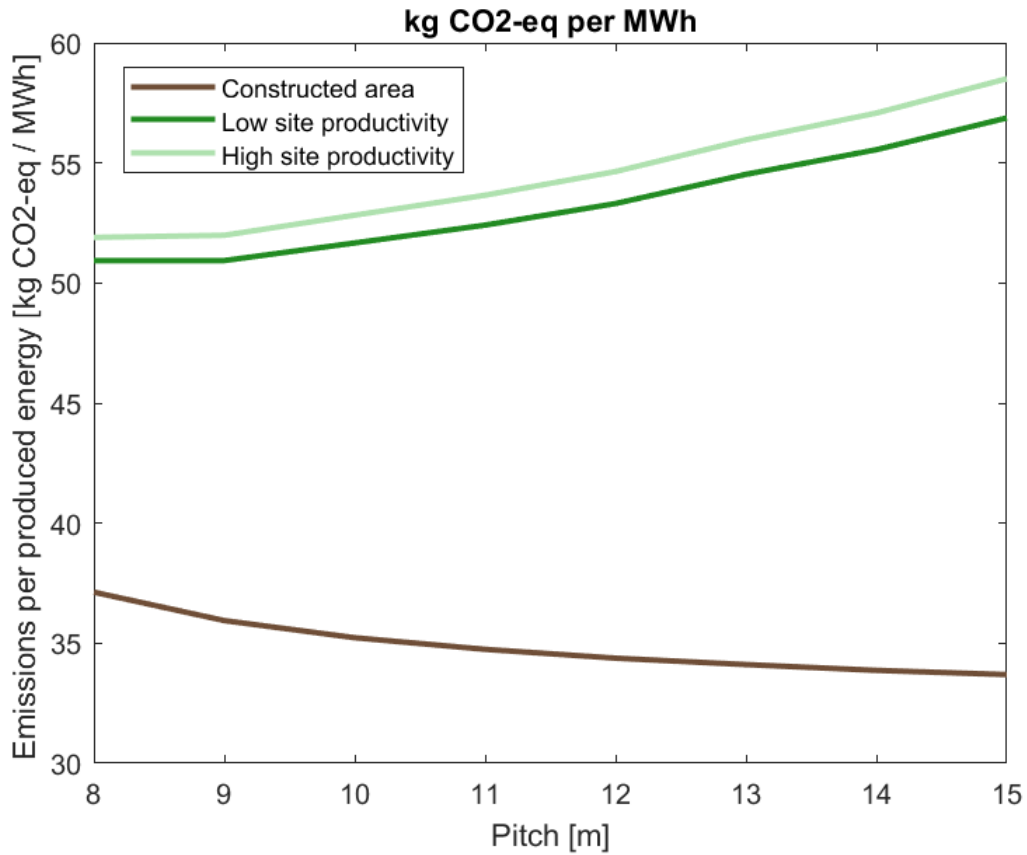


Figure 4.15: Production and emissions [kg CO₂-ekv/MWh]

Table 4.11 presents the results for both the production and total emission for the PV panel’s lifetime. The lifetime includes the production of the panels, transport, land-use change and recycling. The highest energy production over 30 years is for a pitch of 8 meters, with 957 592 MWh and 954 414 MWh for constructed area and forest respectively. The highest total emissions are for high site productivity forest with a pitch of 8 meters, with 50 796 ton CO₂-eq, followed by low site productivity forest with an 8 meter pitch, with 49 899 ton CO₂-eq. The lowest total emissions are for constructed area with a 15 meter pitch, with 20 135 ton CO₂-eq.

Table 4.11: Production and total emission over the panels lifetime.

Pitch [m]	Production over 30 years [MWh]		Total emissions [ton CO ₂ -eq]		
	Constructed area	Forest	Constructed area	High site productivity	Low site productivity
8	957 592	954 414	37 250	50 796	49 899
9	882 196	878 877	33 223	46 769	45 872
10	804 606	801 288	29 699	43 246	42 348
11	746 506	744 003	27 177	40 723	39 825
12	698 754	695 520	25 169	38 715	37 818
13	647 881	644 759	23 155	36 702	35 804
14	609 944	606 907	21 645	35 192	34 294
15	570 348	567 451	20 135	33 682	32 784

The ratio between the production and total emissions in Table 4.11 are presented in Table 4.12. A low ratio indicates a high production in relation to emission. For forest, the lowest ratio is for a pitch of 9 meters. The ratio is then 53.22 kg CO₂-eq/MWh for high site productivity and 52.19 kg CO₂-eq/MWh for low site productivity. The lowest ratio for constructed area is for a pitch of 15 meters, and is 35.30 kg CO₂-eq/MWh.

Table 4.12: kg CO₂-eq per MWh energy production.

Pitch [m]	Constructed area [kg CO₂2/MWh]	High site productivity [kg CO₂2/MWh]	Low site productivity [kg CO₂2/MWh]
8	38.8997	53.2225	52.2821
9	37.6594	53.2148	52.1935
10	36.9117	53.9702	52.8500
11	36.4052	54.7350	53.5285
12	36.0198	55.6638	54.3733
13	35.7404	56.9232	55.5311
14	35.4875	57.9853	56.5063
15	35.3034	59.3558	57.7740

5 Discussion

In this chapter the methods, assumptions and results from the LCA in SimaPro, land-use change calculations and simulations in PVsyst will be discussed. In addition, the comparing results and reflections of both production and emissions will be discussed.

5.1 Life Cycle Interpretation

The discussion part of an LCA, called life cycle interpretation, is the fourth phase of the analysis and is described in ISO 14040. In this section, the results from the earlier phases in the LCA will be compared, evaluated and discussed based on the goal and scope specified for this analysis.

5.1.1 Methodology

In order to estimate the total greenhouse gas emissions for the life cycle of the PV panels, the IPCC 2013 GWP100a methodology was used as it has the impact category Climate Change. This category includes factors and substances that contribute to climate change, such as CO₂. In addition, the method is developed by a wide range of researchers on climate change and experts from IPCC within climate assessment. However, the method is based on data retrieved from 2013. From 2013 to 2023 there have been collected more information, data and knowledge within the field related to global warming and its impacts. This development has not been taken into account in the analysis, as the method from 2013 was used for this LCA.

According to SimaPro's database manual, there is a successor called IPCC 2021 GWP100 based on updated data from an IPCC report from 2021. This method was not available in the SimaPro version used to collect the LCA results for this analysis. Potentially, this method could have provided more updated and correct results for the greenhouse gas emissions for the ground-mounted solar park.

GWP100 is the most commonly used indicator in SimaPro for the chosen methodology. It indicates how much greenhouse gases contribute to climate change over a time span of 100 years. As the solar park is assumed to be operative for 30 years, it could have been applicable to use GWP20 with a time horizon of 20 years. In spite of this, GWP20 only considers impacts within 20 years after the emissions occur and focuses mainly on gases with a short life span. As a result, the GWP would have been higher for some greenhouse gases, such as CH₄ which has a shorter lifetime in the atmosphere before it is naturally broken down, than CO₂. Therefore, GWP100 was chosen, as the method is assumed to give the most correct results in relation to most of the different greenhouse gases' lifetime.

It was assumed that the backsheet for the monofacial PV panel can be replaced by glass or transparent backsheet to get a bifacial panel. This assumption was made as there was not any inventory lists available online from trustworthy sources that were applicable to the bifacial JA-solar panel studied in this thesis. Therefore, materials from the backsheet were replaced by the same glass used as the top layer of the PV panel. It was assumed that the material was included for the first time in the composition of the PV panel. If some materials in the backsheet were included in an earlier process, these materials are still included in the results from the analysis. Additionally, other materials from the bifacial panel may have been omitted as the inventory list consists of various materials, and the materials assumed for the backsheet and front glass might have been wrong.

5.1.2 Results

Table 4.2 shows the emissions for the various processes in the LCA analysis, where the total greenhouse gas emissions for one panel, excluding the transport from China to Norway, is 582.61 kg CO₂-eq. PV panel production has the highest CO₂ emissions, followed by PV panel mounting and recycling. The least amount of emissions come from transporting the solar panels to Halden.

The emissions from the PV panel production are mainly from the production of the PV cell as shown in Figure 4.1. This is as expected as there are many processes leading up to the production of the cell. These processes are the extraction of materials, the processing of silicon and the production of the silicon wafer. All of these processes are energy-intensive and release a high amount of greenhouse gases. A PV panel requires 17.6 kg of solar glass per square meter. Because the solar glass covers both the front and the back side of the panel, it is reasonable to assume that bifacial panels have higher emissions from glass production than monofacial panels.

Another process that contributes to the total emissions is aluminum alloy. In the production of the PV panels there is only 2.13 kg aluminum alloy, but this process alone releases 14.5 kg CO₂-eq. This might be because SimaPro includes the production of aluminum in the emissions. The flow chart for the production presented in Figure 4.1, shows that electricity releases 51.48 kg CO₂-eq per 1 m² PV panel throughout the entire process. Electricity is one of the processes that release the most emissions, which could be expected as the electricity in China is mostly produced by coal and oil. The results from the production process would differ if alternative glass and different materials had been used for the frame. As SimaPro includes the entire process of producing the materials, would these processes been included in the result.

Figure 4.3 shows the emissions from the transport from Nanjing to Halden. This transport releases 220 kg CO₂-eq for all the panels, regardless of how many panels are needed for the park. Large solar parks require many panels, so the assumption that all these panels are transported by only one ship might not be accurate. If more ships are needed, the emissions from the transport might increase. Another assumption that was made in the analysis was the type of transport used for the distance between China and Halden. Ideally, a transoceanic ship should have been used in the analysis, because this is a ship that is intended to cross oceans and travel longer distances. This would have given a different and more realistic amount of emissions compared to the emission from the chosen ship.

The mounting process releases 91.9 kg CO₂-eq per square meter as shown in Figure 4.4. This is 30.1 kg CO₂-eq less than the emission from the production of the PV panel. The largest part of the emissions in the mounting process comes from reinforcing steel. There are various factors that may change the emissions from the analysis of the mounting process. Firstly, the values in the IEA PVPS report are from 2012. The amount of materials needed for the mounting might have changed during the last 11 years, as there has been a high technology development in the solar industry over the last decade. Because of this, the emissions from the analysis might not reflect the actual emissions today.

Another factor is the size of the panels, as less material is required per square meter for the mounting of larger panels. In the simulations done in PVsyst there are two panels in height and 27 panels in length in one table. The size of the tables was not taken into account in the LCA analysis. The size of the tables might affect the amount of materials required for the mounting, especially the amount of steel. Using another material than steel in the mounting might decrease the emissions, as reinforcing steel contributes to 84.87% of the emissions. The mounting structure used in the analysis is based on a mounting structure in Switzerland. The structure and foundation might be different in Norway with varying amounts and different types of materials.

The recycling process releases 30.05 kg CO₂-eq per panel, where the biggest emissions come from plastic waste as shown in the flow charts for the various processes. Figure 4.5, 4.6, 4.7 and 4.8 shows these processes. Since the results from the recycling process are composed of the results from four different processes, the results might not represent reality. The amount of glass, aluminum and copper may vary from different panels. Therefore, each process might release a different amount of emission than calculated. In addition, more materials recovered from the c-Si panels could be considered. The recovery of these materials would also release emissions and might alter the total results.

The recycling process is based on the IEA PVPS report, which takes place in Western Europe. This process might be different in Norway, and the amount of emission may differ. The JA-solar panels have a warranty of 30 years. It is reasonable to assume that the recycling process will be improved over the next 30 years. As a result, emissions from the recycling process can be reduced.

The results from this analysis is mainly based on the IEA PVPS report. The panel in the IEA PVPS report is not the exact same PV panel as the JA-Solar 550 Wp panel. The JA-Solar panel might not have the same amount of materials, and use processes and materials from the same places as the IEA report. Therefore, the results of the analysis may not represent the actual emissions in life cycle of the JA-solar panel. The production process, the transport, the mounting and the recycling of the panel might be different then the ones used in this analysis.

5.1.3 Production in China

In the LCA, it was assumed that the panels were produced in China, since JA-solar produces most of their panels in China. By choosing a panel produced in Europe instead, the emissions might decrease as the energy mix in Europe consists of less coal than in China. The energy consumption during the production of the PV panels releases 51.48 kg CO₂-eq per m². The EU solar energy strategy in the REPowerEU plan has a goal to increase the solar photovoltaic capacity in Europe, which includes the production of PV panels. If the production is moved from China to Europe, this could increase the availability of more sustainable solar panels, as the energy mix in Europe consists of more renewable energy sources and energy sources.

PV panels produced in Europe would also reduce the transport distance to solar parks in Norway. There is transport included in the production processes as well as the transport from the production site to the mounting site. The emissions from the transport between the extraction sites and the production site might not change that much, but the emissions from transport to the mounting site will be considerably smaller. In addition, different means of transportation might be used if the production is in Europe compared to China.

5.1.4 Uncertainties

There are some other uncertainties with the results besides the ones previously mentioned. The LCA analysis is based on the inventory lists from the IEA PVPS report, with specific materials and processes. In SimaPro there are multiple materials and processes. As a result, chosen processes and materials may differ from the report by accident. Since SimaPro includes the entire life cycle of many of these processes, a wrong process could lead to more or less emissions than the actual process. Another uncertainty is that the IEA PVPS report, as well as the analysis in this thesis, does not include emissions during the years the PV panels are installed and operative. The analysis does not include energy used for construction work, maintenance, disassembly and infrastructure. To make an analysis of the complete life cycle of a PV panel, all the required energy and all the processes that could potentially release CO₂ emissions should be included. As a result, the total emissions from the LCA for the solar park are even higher as not all the life cycle parts were included.

5.2 Land-Use Change

This section will discuss the results, methodology and uncertainties surrounding the land-use change calculations.

5.2.1 Results

Table 4.3 and 4.4 shows that the emission from a land-use change from forest with low site productivity to settlement is approximately 12 650 ton CO₂-eq, and the emission from forest with high site productivity is approximately 13 550 ton CO₂-eq. It was expected that the emissions from a forest with high site productivity would be a bit higher than one with low site productivity, since that land-use change has higher emission factors. The results meet this expectation, as the high site productivity forest had around 900 ton CO₂-eq more emission than forest with low site productivity.

Table 4.3 and 4.4 shows that the forest with high site productivity has both more absorption of CO₂ in case of no land-use change and higher emission in case of land-use change. The reason for this might be that high site productivity means high capacity of wood production, and growing trees and vegetation absorb carbon at a high rate. In addition, forest with high site productivity often have more biomass and larger trees, meaning more carbon is sequestered than in a forest with low site productivity. All of this contribute to the higher value of total emissions for a high site productivity forest.

Potential emissions from CH₄ and N₂O without land-use change were taken into account in the calculations. As future emissions from CH₄ and N₂O are avoided when the forest is removed, this contributes with a negative value that helps reduce the total carbon footprint. However, the potential absorption of CO₂ in the forest with no land-use change is a fair bit higher than the potential emission of CH₄ and N₂O. Because of this, the carbon storage in forest will increase over time, and removal of the forest has a considerable contribution to the carbon footprint from a land-use change. The values for potential emissions from CH₄ and N₂O without land-use change were the same for both forest with high and low site productivity, and therefore did not affect the difference between these two cases.

For the case with constructed area, all absorption and emission was set to zero, as shown in Table 4.5. This was done as a constructed area falls under the area type settlement. Because of this classification there is no land-use change, even if the use of the land changes. The actual total emissions might not be zero, but most likely close enough that it is reasonable to assume zero. A constructed area is highly impacted by humans, which means that the land-use change has already happened. The soil is very little biologically productive, which means that potential vegetation that might grow there is small. In case of growth of grass and smaller plants, these could absorb some CO₂ over the spring and summer months, but this would be released again as they die over the winter. For the area to absorb a significant amount of CO₂, trees need to grow there, which would be impractical in a solar park as they would create shade.

5.2.2 Methodology

It is important to be aware that there has been a lot of recent and ongoing research on emissions from land-use change, and the values for emission factors might change in a few years as more research is done. The Excel spreadsheet from the Norwegian Environment Agency used for the calculations in this thesis is from 2019, and has been updated since then. However, the new spreadsheet is still for consultation, which is why it was chosen to use the older version. This decision was discussed with an expert from the Norwegian Environment Agency. As only land-use change from forest to settlement was calculated in this thesis, using the older spreadsheet was reasonable as there was little change in these emission factors. The biggest modification was in the emission factors for bog and organic soil, which was not relevant for this thesis.

The Excel spreadsheet calculates greenhouse gas emission over a period of 20 years. These calculations were adapted to 30 years, to include all the operational years of the solar park. This was done by using a separate emission factor for the area after the transition phase of 20 years. There might be uncertainties associated with these calculations, mostly surrounding the emission factor. The emission factors were extracted from the Excel spreadsheet from the Norwegian Environment Agency for the type of area analysed in the thesis. The methodology was also discussed with an expert in the field from the agency, which assured quality to the calculations. Uncertainties associated with emission factors will be discussed in Section 5.2.3.

The area used in this thesis is an unspecified area close to Halden. Mineral soil was assumed for this area, as that is normal practice when the area is unspecified. The difference in emission factors between mineral soil and organic soil is considerable. The amount of organic matter in the soil can vary, and this will affect the emission. If the area where the solar park will be built is known, the actual soil condition in that area can be checked. This can be done in NIBIO's map with area information called Kilden. This map also contains information about site productivity. Often, forest with high site productivity and low site productivity can overlap. When looking at an area as large as a solar park, in this case 300 000 m², it is likely that the area will contain forest with more than one type of site productivity. Using NIBIO's map when planning the development of a solar park can be beneficial to avoid areas of soil with a high amount of organic matter and high site productivity.

5.2.3 Uncertainties

An uncertainty in the land-use change calculations is that the age of the forest is not specified. Older forests often store more carbon than younger forests, while younger forests have a higher rate of carbon absorption. If the deforested area was an old-growth forest, there might be more emissions released immediately as the forest is cut. A younger forest might release less CO₂ from deforestation, but if it remains untouched, it can absorb more CO₂ over the coming decades. The potential absorption of CO₂ without deforestation is accounted for in the land-use change calculations. This value might be inaccurate, as the age of the forest is not considered and could affect this value.

Another uncertainty with the land-use change calculations is that the definition of settlement is wide, and includes all types of developed areas. This could be everything from parks, gardens, and golf courses to buildings, parking lots and gravel pits. There might be small differences between these areas, which are not accounted for in the calculations. Construction of buildings and roads includes removal of both trees and soil to create a solid foundation. Other constructions, for example power lines, would only require cutting of tall trees in conflict with the power line, which means soil and lower vegetation will be affected to a smaller extent. This might be the case for ground-mounted solar panels as well, depending on how they are mounted.

Often, profiles are piled into the ground to form the foundation of open ground systems. In situations where piled profiles cannot be used, it is normal to use concrete foundations. Piled profiles are likely to have a smaller impact to the soil than the concrete foundations, as a lot less soil would be removed. In addition, the pitch will affect how much of the ground is impacted. A higher pitch will leave more ground between the rows of solar panels. If the solar park is mounted with concrete foundations, a small pitch would mean more concrete and removal of soil than a higher pitch. This is not considered in the carbon footprint calculations from land-use change.

There will also be uncertainties related to the emission factors. There are several factors affecting these uncertainties, such as having deficient data or not representative data when developing emission factors. The uncertainty can be reduced by getting better adapted models and more measurements. Here, the requirements for precision must be balanced with what is practically feasible. It is in general a greater uncertainty related to emissions from soil, as collecting soil samples is expensive and it often takes a long time before changes in soil carbon are seen. It should also be noted that emission factors for land-use change are national factors, and are not adapted regionally. This adds an uncertainty to the results. If the emission factors were adapted regionally, the results may be more accurate.

5.2.4 Other Area Types

The largest emissions come the first year when living biomass is removed. Then, emissions from the soil are calculated for a period of 20 years, as it is assumed that the amount of carbon in the soil have stabilised after 20 years. Using an area with less living biomass, such as trees and plants, will therefore lessen the immediate emissions. Logging sites where the vegetation is already cut, as well as abandoned pastures and farmlands, will therefore have little emission from living biomass, mostly the soil. In addition to a lower carbon footprint, advantages of using these kind of areas are that deforestation will be avoided, and the development of a solar park will have less impact on biodiversity and ecosystems in forests.

A type of area that should absolutely be avoided is bog. The emission factor for bog is more than five times the emission factor of forest with low site productivity, and using an area with bog for building the solar park would therefore significantly increase the emission from land-use change. Avoiding areas with bog would be highly preferable to minimise greenhouse gas emission when building a solar park.

5.2.5 Land-Use Change for Other Renewable Technologies

When comparing area required for ground-mounted solar parks to wind farms, solar parks have a lot more area that will be directly impacted by land-use change per TWh than wind farms. Area used for wind farms are usually on top of hills and ridges with relatively poor soil. Also, most of the land-use change for wind farms are due to roads, and it might be possible to avoid the most carbon-rich soil in the area when deciding where to put the roads. Because of this, one can assume that there is less emission from land-use change associated with wind farms than ground-mounted solar parks. This only applies if a forested area is used for the solar park. If the solar park is built on an already developed area, for example a constructed area, it is reasonable to assume that emissions from land-use change will be higher for the wind farm.

It is harder to compare the emissions from land-use change with hydropower, as the area required for hydropower varies a lot and is very dependent on whether regulating reservoirs are a part of the equation or not. The potential for hydropower in Norway is already well utilized, and it is more likely that already existing hydropower plants will be further developed than that new ones will be built.

5.3 PV Production

In this section, the methods and results related to the simulated PV production in PVsyst will be discussed. This includes topics such as the PVsyst software, orientation settings, albedo, solar irradiance, and losses.

5.3.1 PVsyst Software

Generally, for the simulations in PVsyst, some simplifications have been done that may give results that differ from reality. It is a simplified PV system where some settings in PVsyst have not been taken into consideration. This will be discussed later in this section. However, the main focus and goal of the thesis is to compare the cases and find the ratio between production and greenhouse gas emission, and the ideal combination of pitch and area type.

The simulation program, PVsyst student version, was used to simulate solar production for the different cases. Pvsyst also offers other licenses where there are unlimited features and unrestricted access to the components database. The student version used in this study has many of these features, but is limited to the use of generic components. A version with unlimited features could potentially generate more correct results for the total PV production. Another uncertainty is that the Meteonorm software, which provides meteorological data for a given location in PVsyst, does not include the effect of far shadings from mountains at sunrise and sunset. This could potentially have affected the PV production results, as the shadows from mountains and hills are omitted.

5.3.2 Methodology

The geographical site for all the simulations was an area close to Halden, in the southeast part of Norway. Therefore, the results from the simulations in PVsyst are not representative for all places in Norway. However, the simulations could give a relatively correct indication of PV production at locations nearby the chosen area or sites characterized by the same climate, solar radiation and weather conditions as Halden.

The total time interval for the simulations was set to one year of solar energy production. It is assumed that the solar park has an operation time of 30 years. During this period the climate and weather conditions may vary and change, especially because of the climate change. As a result, the estimated solar radiation in PVsyst based on data collected from the Meteonorm may differ from reality.

The PV system designed in PVsyst had a constant azimuth and tilt angle. In addition, the simulations were optimized with respect to yearly irradiation yield. As the sun's path varies throughout the year, the PV production from the solar park could have been improved by changing the field type of the panels. As a result of solar technology development, there have been released PV panels with sun tracker systems, where the panels can rotate and change their tilt relative to the sun's path across the sky. This development has not been taken into account in the simulation, and could potentially give a greater yearly and monthly PV production.

In the simulations in PVsyst, only the shades from the panels were taken into consideration. This simplification is not realistic, especially for ground-mounted solar parks installed in a Norwegian landscape with natural shading elements such as mountains, woods as well as plants and crops. These elements could reduce the energy production results for the simulated solar park, especially during wintertime when the sun's path is low across the sky and the shadow for the panels could potentially increase.

The 3D-scene of the solar park was mainly designed to include the shades from the panels. This 3D-scene is a rectangle of 300 000 m² filled with tables, which is not a realistic design. Firstly, it is unlikely that a solar park of such a size would have a rectangular shape, as the geographic area occupied by the solar park is likely to encompass a wide variety of shapes. The setup and number of tables will differ depending on the shape of the solar park, and therefore affect the solar energy production. However, the shape of the solar park is not important when comparing cases, as long as the shape is consistent in all the cases being compared. This applies to the simulations done in this thesis. An area adapted to the surroundings would give more realistic results.

Another fact that makes the 3D-scene unrealistic is that the area is assumed flat ground by PVsyst. The probability that the entire area is flat is low, so the fact that PVsyst assumes flat ground is unrealistic. The shadows that can appear on the panels because of uneven ground will not be included in the simulation. Because of this, the simulations will be representative for areas with flat ground. However, the horizon for the chosen location in Halden was included in the simulations. As shown in Figure 3.3, the horizon only blocks a small amount of the incoming solar irradiance, as the chosen place has relatively flat terrain with no hills. This is positive in terms of ensuring optimal and high solar energy production in a ground-mounted solar park for a specific location.

As presented in Section 3.4.5, the wind loss factor was excluded when calculating the thermal parameter because of recommendations by PVsyst. Wind can have a cooling effect on the PV panels and potentially improve their overall performance and efficiency. As a result, the total yearly solar energy production could have been higher and more realistic if the wind factor was included for all cases.

For the simulations in PVsyst it was assumed one transformer and park transformer for the entire system. In reality, more transformers are often implemented in a PV system. The number of transformers in a PV system varies depending on factors such as the size of the solar park, with its number of solar panels as well as the electrical distribution system. In addition, more transformers could reduce the sensitivity of power distribution if the transformer is inoperative or needs maintenance. In this case, a park with more transformers could increase the security of supply to the distribution network. This provides an increase in reliability.

Albedo Value

The albedo values were different for constructed area and the forests, as the surfaces are different. Although the albedo values did not have the biggest impact on the production, the values presented in Table 3.14a and 3.14b could have been more accurate. Firstly, the snow cover values could have been more accurate as the data extracted from The Norwegian Climate Service Center was the monthly average snow cover from 2017 to 2022. To get more specific values, daily data could have been used instead of monthly data. In addition, data from even more years could have been studied, but this was not possible as there was no available data from before 2017. By looking at data from a longer period, a more accurate snow pattern could have been detected.

With more detailed information about the ground surface of the solar park each month, the albedo values would be more accurate. Green grass and brown ground would reflect light differently, and therefore have different albedo values. The albedo values used in this thesis are based on assumptions of the amount of snow, brown ground and grass for the various months. These assumptions may be inaccurate, and more detailed information would reduce this uncertainty. Another assumption was that forest with high and low site productivity reflect light in a similar manner. This assumption was based on the fact that the forest types have vegetation with similar colors. However, the vegetation in a forest might vary, and therefore reflect the light differently.

As mentioned, the albedo values did not have a big impact on the production. This may be because there is not much difference between the albedo values for constructed area and forest for the various months. Equation 2.3 shows how the albedo value impacts the ground-reflected radiation on a tilted surface. When the albedo value is similar for the different area types and months, the ground-reflected radiation will not change much. As the bifacial panel converts the solar irradiance from both the front and back side, the ground reflection will have a direct impact on the production. Small differences in reflection between the area types will result in small differences in production between area types. The production from constructed area is higher than the production from the forest. This is because the albedo values for concrete are higher than the value for grass, and the bifacial part of the PV panel will produce more with higher reflection from the ground.

5.3.3 Results

The simulation results presented in Table 4.6 indicate that there are almost twice as many numbers of modules when the pitch is 8 meters, with 63 936 panels, compared to 15 meters where there are 34 560 panels. This is related to the fact that a solar park with a pitch of 15 meters has more unused area between the rows. This is also seen in the module area. A solar park with a pitch of 8 meters has a module area of 165 163 m², and a park with a pitch of 15 meters has a module area of 89 277 m². The number of modules also affects the number of inverters. As a result, the cases with a pitch of 8 meters have in total 161 inverters, and cases with 15 meters have 87 inverters. As there are more panels and active module area for a low pitch, this increases solar energy production. The system power for 8 meters was estimated to 35.16 MWp with a total power of 25.7 MWac, and a system power of 19.01 MWp as well as 13.9 MWac in total power for 15 meters.

Main Results

Table 4.7 and 4.8 present the main results for forest and constructed area respectively. All cases have the same values for the monthly global and diffuse horizontal irradiation and ambient average temperature. This is because they are based on the same solar and weather data collected from Meteonorm. However, the values are different throughout the year. The global irradiance for the cases indicates that the solar irradiance reaches its highest point in June with 173.5 kWh/m². This is over 33 times more solar radiation than in December where the horizontal radiation is 5.2 kWh/m². This difference appears as the PV system was optimized with respect to yearly irradiance yield. It is conceivable that the difference would have been smaller if the orientation of the PV panels had been optimized for winter months.

The total amount of diffuse and direct irradiance is the global irradiance. The ratio between diffuse and total horizontal irradiance is greatest during the autumn and winter months. In December, the diffuse counts for 81.7% of the total global horizontal irradiance. This is connected with the fact that Halden, as well as the Norwegian climate, is known for more cloudy and rainy weather in this specific period. This could also explain the lower solar irradiance on PV panels in the winter season.

PV solar irradiance affects solar energy production and the amount of energy injected into the grid (E_{grid}). E_{grid} is highest for Case A, representing a constructed area with a pitch of 8 meters. In total for the whole year, the system delivered 34 050 MWh to the grid. This is 113 MWh more than for forest with the same pitch. This may be explained by the fact that the albedo values in total are generally higher for constructed area throughout the year, and during the summer when the solar irradiance is higher. As a result, this will increase the yearly solar energy production.

E_{grid} is highest June for Case A, where it is estimated to 5 496 MWh. The production is significantly lower during winter months due to the low solar irradiance discussed above. In addition to this, the winter period generally has reduced daylight due to the location of the solar park north in the Northern Hemisphere. The further north, the lower the sun's path across the sky in winter. This is reflected in the results for E_{grid} during November, December and January. In this period, Case A had the highest E_{grid} value of only 781 MWh.

Performance Ratio

The cold temperature during winter affects the performance ratio positively. The performance ratio is presented in Table 4.10 for forest and Table 4.13 for the constructed area. For Case A, C and E, with 8 meters pitch, the performance ratio is highest in April, while it is highest in February for Cases B, D and F where the pitch is 15 meters. This is caused by the fact that the ambient temperatures in these months are low. As a result, the performance ratio is higher even though the solar irradiance is greater in June.

The ambient temperature for all cases is 6.01°C in April and -0.93°C for all cases in February. The reason why the performance ratio is highest in April for the 8 meters pitch may be explained by the fact that there are more panels that could produce solar energy, the high solar irradiance this month, and the low temperature. This point is shown in the loss diagram in Figure 4.11 and 4.14, where both diffuse and direct irradiance is generally higher for a pitch of 8 meters. For the pitch of 15 meters, the performance ratio is highest in February. This might be because there is typically more snow that month, which could reflect more of the incoming solar irradiance to the panel. In addition, it is the coldest month, and low temperatures generally increase the solar cells' efficiency.

Additionally, Table 4.10 for forest and Table 4.13 for constructed area indicates that the performance ratio for Case A, C and E, are, in general, significantly lower than for Case B, D and F. This might be connected to shading, as the rows of panels are closer when the pitch is 8 meters compared to 15 meters. In addition, the sun's path is also lower during winter when the ambient temperature is low. As a result, the south-orientated panels in the front rows will create shade for panels further back. Because of this, the performance ratio is greater when the pitch is higher. The shading does also represent an irradiance loss as an amount of the incoming solar irradiance does not reach some of the PV cells due to shading from other panels in front. As seen in Figure 4.11 and Figure 4.14, the irradiance losses are higher for Case A, C and E, with -7.8% , compared to Case B, D and F where the loss is -2.7% . The reason for this is, as mentioned, that there are more panels when the pitch is 8 meters, which creates more shade for the other panels in the solar park.

Losses in the PV System

E_{array} in Table 4.7 and 4.8, represents the effective energy at the output of the array. For all cases, there is a small deviation between E_{array} and E_{grid} . This is because there are losses in the PV system. Figure 4.9 for forest and Figure 4.12 for constructed area shows a monthly overview of energy production as well as the losses. They indicate that solar energy production during the year is quite unstable. As mentioned, energy production is greater in the summer months compared to the winter months due to more solar irradiance, as there is more sun and daylight. In spite of that, the collection and system losses are also highest in this period. The collection loss (PV-array losses) dominates the most. This loss is also represented in the loss diagrams, Figure 4.11 for forest and Figure 4.14 for constructed area. This array loss dominates because the ambient temperature in Halden is higher in these months, as shown in Table 4.7. Higher temperature causes more losses and lower efficiency for PV panels. In spite of this, the monthly solar energy production is still greatest in June for all cases, as there is significantly more solar irradiance in this month.

Both the loss diagrams in Figure 4.11 and 4.14, as well as Figure 4.9 and 4.12 for normalized production for forest and constructed area respectively, present the system losses. System losses are losses mainly related to the inverter and its efficiency. It occurs often when the DC solar power is converted to AC due to ohmic resistance in the inverter. In addition, the inverter components represent resistance that generates heat loss.

Based on the simulation results, the inverter loss is relatively similar and small for all cases, as the system loss for 8 meters is 0.16 kWh/kW_p/day and 0.17 kWh/kW_p/day for a 15 meters pitch. This may be explained by the fact that the same inverter has been used for all cases. However, the system losses are highest during the summer season for all cases, as seen in Figure 4.9 and Figure 4.12. The system losses may increase during the summer season as the temperature is higher. When the temperature rises, the electrical resistance and wire loss increase. This results in a higher loss during this period and the efficiency of the inverter decreases. In addition, several types of inverter losses in the loss diagrams in Figure 4.11 and 4.14 are usually zero according to PVsyst. They will not be accounted for because of limitations in the thesis. In reality, these losses could impact the PV production results, but because this thesis mainly looks at comparison between cases, this impact will not be of much importance.

There are also losses related to the transformer and its wiring. These losses are represented at the bottom of the loss diagrams in Figure 4.9 and Figure 4.12. The MV transformer loss is about -1.3% for 8 meters and -1.25% for 15 meters. For all cases, the HV transformer loss is about -1.6% and the AC ohmic loss, from wiring up to the injection point, is about -1.2%. Just as for the inverter, the losses related to the transformer and wiring are relatively similar and small for all cases, as the same transformer and wiring have been used for all cases. However, the amount of energy loss in the inverter, transformer and wiring could be high as there is a high amount of solar energy injected into the grid per year.

The detailed losses for the whole year for the PV system are presented in Figure 4.11 for forest and Figure 4.14 for constructed area. As all cases are located at the same location in Halden, the general solar irradiation on top of the losses diagram is 1 000 kWh/m² for all cases. However, the global incident in collector plane value contributes with about 24% more irradiance for all cases. This represents the obtained gain from the fact that all the PV panels have tilted planes. As a result, the panels are able to produce more energy as the sun's path varies throughout the year compared to a tilt angle of zero, which is normal near the equator.

Some of the main results in the PVsyst simulations shown in the losses diagrams are related to the bifacial panels' positive contribution of solar irradiance on the PV panels. Global incident on the ground for Case A, C and E is 339 kWh/m² on an area of 288 746 m², and 626 kWh/m² on an area of 292 648 m² for Case B, D and F. This value indicates the global irradiance reaching the backside of the solar panel. The value is higher for a pitch of 15 meters as there is minimal shading compared to the cases with a pitch of 8 meters.

PVsyst also calculates losses related to the albedo value, called ground reflection loss in the loss diagram, which is connected to the loss of irradiance due to the surface's area ability to reflect solar radiation. An albedo value of 100% represents "perfect reflection", however the average albedo values for one year used in the different PVsyst simulations were between 24% and 26%. This indicates that the rest of the incoming solar radiation is absorbed by the surface, and represents the ground reflection loss of -74% and -76% for the PV system for all cases. In addition to the bifacial effect, some incoming solar irradiance was reflected from the ground and reached the PV panels' front side. The ground reflection on the front side was 0.3% for a pitch of 8 meters, and about 0.8% for a pitch of 15 meters. The reason for this is the same as explained above.

The view factor from the loss diagram represents the ratio between solar irradiance reflected from the ground that reaches the backside of the bifacial panel, and the irradiance lost and reflected back to the sky. For Case A, C and E, the view factor is about -58%, and for Case B, D and F it is about -80%. This value is higher for Case B, D and F, because the pitch is higher and less panels are installed in the solar park. As a result, there are more unused area where incoming solar irradiance can be reflected out in the sky.

As mentioned in Section 3.4.5, the yearly soiling losses factor was set to default and 3%. This is also presented in the loss diagram Figure 4.11 and 4.14. As there are different seasons in Norway with pollen dust during spring, leaves in the autumn season as well as snow and ice during winter, it could have been appropriate to define a soiling factor for each month, and not for the whole year, as soiling conditions varies with the different seasons throughout the year. Potentially this could have improved the result and made them more precise and representative of reality.

5.4 Ratio between Production and Emissions

In this section, the results from the simulated PV production and calculated emissions in Section 4.4 will be discussed and analyzed. The result for the different cases will be compared, as well as the additional pitches between 8 and 15 meters.

Table 4.10 presents the ratio between production and emission for the Cases A-F. Case B has the lowest ratio of 35.30 kg CO₂-eq/MWh. The second lowest is Case A with a ratio of 38.90 kg CO₂-eq/MWh. This is expected, as these two cases are for constructed area, where the emissions from land-use change are assumed to be zero. There is only greenhouse gas emission from the life cycle of the solar panels in these cases. In addition, the PV production is highest for these cases, which reduces the ratio. Case D and F have the highest ratio between emissions and production, with a ratio of 57.77 kg CO₂-eq/MWh and 59.36 kg CO₂-eq/MWh. Case D has low site productivity and Case F has high site productivity, both these cases have a pitch of 15 meters. This means that when looking at a forested area, it might be better with a shorter pitch closer to 8 meters.

Case F with high site productivity has the highest ratio as this forest type has the largest total carbon footprint. In addition, the PVsyst simulation results estimated that forest with a pitch of 15 meters has the lowest PV production. The production combined with the emissions gives the high ratio between emission and production, which indicates that the worst case might be Case F with high site productivity forest and a pitch of 15 meters.

Looking at Figure 4.15, it is evident that the constructed area has the lowest emission of CO₂-eq per MWh produced solar energy. As previously mentioned, this is expected as it is assumed zero emission from land-use change for constructed area. Looking at the graph for constructed area, the emission per MWh decreases with a higher pitch. However, it kind of evens out a bit after a pitch of 11-12 meters. A pitch of 15 meters is the one with the least amount of emission, but also the least amount of production. One could therefore argue that the optimal pitch for this type of area is 12 meters, as the change in ratio between emission and production is minor, but the production is higher. Looking at Table 4.11, the production for a pitch of 12 meters for constructed area is 698 750 MWh, which is over 100 000 MWh higher than the production with a 15 meter pitch.

The graphs for forest with high and low site productivity in Figure 4.15 look very similar. However, the high site productivity is a bit higher than low site productivity. Both graphs do not change much between pitch 8 and 9 meters, but start increasing after the pitch of 9 meters. The lowest value for both high and low site productivity is at a pitch of 9 meters, being slightly lower than for the 8 meters pitch. Table 4.12 shows that the ratio for an 8 meters pitch is 52.28 kg CO₂-eq/MWh for low site productivity forest and 53.22 kg CO₂-eq/MWh for high site productivity forest. The ratio for a 9 meter pitch is 52.19 kg CO₂-eq/MWh for low site productivity forest and 53.21 kg CO₂-eq/MWh for high site productivity forest. Because of this, one can argue that 9 meters is the optimal pitch for forest. In addition, a low site productivity forest is preferable to high site productivity.

Like mentioned before, the least favorable case is Case F with a pitch of 15 meters and forested area with high site productivity. This becomes evident when looking at Figure 4.15. Not far behind is a 14 meters pitch on high site productivity forest with a little bit higher ratio than a 15 meter pitch on low site productivity forest.

The results make it clear that it is preferable to build solar parks on constructed areas, as the emissions are considerably smaller and energy production higher. Moving the construction of solar parks from areas with large carbon storage and CO₂ absorption, such as forest, to already developed areas with smaller or no carbon storage or absorption, will help cut greenhouse gas emissions significantly. This will also be in line with UNs SDG 15 about protecting life on land. An alternative to ground-mounted solar power is to increase the installation of solar panels on roofs and buildings.

Even though there are large greenhouse gas emissions linked to ground-mounted solar power in carbon-rich areas such as forest, one can argue that the rapid and large volume of new renewable energy from solar parks might make up for the emissions from deforesting. Areas with the right solar conditions are limited, and it might be necessary to use forested areas as well to have the desired growth in solar power. If areas with high site productivity, organic soil and bog are avoided as much as possible, that will lessen the emission from the deforestation.

Another argument that building solar parks in forested areas is worth the CO₂ emissions from the land-use change is that developing new renewable energy can help cut greenhouse gas emissions in other sectors. The energy consumption is expected to grow in the coming years. An example is the electrification of the transportation sector, which will contribute to increase the power consumption. Developing solar parks can therefore contribute to phasing out the use and need for fossil fuels.

6 Further Work

While working on this thesis, several topics that could be interesting to investigate further have been identified. The main focus of the thesis has been on environmental sustainability, and how the construction of a ground-mounted solar park will affect the climate in terms of greenhouse gas emissions. It could also be interesting to examine how a land-use change will affect biological diversity and ecosystems. This is because a land-use change from forest to settlement will change the ecosystem in that area, and greatly affect the biological diversity. In addition, it would be interesting to further investigate the social and economic sustainability of the development of a solar park.

In the LCA, only the life cycle of the PV panels is studied. The solar park has a number of other components, such as the junction box, the inverter, the infrastructure, and the transformers. An LCA of the entire system would give a complete understanding of the carbon footprint from the installation of a solar park. It could also be useful to investigate the effect of moving the PV panel production to other countries than China, and how this could affect greenhouse gas emissions. A country with an energy mix of more renewable energy could potentially reduce the carbon footprint.

For the LCA, it could also be relevant to try different methods in SimaPro. A different method could give more updated or accurate results, for example if the IPCC 2021 method is used instead of IPCC 2013. Other methods could also look at different impact categories than just global warming potential, for example human toxicity, ozone depletion and acidification.

When it comes to land-use change, it would be useful to investigate more types of areas. For example abandoned farmland or pastures, logging sites, or other areas that have already been through a land-use change, and where the carbon footprint would likely be smaller than for a forest. It would also be interesting to look at the emissions from land-use change due to infrastructure, transformers and power lines, not only the solar park itself.

The simulations done in PVsyst are based on a location close to Halden. The results in this thesis would be inaccurate if the solar park is to be located somewhere else with other climate and weather conditions. Further work could include investigating PV production on other locations in Norway. It would be interesting to see how much the results would change if moving the solar park to other locations. In addition, other types of solar panels and inverter technologies could have been simulated and analyzed how this could change the solar energy production.

Lastly, it would be relevant to further investigate and compare the carbon footprint from a solar park with a wind farm or a hydropower plant. This was briefly discussed in this thesis and has a lot of potential for further work. This could potentially indicate which renewable energy source has the smallest greenhouse gas emission.

7 Conclusion

The purpose of this thesis was to investigate the climate and environmental effect of an installed ground-mounted solar energy park in Norway. This has been done through an LCA of the PV panels, land-use change calculations and PV production simulations. The main focus was on six cases, with a pitch of 8 and 15 meters for constructed area and forest with high and low site productivity.

The results from the LCA showed that the largest part of the emissions in the LCA comes from the production of the PV panel. This includes all processes that are a part of the production of the panel, such as the production of the cell, production of monocrystalline silicon, and the extraction of MG-silicon. The PV panels are produced in China, where a large part of the energy mix comes from coal and oil. Moving the production to for example Europe could potentially reduce the emissions from the production, as well as the transport. The mounting part of the PV panels also has a lot of emissions, most of it from steel production.

The land-use change calculations indicated that the best area for building a solar park is a constructed area, as the area has already been through a land-use change and it is reasonable to assume zero emission from using this area. The area associated with most green house gas emissions from a land-use change is forest with high site productivity. If a solar park is planned to be installed on a forested area, it would be preferable to find forest with low site productivity and mineral soil.

The results from the simulated PV production indicated that a solar park built on a constructed area with a pitch of 8 meters injects most energy to the grid, with a yearly contribution of 34 050 MWh. This is because this case has the highest albedo values and more panels that can produce energy, despite more shading loss. From these simulations, it was also evident that bifacial PV panels increased the production as they can collect solar irradiance from both sides. In addition, lower temperatures generally reduced losses in the system and increased the performance of the PV system.

Looking at the ratio between emission and production for the six cases, the best case is Case B for a constructed area with a 15 meters pitch. The worst case is Case F with a 15 meters pitch and high site productivity forest. When looking at every meter pitch between 8 and 15 meters, the results indicate that the best pitch for a constructed area might be around 12 meters. The best pitch for an area with forest might be 9 meters.

Despite large greenhouse gas emission from land-use change when a forested area is used for building a solar park, the large and rapid growth of new renewable energy a solar park can contribute with might make up for the emissions. Building solar parks on constructed areas or other already developed areas would be preferable. If building on a forested area, avoiding areas with high site productivity and organic soil would reduce the greenhouse gas emission.

References

- [1] Robert A. Adams, Christopher Essex, and Morten Andreas Nome. *Calculus 1: selected chapters from: Calculus: a complete course*. 9th ed. Pearson, 2018. ISBN: 9781787267763.
- [2] European Environment Agency. *cradle to grave — European Environment Agency*. en. Term. URL: <https://www.eea.europa.eu/help/glossary/eea-glossary/cradle-to-grave> (visited on 05/21/2023).
- [3] Anja Ahlstrøm, Knut Bjørkelo, and Kjetil Damsberg Fadnes. *AR5 Klassifikasjonssystem*. Research report 5(5). NIBIO, May 2019. URL: <http://hdl.handle.net/11250/2596511> (visited on 05/21/2023).
- [4] Otto Andersen et al. “CO2 emissions from the transport of China’s exported goods”. en. In: *Energy Policy* 38.10 (Oct. 2010), pp. 5790–5798. ISSN: 03014215. DOI: 10.1016/j.enpol.2010.05.030. URL: <https://linkinghub.elsevier.com/retrieve/pii/S0301421510004015> (visited on 05/01/2023).
- [5] Aneo. *Aneo skal bygge ut solkraft i Sverige*. nb. URL: <https://www.aneo.com/om-oss/nyheter/aneo-skal-bygge-ut-solkraft-i-sverige/> (visited on 05/15/2023).
- [6] Aneo. *Fra TrønderEnergi og Ohmia til Aneo*. nb. URL: <https://www.aneo.com/om-oss/om-aneo/> (visited on 05/15/2023).
- [7] Cooper B-Line. *Solar Power Panel Orientation: Landscape vs. Portrait - PDF Free Download*. URL: <https://docplayer.net/13272966-Solar-power-panel-orientation-landscape-vs-portrait.html> (visited on 05/03/2023).
- [8] Kristine Bekkelund. *A Comparative Life Cycle Assessment of PV Solar Systems*. English. 2013. URL: https://ntnuopen.ntnu.no/ntnu-xmlui/bitstream/handle/11250/235329/654872_FULLTEXT01.pdf?sequence=1 (visited on 05/17/2023).
- [9] Steinar Brandslet. *Nytt materiale gjør solceller enda mer miljøvennlige*. no. Publication Title: SINTEF. Jan. 2021. URL: <https://www.sintef.no/siste-nytt/2021/nytt-materiale-gjor-solceller-enda-mer-miljovennlige/> (visited on 05/10/2023).
- [10] Melissa Kreye Calvin Norman. *How Forests Store Carbon*. en. URL: <https://extension.psu.edu/how-forests-store-carbon> (visited on 05/04/2023).
- [11] Justin CatanosoJ. *With British Columbia’s last old-growth at risk, government falters: Critics*. en-US. Section: Environmental news. Apr. 2021. URL: <https://news.mongabay.com/2021/04/with-british-columbias-last-old-growth-at-risk-government-falters-critics/> (visited on 05/05/2023).
- [12] Bjerknnes Centre for Climate Research. *Opptak i skog*. nb. May 2021. URL: <http://bjerknnes.uib.no/artikler/fns-klimapanel/opptak-i-skog> (visited on 04/03/2023).
- [13] European Commission. *Paris Agreement*. en. URL: https://climate.ec.europa.eu/eu-action/international-action-climate-change/climate-negotiations/paris-agreement_en (visited on 05/05/2023).
- [14] European Commission. *Solar energy*. en. URL: https://energy.ec.europa.eu/topics/renewable-energy/solar-energy_en (visited on 05/07/2023).
- [15] European Commission. *Communication from the Commission of the European Parliament, the Council, to the European Parliament, the European Economic and social committee and the Committee of the Regions*. en. May 2022. URL: https://eur-lex.europa.eu/resource.html?uri=cellar:516a902d-d7a0-11ec-a95f-01aa75ed71a1.0001.02/D0C_1&format=PDF (visited on 05/05/2023).

REFERENCES

- [16] My NASA Data. *Albedo Values*. en. Basic page. Publisher: My NASA Data. Nov. 2019. URL: <https://mynasadata.larc.nasa.gov/basic-page/albedo-values> (visited on 05/17/2023).
- [17] Chris Deziel. *Which Colors Reflect More Light?* en. URL: <https://sciencing.com/colors-reflect-light-8398645.html> (visited on 05/17/2023).
- [18] Oslo Economics. “Nettkundenes nytte av en oppgradering av lavspenningsnettet”. no. In: (Feb. 2019).
- [19] Mayuri Ejgar, Bashirahamad Momin, and Tanuja Ganu. “Intelligent monitoring and maintenance of solar plants using real-time data analysis”. In: Oct. 2017, pp. 133–138. DOI: 10.1109/ICCE-ASIA.2017.8307844.
- [20] Office of Energy Efficiency Renewable Energy. *Solar Photovoltaic Cell Basics*. en. URL: <https://www.energy.gov/eere/solar/solar-photovoltaic-cell-basics> (visited on 05/17/2023).
- [21] UN. Secretary-General; World Commission on Environment and Development. *Our common future*. eng. Oxford: World Commission on Environment and Development, 1987.
- [22] SolarPower Europe. *EU Solar Strategy Explained - SolarPower Europe*. URL: <https://www.solarpowereurope.org/advocacy/eu-solar-strategy> (visited on 05/05/2023).
- [23] Torje Evensen et al. *Bakkemonterte solkraftverk i Norge — prosess og beste praksis*. Nov. 2022. URL: <https://www.solenergiklyngen.no/wp-content/uploads/2022/11/Bakke-monterte-solkraftverk-i-Norge.pdf> (visited on 05/02/2023).
- [24] Fortum. *Solar power - unlimited source of energy*. en. URL: <https://www.fortum.com/energy-production/solar-power> (visited on 05/04/2023).
- [25] Rolf Frischknecht et al. *Life Cycle Inventories and Life Cycle Assessments of Photovoltaic Systems*. Report IEA-PVPS T12-19:2020. ISBN 978-3-907281-14-7. Golden, CO, USA: International Energy Agency (IEA) PVPS Task 12, Dec. 2020.
- [26] Henrik Gade et al. *Grønn omstilling: Klimatiltaksanalyse for petroleum, industri og energiforsyning - Miljødirektoratet*. no. URL: <https://www.miljodirektoratet.no/publikasjoner/2022/september/gronn-omstilling-klimatiltaksanalyse/> (visited on 05/12/2023).
- [27] Melissa Ha and Rachel Schleiger. *Environmental Science (Whittinghill) - 6.06: Soils*. Yuba College & Butte College via ASCCC Open Educational Resources Initiative. University of Pittsburgh. n.d. URL: [https://bio.libretexts.org/Courses/University_of_Pittsburgh/Environmental_Science_\(Whittinghill\)/06%3A_Geology/6.06%3A_Soils](https://bio.libretexts.org/Courses/University_of_Pittsburgh/Environmental_Science_(Whittinghill)/06%3A_Geology/6.06%3A_Soils) (visited on 05/21/2023).
- [28] Seyed M. Heidari and Annick Anctil. “Country-specific carbon footprint and cumulative energy demand of metallurgical grade silicon production for silicon photovoltaics”. en. In: *Resources, Conservation and Recycling* 180 (May 2022), p. 106171. ISSN: 0921-3449. DOI: 10.1016/j.resconrec.2022.106171. URL: <https://www.sciencedirect.com/science/article/pii/S0921344922000192> (visited on 05/03/2023).
- [29] Jinglan Hong et al. “Life cycle assessment of multicrystalline silicon photovoltaic cell production in China”. en. In: *Solar Energy* 133 (Aug. 2016), pp. 283–293. ISSN: 0038-092X. DOI: 10.1016/j.solener.2016.04.013. URL: <https://www.sciencedirect.com/science/article/pii/S0038092X16300366> (visited on 05/20/2023).
- [30] IEA. *China - Countries & Regions*. en-GB. URL: <https://www.iea.org/countries/china> (visited on 05/08/2023).

REFERENCES

- [31] IEA. *Clean energy supply chains vulnerabilities – Energy Technology Perspectives 2023 – Analysis*. no. URL: <https://www.iea.org/reports/energy-technology-perspectives-2023/clean-energy-supply-chains-vulnerabilities> (visited on 05/08/2023).
- [32] IEA. *Europe – Countries & Regions*. en-GB. URL: <https://www.iea.org/regions/europe> (visited on 05/20/2023).
- [33] ISO. *ISO - ISO 14044:2006 - Environmental management — Life cycle assessment — Requirements and guidelines*. 2006. URL: <https://www.iso.org/standard/38498.html> (visited on 04/24/2022).
- [34] ISO. *ISO 14040:2006(en), Environmental management— Life cycle assessment— Principles and framework*. URL: <https://www.iso.org/obp/ui/#iso:std:iso:14040:ed-2:v1:en> (visited on 04/24/2022).
- [35] ISO. *ISO 14044:2006*. en. Aug. 2014. URL: <https://www.iso.org/standard/38498.html> (visited on 04/04/2023).
- [36] JA Solar. *Technical Datasheet: Photovoltaic Modules*. 2022. URL: <https://www.jasolar.com/uploadfile/2022/0224/20220224052158249.pdf>.
- [37] Yaman Abou Jieb. *Photovoltaic systems : fundamentals and applications*. eng. ISBN: 9783030897802 Place: Cham, Switzerland. 2022.
- [38] Niels Jungbluth et al. *Life Cycle Inventories of Photovoltaics*. Version 174-LCI-Photovoltaics-2012_v1.1. Commissioner: Swiss Federal Office of Energy SFOE. Kanzleistr. 4, CH-8610 Uster: ESU-services Ltd., fair consulting in sustainability, May 2012. URL: www.esu-services.ch.
- [39] Soteris A Kalogirou. *Solar energy engineering : processes and systems*. eng. Edition: Second edition. ISBN: 0-12-397256-6 Place: Amsterdam. 2014.
- [40] Henrik Kirkeby. *Plusskunder - hvor stor innvirkning har de på spenningskvaliteten?* nb-NO. Sept. 2017. URL: <https://pqa.no/plusskunder-innvirkning-spenningkvalitet/> (visited on 05/17/2023).
- [41] Kia Luise Klavenes. “Integrering av bærekraft i strategiprosessen – en forutsetning for lønnsom drift?” nor. In: *Praktisk økonomi og finans* 37.2 (2021), pp. 118–128. ISSN: 1501-0074.
- [42] Norsk klimaservicesenter. *Norsk klimaservicesenter*. URL: <https://klimaservicesenter.no/> (visited on 04/28/2023).
- [43] Norsk klimaservicesenter. *Observasjoner og værstatistikk - Seklima*. URL: <https://seklima.met.no/observations/> (visited on 05/20/2023).
- [44] Radovan Kopecek and Joris Libal. “Bifacial Photovoltaics 2021: Status, Opportunities and Challenges”. en. In: *Energies* 14.8 (Jan. 2021). Number: 8 Publisher: Multidisciplinary Digital Publishing Institute, p. 2076. ISSN: 1996-1073. DOI: 10.3390/en14082076. URL: <https://www.mdpi.com/1996-1073/14/8/2076> (visited on 05/01/2023).
- [45] Christopher Kranz et al. “Analysis of Local Aluminum Rear Contacts of Bifacial PERC+ Solar Cells”. In: *IEEE Journal of Photovoltaics* 6.4 (2016), pp. 830–836.
- [46] InSolare Energy Pvt. Ltd. (1) *A Designer’s Guide to PVsyst: Part 05 — LinkedIn*. URL: https://www.linkedin.com/pulse/designers-guide-pvsyst-part-05-insolare-energy-pvt-ltd-/?trk=organization_guest_main-feed-card_feed-article-content (visited on 05/03/2023).
- [47] NVE M.fl. Miljødirektoratet. *Tiltaksanalyse for skog- og arealbrukssektoren (LULUCF)*. 2023. URL: <https://www.miljodirektoratet.no/publikasjoner/2023/april-2023/tiltaksanalyse-for-skog-og-arealbrukssektoren/> (visited on 04/17/2023).

REFERENCES

- [48] Worry Free Marketing. *Solar Modules – Why Do Tilt And Orientation Matter?* en-US. Apr. 2019. URL: <https://solarislandenergy.com/2019/04/solar-modules-why-do-tilt-and-orientation-matter/> (visited on 05/03/2023).
- [49] Erik Marstein et al. *Veikart for den norske solkraftbrnasjen mot 2030*. Dec. 2020. URL: https://www.regjeringen.no/contentassets/66de7ddcf7a6494694202b760fa3f50f/susoltech_.pdf (visited on 05/02/2023).
- [50] Dina Christensen Martinsen. *Performance Modeling of Bifacial PV Power Plants in a Nordic Climate*. eng. 2022. URL: <https://hdl.handle.net/11250/3024751>.
- [51] Green match. *How are Solar Panels Made? — GreenMatch*. en-GB. 2023. URL: <https://www.greenmatch.co.uk/blog/2014/12/how-are-solar-panels-made> (visited on 05/17/2023).
- [52] Sarah Number Matthew Eckelman. *Life Cycle Assessment Explained*. en-US. Oct. 2021. URL: <https://stich.culturalheritage.org/life-cycle-assessment-explained/> (visited on 05/20/2023).
- [53] Klima-og miljødepartementet. *Derfor er myr og våtmark viktige*. no. Redaksjonellartikkel. Publisher: regjeringen.no. Oct. 2021. URL: <https://www.regjeringen.no/no/tema/klima-og-miljo/naturmangfold/innsiktsartikler-naturmangfold/vatmark/id2339659/> (visited on 05/11/2023).
- [54] Miljødirektoratet. *Arealbruksendringer*. Excel file. 2022. URL: <https://www.miljodirektoratet.no/sharepoint/downloaditem/?id=01FM3LD2X7X3ZR625A2FA2NC2UVCVA6ZL6>.
- [55] Miljødirektoratet. *Om Miljødirektoratet - Miljødirektoratet*. no. URL: <https://www.miljodirektoratet.no/om-oss/> (visited on 05/20/2023).
- [56] Barbara Moran. *As Forests Decline Globally, New England Is Not Immune*. en. May 2020. URL: <https://www.wbur.org/news/2020/05/28/study-old-growth-trees-climate-change> (visited on 05/05/2023).
- [57] United Nations. *Goal 15 — Department of Economic and Social Affairs*. URL: <https://sdgs.un.org/goals/goal15> (visited on 05/03/2023).
- [58] United Nations. *THE 17 GOALS — Sustainable Development*. URL: <https://sdgs.un.org/goals> (visited on 05/03/2023).
- [59] NIBIO. *Kilden - Arealinformasjon*. URL: https://kilden.nibio.no/?topic=arealinformasjon&lang=nb&X=6562199.04&Y=293661.14&zoom=8.127285180805103&bgLayer=graa_tone_cache&catalogNodes=2&layers=ar5_treslag&layers_opacity=0.75 (visited on 05/04/2023).
- [60] NIBIO. *Myr og klimagasser*. no. URL: <https://www.nibio.no/tema/miljo/tiltaksveileder-for-landbruket/klimagassutslipp/myr-og-klimagasser> (visited on 05/11/2023).
- [61] Nibio. *Klassifikasjonssystem AR5*. no. URL: <https://www.nibio.no/tema/jord/arealressurser/arealressurskart-ar5/klassifikasjonssystem-ar5> (visited on 04/24/2023).
- [62] Nibio. *Skogbonitet*. no. 2020. URL: <https://www.nibio.no/tema/jord/arealressurser/arealressurskart-ar5/skogbonitet> (visited on 04/24/2023).
- [63] NVE. *Solkraft - NVE*. no. 2023. URL: <https://www.nve.no/energi/energisystem/solkraft/> (visited on 02/22/2023).
- [64] Ports.com. *Sea routes and distances*. URL: <http://ports.com/sea-route/> (visited on 04/04/2023).

REFERENCES

- [65] Henrik Kirkeby og Thor Holm PQA AS v/Martin Lillebo. *Prosumenterers innvirkning på lavspente distribusjonsnett*. nb-NO. 2020. URL: https://publikasjoner.nve.no/rme_eksternrapport/2020/rme_eksternrapport2020_09.pdf (visited on 05/17/2023).
- [66] Database & Support team at PRé Sustainability. *SimaPro database manual Methods library*. en. June 2022. June 2022. URL: <https://example.com/simapro-database-manual> (visited on 05/20/2023).
- [67] PVEducation. *Module Materials — PVEducation*. URL: <https://www.pveducation.org/pvcdrom/modules-and-arrays/module-materials> (visited on 05/01/2023).
- [68] PVsyst. *Overview & General description of the PVsyst Software*. URL: https://www.pvsyst.com/help/general_descr.htm (visited on 02/15/2023).
- [69] PVsyst. *Performance ratio*. URL: https://www.pvsyst.com/help/performance_ratio.htm (visited on 05/21/2023).
- [70] PVsyst. *PNom Ratio - DC:AC*. URL: <https://www.pvsyst.com/help/pnomratio.htm> (visited on 05/21/2023).
- [71] PVsyst. *Project design & Array and system losses & Array losses, general considerations*. URL: https://www.pvsyst.com/help/array_losses_general.htm (visited on 05/20/2023).
- [72] PVsyst. *Project design & Array and system losses & Array Thermal losses*. URL: https://www.pvsyst.com/help/thermal_loss.htm (visited on 05/17/2023).
- [73] PVsyst. *Project design & Array voltage sizing*. URL: https://www.pvsyst.com/help/index.html?systemgrid_vocond.htm (visited on 05/21/2023).
- [74] PVsyst. *Project design & Bifacial system*. URL: https://www.pvsyst.com/help/index.html?bifacial_system_2d.htm (visited on 05/21/2023).
- [75] PVsyst. *Project design & Bifacial Systems & Bifacial systems results*. URL: https://www.pvsyst.com/help/bifacial_results.htm (visited on 05/21/2023).
- [76] PVsyst. *Project design & Multi-MPPT inverters*. URL: https://www.pvsyst.com/help/index.html?multi_mppt_use.htm (visited on 05/21/2023).
- [77] PVsyst. *Project design & Shadings*. URL: https://www.pvsyst.com/help/shadings_general.htm (visited on 05/21/2023).
- [78] PVsyst. *PVsyst – Logiciel Photovoltaïque*. en-US. URL: <https://www.pvsyst.com/> (visited on 02/15/2023).
- [79] PVsyst. *PVsyst 7 — Tutorial*. en. URL: https://www.pvsyst.com/wp-content/uploads/2020/10/PVsyst_Tutorials_V7_Grid_Connected.pdf (visited on 05/21/2023).
- [80] Regjeringen. *Norges Batteristrategi*. no_NO. Feb. 2022. URL: https://www.regjeringen.no/contentassets/a894b5594dbf4eccbec0d65f491e4809/batteristrategien_web2.pdf (visited on 03/03/2023).
- [81] Regjeringen. *NOU 2023: 3*. no_NO. Publisher: regjeringen.no. Feb. 2023. URL: <https://www.regjeringen.no/no/dokumenter/nou-2023-3/id2961311/> (visited on 05/07/2023).
- [82] FN-sambandet. *FNs bærekraftsmål*. no_NO. Apr. 2023. URL: <https://www.fn.no/om-fn/fns-baerekraftsmaal> (visited on 05/05/2023).
- [83] Statistisk sentralbyrå. *Hva er bærekraftig utvikling?* no. June 2014. URL: <https://www.ssb.no/natur-og-miljo/barekraft/hva-er-barekraftig-utvikling> (visited on 04/09/2023).
- [84] Priyadarshi R Shukla et al. “Climate Change 2022 Mitigation of Climate Change”. en. In: (Apr. 2023). URL: <https://www.ipcc.ch/report/ar6/wg3/> (visited on 05/05/2023).
- [85] Simapro. *About Simapro*. en-US. URL: <https://simapro.com/about/> (visited on 02/23/2023).

REFERENCES

- [86] Gunnhild Sjøgaard et al. *Skogens klimagassregnskap*. no-NO. June 2022. URL: <https://www.skogbruk.nibio.no/klimagassregnskapet-for-norske-skoger> (visited on 02/07/2023).
- [87] Norsk solenergiforening. *Solceller*. en-US. URL: <https://www.solenergi.no/solstrm> (visited on 05/21/2023).
- [88] Solenergiklyngen. *Solparker – Solenergiklyngen The Norwegian Solar Energy Cluster*{:}. URL: <https://solenergiklyngen.no/solparker/> (visited on 05/01/2023).
- [89] Joshua Stein et al. *IEA PVPS Task 13 Performance, Operation and Reliability of Photovoltaic Systems - Bifacial Photovoltaic Modules and Systems: Experience and Results from International Research and Pilot Applications*. Apr. 2021.
- [90] Jason Svarc. *Solar Panel Construction — Clean Energy Reviews*. 2020. URL: <https://www.cleanenergyreviews.info/blog/solar-panel-components-construction> (visited on 05/17/2023).
- [91] Kristian Bjørndal Vigsø Tveiten. *Solceller i lavspenningsnettet*. nb-NO. 2020. URL: <https://www.nve.no/media/15051/sommerprosjekt-2019.pdf> (visited on 05/17/2023).
- [92] Philippe Bédos Ulvin. *Vil 33-doble solkraft i Norge på syv år: – Realistisk*. nb-NO. Section: annet. Feb. 2023. URL: <https://www.nrk.no/klima/vil-33-doble-solkraft-i-norge-pa-syv-ar--realistisk-1.16279839> (visited on 05/07/2023).
- [93] OAR US EPA. *Understanding Global Warming Potentials*. en. Overviews and Factsheets. Jan. 2016. URL: <https://www.epa.gov/ghgemissions/understanding-global-warming-potentials> (visited on 05/20/2023).
- [94] OLEM US EPA. *Solar Panel Recycling*. en. Guidance (OMB). Aug. 2021. URL: <https://www.epa.gov/hw/solar-panel-recycling> (visited on 05/05/2023).
- [95] Database & Support team PRé Sustainability Various authors. *SimaPro database manual Methods library*. en. Version 4.17. Version 4.17, December 2021. Dec. 2021. URL: <https://example.com/simapro-database-manual> (visited on 05/20/2023).
- [96] Håkon Sverke Vindenes. “Metoder for å beregne klimagassutslipp fra arealbeslag”. no. In: ().

A JA-solar 550 Wp Panel

Harvest the Sunshine

DEEP BLUE 3.0

Mono 550W MBB Bifacial Mono PERC Half-cell Double Glass Module
JAM72D30 525-550/MB Series

Introduction

Assembled with 11BB bifacial PERCIUM cells and half-cell configuration, these double glass modules have the capability of converting the incident light from the rear side together with the front side into electricity, providing higher output power, lower temperature coefficient, less shading loss, as well as enhanced tolerance for mechanical loading.



Higher output power



More reliable, more stable power generation



Less shading effect

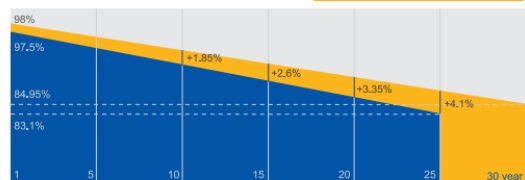


Lower temperature coefficient

Superior Warranty

- 12-year product warranty
- 30-year linear power output warranty

0.45% Annual Degradation Over 30 years



■ Bifacial double glass module linear power warranty ■ Standard module linear power warranty

Comprehensive Certificates

- IEC 61215, IEC 61730, UL 61215, UL 61730
- ISO 9001: 2015 Quality management systems
- ISO 14001: 2015 Environmental management systems
- ISO 45001: 2018 Occupational health and safety management systems
- IEC TS 62941: 2016 Terrestrial photovoltaic (PV) modules – Guidelines for increased confidence in PV module design qualification and type approval



JA SOLAR

www.jasolar.com

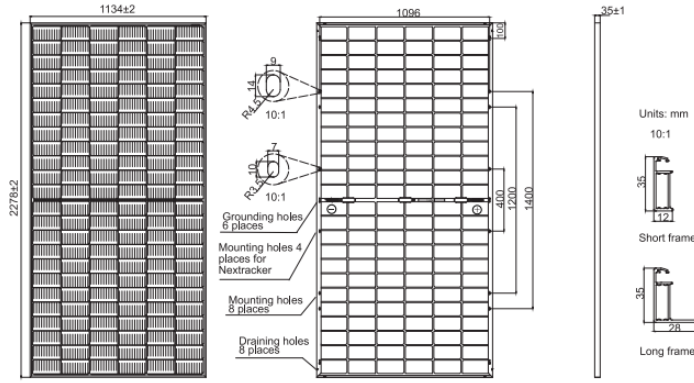
Specifications subject to technical changes and tests. JA Solar reserves the right of final interpretation.





JAM72D30 525-550/MB Series

MECHANICAL DIAGRAMS



Remark: customized frame color and cable length available upon request

SPECIFICATIONS

Cell	Mono
Weight	31.8kg±3%
Dimensions	2278±2mm×1134±2mm×35±1mm
Cable Cross Section Size	4mm ² (IEC), 12 AWG(UL)
No. of cells	144(6×24)
Junction Box	IP68, 3 diodes
Connector	QC 4,10-35
Cable Length (Including Connector)	Portrait:300mm(+)/400mm(-); Landscape:1300mm(+)/1300mm(-)
Front Glass/Back Glass	2.0mm/2.0mm
Packaging Configuration	31pcs/Pallet 620pcs/40HQ Container

ELECTRICAL PARAMETERS AT STC

TYPE	JAM72D30 -525/MB	JAM72D30 -530/MB	JAM72D30 -535/MB	JAM72D30 -540/MB	JAM72D30 -545/MB	JAM72D30 -550/MB
Rated Maximum Power(Pmax) [W]	525	530	535	540	545	550
Open Circuit Voltage(Voc) [V]	49.15	49.30	49.45	49.60	49.75	49.90
Maximum Power Voltage(Vmp) [V]	41.15	41.31	41.47	41.64	41.80	41.96
Short Circuit Current(Isc) [A]	13.65	13.72	13.79	13.86	13.93	14.00
Maximum Power Current(Imp) [A]	12.76	12.83	12.90	12.97	13.04	13.11
Module Efficiency [%]	20.3	20.5	20.7	20.9	21.1	21.3
Power Tolerance	0~+5W					
Temperature Coefficient of Isc(α _{Isc})	+0.045%/°C					
Temperature Coefficient of Voc(β _{Voc})	-0.275%/°C					
Temperature Coefficient of Pmax(γ _{Pmp})	-0.350%/°C					
STC	Irradiance 1000W/m ² , cell temperature 25°C, AM1.5G					

Remark: Electrical data in this catalog do not refer to a single module and they are not part of the offer.They only serve for comparison among different module types.

ELECTRICAL CHARACTERISTICS WITH 10% SOLAR IRRADIATION RATIO

TYPE	JAM72D30 -525/MB	JAM72D30 -530/MB	JAM72D30 -535/MB	JAM72D30 -540/MB	JAM72D30 -545/MB	JAM72D30 -550/MB
Rated Max Power(Pmax) [W]	562	567	572	578	583	589
Open Circuit Voltage(Voc) [V]	49.54	49.67	49.80	49.93	50.03	50.21
Max Power Voltage(Vmp) [V]	41.14	41.31	41.47	41.65	41.78	41.95
Short Circuit Current(Isc) [A]	14.61	14.68	14.76	14.83	14.91	14.98
Max Power Current(Imp) [A]	13.65	13.73	13.80	13.88	13.95	14.03
Irradiation Ratio(rear/front)	10%					

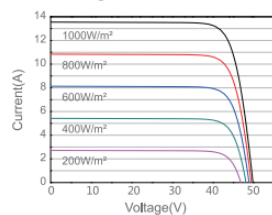
*For NexTracker installations, Maximum Static Load, Front is 2400Pa while Maximum Static Load, Back is 2400Pa.
**Bifaciality=Pmax,rear/Rated Pmax,front

OPERATING CONDITIONS

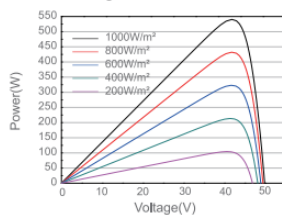
Maximum System Voltage	1500V DC
Operating Temperature	-40°C~+85°C
Maximum Series Fuse Rating	30A
Maximum Static Load,Front*	5400Pa(112 lb/ft ²)
Maximum Static Load,Back*	2400Pa(50 lb/ft ²)
NOCT	45±2°C
Bifaciality**	70%±10%
Fire Performance	UL Type 29

CHARACTERISTICS

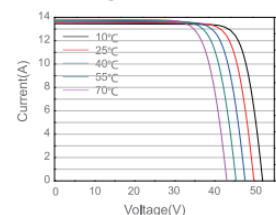
Current-Voltage Curve JAM72D30-540/MB



Power-Voltage Curve JAM72D30-540/MB



Current-Voltage Curve JAM72D30-540/MB



Premium Cells, Premium Modules

Version No. : Global_EN_20211129A

B INVENTORY LIST

B Inventory List

Table 6: Unit process LCI data of MG-Silicon production in Europe (NO), China (CN), North America (US) and Asia & Pacific (APAC)

product	Name	Location	InfrastructureProcess	Unit	MG-silicon, at plant				UncertaintyType	StandardDeviation95%	GeneralComment
					NO	CN	US	APAC			
					kg	kg	kg	kg			
	Location InfrastructureProcess Unit										
	MG-silicon, at plant	NO	0	kg	1	0	0	0			
	MG-silicon, at plant	CN	0	kg	0	1	0	0			
	MG-silicon, at plant	US	0	kg	0	0	1	0			
	MG-silicon, at plant	APAC	0	kg	0	0	0	1			
technosphere	electricity, medium voltage, at grid	NO	0	kWh	1.10E+1	0	0	0	1	1.22	(2,2,4,1,1,3); Literature, lower range to account for heat recovery
	electricity, medium voltage, at grid	CN	0	kWh	0	1.10E+1	0	0	1	1.22	(2,2,4,1,1,3); Literature, lower range to account for heat recovery
	electricity, medium voltage, at grid	US	0	kWh	0	0	1.10E+1	0	1	1.22	(2,2,4,1,1,3); Literature, lower range to account for heat recovery
	electricity, medium voltage, at grid	KR	0	kWh	0	0	0	1.10E+1	1	1.22	(2,2,4,1,1,3); Literature, lower range to account for heat recovery
	wood chips, production mix, wet, measured as dry mass, at forest road & at sawmill	RER	0	kg	3.25E-3	3.25E-3	3.25E-3	3.25E-3	1	1.22	(2,2,4,1,1,3); Literature, 1.35 kg
	hard coal coke, at plant	RER	0	MJ	2.31E+1	2.31E+1	2.31E+1	2.31E+1	1	1.22	(2,2,4,1,1,3); Literature, coal
	graphite, at plant	RER	0	kg	1.00E-1	1.00E-1	1.00E-1	1.00E-1	1	1.22	(2,2,4,1,1,3); Literature, graphite electrodes
	charcoal, at plant	GLO	0	kg	1.70E-1	1.70E-1	1.70E-1	1.70E-1	1	1.22	(2,2,4,1,1,3); Literature
	petroleum coke, at refinery	RER	0	kg	5.00E-1	5.00E-1	5.00E-1	5.00E-1	1	1.22	(2,2,4,1,1,3); Literature
	silica sand, at plant	DE	0	kg	2.70E+0	2.70E+0	2.70E+0	2.70E+0	1	1.22	(2,2,4,1,1,3); Literature
	oxygen, liquid, at plant	RER	0	kg	2.00E-2	2.00E-2	2.00E-2	2.00E-2	1	1.60	(3,4,5,3,1,5); Literature
	disposal, slag from MG silicon production, 0% water, to inert material landfill	CH	0	kg	2.50E-2	2.50E-2	2.50E-2	2.50E-2	1	1.22	(2,2,4,1,1,3); Literature
	silicone plant	RER	1	unit	1.00E-11	1.00E-11	1.00E-11	1.00E-11	1	3.09	(1,2,4,1,3,3); Estimation
	transport, transoceanic freight ship	OCE	0	tkm	2.55E+0	2.55E+0	2.55E+0	2.55E+0	1	2.09	(4,5,n,a,n,a,n,a); Charcoal from Asia 15000km
emission air, low population density	transport, freight, lorry, fleet average	RER	0	tkm	1.56E-1	1.56E-1	1.56E-1	1.56E-1	1	2.09	(4,5,n,a,n,a,n,a); Standard distance 50km, 20km for sand
	transport, freight, rail	RER	0	tkm	6.90E-2	6.90E-2	6.90E-2	6.90E-2	1	2.09	(4,5,n,a,n,a,n,a); Standard distance 100km
	Heat, waste	-	-	MJ	7.13E+1	7.13E+1	7.13E+1	7.13E+1	1	1.22	(2,2,4,1,1,3); Calculation based on fuel and electricity use minus 25 MJ/kg
	Arsenic	-	-	kg	9.42E-9	9.42E-9	9.42E-9	9.42E-9	1	5.34	(3,4,5,3,1,5); Literature, in dust
	Aluminium	-	-	kg	1.55E-6	1.55E-6	1.55E-6	1.55E-6	1	5.34	(3,4,5,3,1,5); Literature, in dust
	Antimony	-	-	kg	7.85E-9	7.85E-9	7.85E-9	7.85E-9	1	5.34	(3,4,5,3,1,5); Literature, in dust
	Boron	-	-	kg	2.79E-7	2.79E-7	2.79E-7	2.79E-7	1	5.34	(3,4,5,3,1,5); Literature, in dust
	Cadmium	-	-	kg	3.14E-10	3.14E-10	3.14E-10	3.14E-10	1	5.34	(3,4,5,3,1,5); Literature, in dust
	Calcium	-	-	kg	7.75E-7	7.75E-7	7.75E-7	7.75E-7	1	5.34	(3,4,5,3,1,5); Literature, in dust
	Carbon monoxide, biogenic	-	-	kg	6.20E-4	6.20E-4	6.20E-4	6.20E-4	1	5.34	(3,4,5,3,1,5); Literature
	Carbon monoxide, fossil	-	-	kg	1.38E-3	1.38E-3	1.38E-3	1.38E-3	1	5.34	(3,4,5,3,1,5); Literature
	Carbon dioxide, biogenic	-	-	kg	1.61E+0	1.61E+0	1.61E+0	1.61E+0	1	1.22	(2,2,4,1,1,3); Calculation, biogenic fuels
	Carbon dioxide, fossil	-	-	kg	3.58E+0	3.58E+0	3.58E+0	3.58E+0	1	1.22	(2,2,4,1,1,3); Calculation, fossil fuels
	Chromium	-	-	kg	7.85E-9	7.85E-9	7.85E-9	7.85E-9	1	5.34	(3,4,5,3,1,5); Literature, in dust
Chlorine	-	-	kg	7.85E-8	7.85E-8	7.85E-8	7.85E-8	1	1.85	(3,4,5,3,1,5); Literature, in dust	
Cyanide	-	-	kg	6.87E-6	6.87E-6	6.87E-6	6.87E-6	1	1.85	(3,4,5,3,1,5); Estimation	
Fluorine	-	-	kg	3.88E-8	3.88E-8	3.88E-8	3.88E-8	1	1.85	(3,4,5,3,1,5); Literature, in dust	
Hydrogen sulfide	-	-	kg	5.00E-4	5.00E-4	5.00E-4	5.00E-4	1	1.85	(3,4,5,3,1,5); Estimation	
Hydrogen fluoride	-	-	kg	5.00E-4	5.00E-4	5.00E-4	5.00E-4	1	1.85	(3,4,5,3,1,5); Estimation	
Iron	-	-	kg	3.88E-6	3.88E-6	3.88E-6	3.88E-6	1	5.34	(3,4,5,3,1,5); Literature, in dust	
Lead	-	-	kg	3.44E-7	3.44E-7	3.44E-7	3.44E-7	1	5.34	(3,4,5,3,1,5); Literature, in dust	
Mercury	-	-	kg	7.85E-9	7.85E-9	7.85E-9	7.85E-9	1	5.34	(3,4,5,3,1,5); Literature, in dust	
NMOC, non-methane volatile organic compounds, unspecified origin	-	-	kg	9.60E-5	9.60E-5	9.60E-5	9.60E-5	1	1.85	(3,4,5,3,1,5); Literature	
Nitrogen oxides	-	-	kg	9.74E-3	9.74E-3	9.74E-3	9.74E-3	1	1.58	(3,2,4,1,1,3); Calculation based on environmental report	
Particulates, > 10 um	-	-	kg	7.75E-3	7.75E-3	7.75E-3	7.75E-3	1	1.58	(3,2,4,1,1,3); Calculation based on environmental report	
Potassium	-	-	kg	6.20E-5	6.20E-5	6.20E-5	6.20E-5	1	5.34	(3,4,5,3,1,5); Literature, in dust	
Silicon	-	-	kg	7.51E-3	7.51E-3	7.51E-3	7.51E-3	1	5.34	(3,4,5,3,1,5); Literature, SiO2 in dust	
Sodium	-	-	kg	7.75E-7	7.75E-7	7.75E-7	7.75E-7	1	5.34	(3,4,5,3,1,5); Literature, in dust	
Sulfur dioxide	-	-	kg	1.22E-2	1.22E-2	1.22E-2	1.22E-2	1	1.24	(3,2,4,1,1,3); Calculation based on environmental report	
Tin	-	-	kg	7.85E-9	7.85E-9	7.85E-9	7.85E-9	1	5.34	(3,4,5,3,1,5); Literature, in dust	

B INVENTORY LIST

Table 7: Unit process LCI data of solar grade silicon production in Europe (RER), China (CN), North America (US) and Asia & Pacific (APAC)

Name	Location	Infrastructure	Process	Unit	silicon, solar grade, modified Siemens process, at plant	silicon, solar grade, modified Siemens process, at plant	silicon, solar grade, modified Siemens process, at plant	silicon, solar grade, modified Siemens process, at plant	Uncertainty Type	Standard Deviation 5%	General Comment
					RER	CN	US	APAC			
product	Location Infrastructure Process Unit				0 kg	0 kg	0 kg	0 kg			
silicon, solar grade, modified Siemens process, at plant	RER	0	kg	1	0	0	0	0			
silicon, solar grade, modified Siemens process, at plant	CN	0	kg	0	1	0	0	0			
silicon, solar grade, modified Siemens process, at plant	US	0	kg	0	0	1	0	0			
silicon, solar grade, modified Siemens process, at plant	APAC	0	kg	0	0	0	1	0			
technosphere											
MG-silicon, at plant	NO	0	kg	1.13E+0	0	0	0	0	1	1.23	(2,3,4,2,1,3); Literature
MG-silicon, at plant	CN	0	kg	1.13E+0	0	0	0	0	1	1.23	(2,3,4,2,1,3); Literature
MG-silicon, at plant	US	0	kg	0	0	1.13E+0	0	0	1	1.23	(2,3,4,2,1,3); Literature
MG-silicon, at plant	APAC	0	kg	0	0	0	1.13E+0	0	1	1.23	(2,3,4,2,1,3); Literature
hydrochloric acid, 30% in H2O, at plant	RER	0	kg	1.60E+0	1.60E+0	1.60E+0	1.60E+0	1.60E+0	1	1.25	(3,3,4,2,1,3); de Wild 2007, share of NaOH, HCl and H2 estimated with EG-Si data
hydrogen, liquid, at plant	RER	0	kg	5.01E-2	5.01E-2	5.01E-2	5.01E-2	5.01E-2	1	1.25	(3,3,4,2,1,3); de Wild 2007, share of NaOH, HCl and H2 estimated with EG-Si data
sodium hydroxide, 50% in H2O, production mix, at plant	RER	0	kg	3.48E-1	3.48E-1	3.48E-1	3.48E-1	3.48E-1	1	1.25	(3,3,4,2,1,3); de Wild 2007, share of NaOH, HCl and H2 estimated with EG-Si data
transport, freight, lorry, fleet average	RER	0	tkm	2.87E+0	2.87E+0	2.87E+0	2.87E+0	2.87E+0	1	2.09	(4,5,na,na,na,na); Transport distance MG-Si: 2000 km; Chemicals: 100 km
transport, freight, rail	RER	0	tkm	3.65E+0	3.65E+0	3.65E+0	3.65E+0	3.65E+0	1	2.09	(4,5,na,na,na,na); Transport distance chemicals: 600 km
electricity, at cogen 1MWe lean burn, allocation exergy	RER	0	kWh	1.75E+1	0	0	0	0	1	1.10	(2,3,1,2,1,3); Total electricity demand: 49 kWh/kg (IEA-PVPS Trends Report 2019)
electricity, hydropower, at run-of-river power plant	RER	0	kWh	3.93E+0	0	1.18E+1	0	0	1	1.10	(2,3,1,2,1,3); Total electricity demand: 49 kWh/kg (IEA-PVPS Trends Report 2019)
electricity, medium voltage, at grid	DE	0	kWh	2.23E+1	0	0	0	0	1	1.10	(2,3,1,2,1,3); Total electricity demand: 49 kWh/kg (IEA-PVPS Trends Report 2019)
electricity, medium voltage, at grid	NO	0	kWh	5.37E+0	0	0	0	0	1	1.10	(2,3,1,2,1,3); Total electricity demand: 49 kWh/kg (IEA-PVPS Trends Report 2019)
electricity, medium voltage, at grid	CN	0	kWh	0	4.90E+1	0	0	0	1	1.10	(2,3,1,2,1,3); Total electricity demand: 49 kWh/kg (IEA-PVPS Trends Report 2019)
electricity, medium voltage, at grid	US	0	kWh	0	0	3.72E+1	0	0	1	1.10	(2,3,1,2,1,3); Total electricity demand: 49 kWh/kg (IEA-PVPS Trends Report 2019)
electricity, medium voltage, at grid	KR	0	kWh	0	0	0	4.90E+1	0	1	1.10	(2,3,1,2,1,3); Total electricity demand: 49 kWh/kg (IEA-PVPS Trends Report 2019)
heat, at cogen 1MWe lean burn, allocation exergy	RER	0	MJ	2.88E+1	2.88E+1	2.88E+1	2.88E+1	2.88E+1	1	1.10	(2,3,1,2,1,3); Woodhouse et al. (2019); c-Si PV Manufacturing Costs 2018, IEA-PVPS Trends Report 2019
silicone plant	RER	1	unit	1.00E-11	1.00E-11	1.00E-11	1.00E-11	1.00E-11	1	3.05	(1,3,4,2,3,3); Estimation
emission air, high population density emission water, river											
Heat, waste	-	-	MJ	1.76E+2	1.76E+2	1.76E+2	1.76E+2	1.76E+2	1	1.23	(2,3,4,2,1,3); Calculation
AOX, Adsorbable Organic Halogen as Cl	-	-	kg	1.26E-5	1.26E-5	1.26E-5	1.26E-5	1.26E-5	1	1.68	(4,2,4,1,3,3); Environmental report 2002, average Si product
BOD5, Biological Oxygen Demand	-	-	kg	2.05E-4	2.05E-4	2.05E-4	2.05E-4	2.05E-4	1	1.68	(4,2,4,1,3,3); Environmental report 2002, average Si product
COD, Chemical Oxygen Demand	-	-	kg	2.02E-3	2.02E-3	2.02E-3	2.02E-3	2.02E-3	1	1.68	(4,2,4,1,3,3); Environmental report 2002, average Si product
Chloride	-	-	kg	3.60E-2	3.60E-2	3.60E-2	3.60E-2	3.60E-2	1	3.14	(4,2,4,1,3,3); Environmental report 2002, average Si product
Copper	-	-	kg	1.02E-7	1.02E-7	1.02E-7	1.02E-7	1.02E-7	1	3.14	(4,2,4,1,3,3); Environmental report 2002, average Si product
Nitrogen	-	-	kg	2.08E-4	2.08E-4	2.08E-4	2.08E-4	2.08E-4	1	1.68	(4,2,4,1,3,3); Environmental report 2002, average Si product
Phosphate	-	-	kg	2.80E-6	2.80E-6	2.80E-6	2.80E-6	2.80E-6	1	1.68	(4,2,4,1,3,3); Environmental report 2002, average Si product
Sodium, ion	-	-	kg	3.38E-2	3.38E-2	3.38E-2	3.38E-2	3.38E-2	1	5.16	(4,2,4,1,3,3); Environmental report 2002, average Si product
Zinc	-	-	kg	1.96E-6	1.96E-6	1.96E-6	1.96E-6	1.96E-6	1	5.16	(4,2,4,1,3,3); Environmental report 2002, average Si product
Iron	-	-	kg	5.61E-6	5.61E-6	5.61E-6	5.61E-6	5.61E-6	1	5.16	(4,2,4,1,3,3); Environmental report 2002, average Si product
DOC, Dissolved Organic Carbon	-	-	kg	9.10E-4	9.10E-4	9.10E-4	9.10E-4	9.10E-4	1	1.68	(4,2,4,1,3,3); Environmental report 2002, average Si product
TOC, Total Organic Carbon	-	-	kg	9.10E-4	9.10E-4	9.10E-4	9.10E-4	9.10E-4	1	1.68	(4,2,4,1,3,3); Environmental report 2002, average Si product

Table 8: Unit process LCI data of the silicon production mixes 2018 of global and European production (GLO), China (CN), North America (US) and Asia & Pacific (APAC)

Name	Location	Infrastructure	Process	Unit	silicon, production mix photovoltaics, at plant	silicon, production mix photovoltaics, at plant	silicon, production mix photovoltaics, at plant	silicon, production mix photovoltaics, at plant	Uncertainty Type	Standard Deviation 5%	General Comment
					CN	APAC	US	GLO			
product	Location Infrastructure Process Unit				0 kg	0 kg	0 kg	0 kg			
silicon, production mix photovoltaics, at plant	CN	0	kg	1	0	0	0	0			
silicon, production mix photovoltaics, at plant	APAC	0	kg	0	1	0	0	0			
silicon, production mix photovoltaics, at plant	US	0	kg	0	0	1	0	0			
silicon, production mix photovoltaics, at plant	GLO	0	kg	0	0	0	1	0			
silicon, solar grade, modified Siemens process, at plant	CN	0	kg	6.10E-01	0.00E+00	0.00E+00	0.00E+00	0.00E+00	1.00	1.11	(3,1,1,1,1,1); Market share Chinese Polysilicon
silicon, solar grade, modified Siemens process, at plant	APAC	0	kg	1.62E-01	1.00E+00	0.00E+00	0.00E+00	0.00E+00	1.00	1.11	(3,1,1,1,1,1); Market share APAC Polysilicon
silicon, solar grade, modified Siemens process, at plant	US	0	kg	9.28E-02	0.00E+00	1.00E+00	0.00E+00	0.00E+00	1.00	1.11	(3,1,1,1,1,1); Market share US Polysilicon
silicon, solar grade, modified Siemens process, at plant	RER	0	kg	1.35E-01	0.00E+00	0.00E+00	1.00E+00	0.00E+00	1.00	1.11	(3,1,1,1,1,1); Market share European Polysilicon
transport, transoceanic freight ship	OCE	0	tkm	5.37E+00	0.00E+00	0.00E+00	0.00E+00	0.00E+00	1.00	2.09	(4,5,na,na,na,na); Transport distance CN-EU: 19994 km, CN-US: 20755 km, CN-APAC: 4584 km
transport, freight, rail	RER	0	tkm	2.00E-01	2.00E-01	2.00E-01	2.00E-01	2.00E-01	1.00	2.09	(4,5,na,na,na,na); Standard distance 200km
transport, freight, lorry, fleet average	RER	0	tkm	5.00E-02	5.00E-02	5.00E-02	5.00E-02	5.00E-02	1.00	2.09	(4,5,na,na,na,na); Standard distance 50km

B INVENTORY LIST

Table 9: Unit process LCI data of the single-crystalline silicon production in Europe (RER), China (CN), North America (US) and Asia & Pacific (APAC)

product	Name	Location	InfrastructureProcess	Unit	CZ single crystalline silicon, photovoltaics, at plant	CZ single crystalline silicon, photovoltaics, at plant	CZ single crystalline silicon, photovoltaics, at plant	CZ single crystalline silicon, photovoltaics, at plant	Uncertainty Type	Standardization	GeneralComment
	CN				US	APAC	RER				
	Location				CN	US	APAC	RER			
	InfrastructureProcess				0	0	0	0			
	Unit				kg	kg	kg	kg			
product	CZ single crystalline silicon, photovoltaics, at plant	CN	0	kg	1	0	0	0			
	CZ single crystalline silicon, photovoltaics, at plant	US	0	kg	0	1	0	0			
	CZ single crystalline silicon, photovoltaics, at plant	APAC	0	kg	0	0	1	0			
	CZ single crystalline silicon, photovoltaics, at plant	RER	0	kg	0	0	0	1			
technosphere	silicon, production mix, photovoltaics, at plant	CN	0	kg	1.00E+0	0	0	0	1	1.33	(2.4.4.2.1.5); Pot scrap losses (1.5 to 2%, according to Woodhouse (2019)) are accounted for in water manufacturing
	silicon, production mix, photovoltaics, at plant	US	0	kg	0	1.00E+0	0	0	1	1.33	(2.4.4.2.1.5); Pot scrap losses (1.5 to 2%, according to Woodhouse (2019)) are accounted for in water manufacturing
	silicon, production mix, photovoltaics, at plant	APAC	0	kg	0	0	1.00E+0	0	1	1.33	(2.4.4.2.1.5); Pot scrap losses (1.5 to 2%, according to Woodhouse (2019)) are accounted for in water manufacturing
	silicon, production mix, photovoltaics, at plant	GLO	0	kg	0	0	0	1.00E+0	1	1.33	(2.4.4.2.1.5); Pot scrap losses (1.5 to 2%, according to Woodhouse (2019)) are accounted for in water manufacturing
materials	argon, liquid, at plant	RER	0	kg	1.00E+0	1.00E+0	1.00E+0	1.00E+0	1	1.32	(1.4.4.2.1.5); de Wild-Scholten (2014) Life Cycle Assessment of Photovoltaics Status 2011, Part 1 Data Collection (table 9)
	hydrogen fluoride, at plant	GLO	0	kg	1.00E-2	1.00E-2	1.00E-2	1.00E-2	1	1.65	(3.4.5.3.3.5); de Wild-Scholten (2014) Life Cycle Assessment of Photovoltaics Status 2011, Part 1 Data Collection (table 9)
	nitric acid, 50% in H2O, at plant	RER	0	kg	6.68E-2	6.68E-2	6.68E-2	6.68E-2	1	1.65	(3.4.5.3.3.5); de Wild-Scholten (2014) Life Cycle Assessment of Photovoltaics Status 2011, Part 1 Data Collection (table 9)
	sodium hydroxide, 50% in H2O, production mix, at plant	RER	0	kg	4.15E-2	4.15E-2	4.15E-2	4.15E-2	1	1.65	(3.4.5.3.3.5); de Wild-Scholten (2014) Life Cycle Assessment of Photovoltaics Status 2011, Part 1 Data Collection (table 9)
	ceramic tiles, at regional storage	CH	0	kg	1.67E-1	1.67E-1	1.67E-1	1.67E-1	1	1.32	(1.4.4.2.1.5); de Wild-Scholten (2014) Life Cycle Assessment of Photovoltaics Status 2011, Part 1 Data Collection (table 9)
	lime, hydrated, packed, at plant	CH	0	kg	2.22E-2	2.22E-2	2.22E-2	2.22E-2	1	1.65	(3.4.5.3.3.5); waste water treatment, Hagedorn 1992
	electricity, medium voltage, at grid	CN	0	kWh	3.20E+1	0	0	0	1	1.22	(2.2.1.2.1.5); ITRPV 2020, Fig. 6, p.9
	electricity, medium voltage, at grid	US	0	kWh	0	3.20E+1	0	0	1	1.22	(2.2.1.2.1.5); ITRPV 2020, Fig. 6, p.9
	electricity, medium voltage, at grid	KR	0	kWh	0	0	3.20E+1	0	1	1.22	(2.2.1.2.1.5); ITRPV 2020, Fig. 6, p.9
	electricity, medium voltage, production ENTSO, at grid	ENTSO	0	kWh	0	0	0	3.20E+1	1	1.22	(2.2.1.2.1.5); ITRPV 2020, Fig. 6, p.9
	natural gas, burned in industrial furnace low-NOx >100kW	RER	0	MJ	6.82E+1	6.82E+1	6.82E+1	6.82E+1	1	1.32	(1.4.4.2.1.5); de Wild-Scholten (2014) Life Cycle Assessment of Photovoltaics Status 2011, Part 1 Data Collection (table 9)
	water, deionised, water balance according to MbK 2013, at plant	CN	0	kg	4.01E+0	0	0	0	1	1.32	(1.4.4.2.1.5); de Wild-Scholten (2014) Life Cycle Assessment of Photovoltaics Status 2011, Part 1 Data Collection (table 9)
	water, deionised, water balance according to MbK 2013, at plant	US	0	kg	0	4.01E+0	0	0	1	1.32	(1.4.4.2.1.5); de Wild-Scholten (2014) Life Cycle Assessment of Photovoltaics Status 2011, Part 1 Data Collection (table 9)
	water, deionised, water balance according to MbK 2013, at plant	KR	0	kg	0	0	4.01E+0	0	1	1.32	(1.4.4.2.1.5); de Wild-Scholten (2014) Life Cycle Assessment of Photovoltaics Status 2011, Part 1 Data Collection (table 9)
	water, deionised, water balance according to MbK 2013, at plant	RER	0	kg	0	0	0	4.01E+0	1	1.32	(1.4.4.2.1.5); de Wild-Scholten (2014) Life Cycle Assessment of Photovoltaics Status 2011, Part 1 Data Collection (table 9)
resource, in water	Water, coding, unspecified natural origin, CN	-	-	m3	5.09E+0	0	0	0	1	1.32	(1.4.4.2.1.5); de Wild-Scholten (2014) Life Cycle Assessment of Photovoltaics Status 2011, Part 1 Data Collection (table 9)
	Water, coding, unspecified natural origin, US	-	-	m3	0	5.09E+0	0	0	1	1.32	(1.4.4.2.1.5); de Wild-Scholten (2014) Life Cycle Assessment of Photovoltaics Status 2011, Part 1 Data Collection (table 9)
	Water, coding, unspecified natural origin, KR	-	-	m3	0	0	5.09E+0	0	1	1.32	(1.4.4.2.1.5); de Wild-Scholten (2014) Life Cycle Assessment of Photovoltaics Status 2011, Part 1 Data Collection (table 9)
	Water, coding, unspecified natural origin, RER	-	-	m3	0	0	0	5.09E+0	1	1.32	(1.4.4.2.1.5); de Wild-Scholten (2014) Life Cycle Assessment of Photovoltaics Status 2011, Part 1 Data Collection (table 9)
transport	transport, freight, lorry, fleet average	RER	0	km	1.13E+0	1.13E+0	1.13E+0	1.13E+0	1	2.09	(4.5.nananana); Transport distance: 100km; silicon: 1000km
	transport, freight, rail	RER	0	km	1.41E+0	1.41E+0	1.41E+0	1.41E+0	1	2.09	(4.5.nananana); de Wild-Scholten (2014) Life Cycle Assessment of Photovoltaics Status 2011, Part 1 Data Collection (table 9)
infrastructure	silicon plant	RER	1	unit	1.00E+11	1.00E+11	1.00E+11	1.00E+11	1	3.09	(1.2.4.1.3.3); Estimation
disposal	disposal, waste, Si waferprod., inorg. 9.4% water, to residual material landfill	CH	0	kg	1.67E-1	1.67E-1	1.67E-1	1.67E-1	1	1.32	(1.4.4.2.1.5); de Wild-Scholten (2014) Life Cycle Assessment of Photovoltaics Status 2011, Part 1 Data Collection (table 9)
	treatment, sewage, to wastewater treatment, class 2	CH	0	m3	4.84E+0	4.84E+0	4.84E+0	4.84E+0	1	1.63	(4.3.5.3.1.5); Calculation based on water withdrawal and water emissions
emission air	Heat, waste	-	-	MJ	1.15E+2	1.15E+2	1.15E+2	1.15E+2	1	1.58	(3.3.5.3.1.5); de Wild-Scholten (2014) Life Cycle Assessment of Photovoltaics Status 2011, Part 1 Data Collection (table 9)
	Water, CN	-	-	kg	2.55E+2	0	0	0	1	1.88	(4.3.5.3.1.5); Assumption: 9% evaporation of cooling water; 10% evaporation of process water; Frischknecht & Basser Knöpfel (2013)
	Water, US	-	-	kg	0	2.55E+2	0	0	1	1.88	(4.3.5.3.1.5); Assumption: 9% evaporation of cooling water; 10% evaporation of process water; Frischknecht & Basser Knöpfel (2013)
	Water, KR	-	-	kg	0	0	2.55E+2	0	1	1.88	(4.3.5.3.1.5); Assumption: 9% evaporation of cooling water; 10% evaporation of process water; Frischknecht & Basser Knöpfel (2013)
	Water, RER	-	-	kg	0	0	0	2.55E+2	1	1.88	(4.3.5.3.1.5); Assumption: 9% evaporation of cooling water; 10% evaporation of process water; Frischknecht & Basser Knöpfel (2013)
	Nitrogen oxides	-	-	kg	3.39E-2	3.39E-2	3.39E-2	3.39E-2	1	1.85	(3.4.5.3.1.5); de Wild-Scholten (2014) Life Cycle Assessment of Photovoltaics Status 2011, Part 1 Data Collection (table 9)
emission water, river	Hydroxide	-	-	kg	4.42E-3	4.42E-3	4.42E-3	4.42E-3	1	3.30	(3.4.5.3.1.5); de Wild-Scholten (2014) Life Cycle Assessment of Photovoltaics Status 2011, Part 1 Data Collection (table 9)
	BOD5, Biological Oxygen Demand	-	-	kg	1.30E-1	1.30E-1	1.30E-1	1.30E-1	1	3.33	(5.4.4.1.1.5); Extrapolation for sum parameter
	COD, Chemical Oxygen Demand	-	-	kg	1.30E-1	1.30E-1	1.30E-1	1.30E-1	1	3.33	(5.4.4.1.1.5); Extrapolation for sum parameter
	DOC, Dissolved Organic Carbon	-	-	kg	4.05E-2	4.05E-2	4.05E-2	4.05E-2	1	3.33	(5.4.4.1.1.5); Extrapolation for sum parameter
	TOC, Total Organic Carbon	-	-	kg	4.05E-2	4.05E-2	4.05E-2	4.05E-2	1	3.33	(5.4.4.1.1.5); Extrapolation for sum parameter
	Nitrate	-	-	kg	8.35E-2	8.35E-2	8.35E-2	8.35E-2	1	1.85	(3.4.5.3.1.5); de Wild-Scholten (2014) Life Cycle Assessment of Photovoltaics Status 2011, Part 1 Data Collection (table 9)

B INVENTORY LIST

Table 10: Unit process LCI data of the multi-crystalline silicon production in Europe (RER), China (CN), North America (US) and Asia & Pacific (APAC)

	Name	Location	Infrastructure	Process	Unit	silicon, multi-Si,	silicon, multi-Si,	silicon, multi-Si,	silicon, multi-Si,	Uncertainty Type	StandardDeviation95	GeneralComment
						casted, at plant	casted, at plant	casted, at plant	casted, at plant			
	Location					CN	US	APAC	RER			
	Infrastructure					0	0	0	0			
	Unit					kg	kg	kg	kg			
product	silicon, multi-Si, casted, at plant	CN	0		kg	1	0	0	0			
	silicon, multi-Si, casted, at plant	US	0		kg	0	1	0	0			
	silicon, multi-Si, casted, at plant	APAC	0		kg	0	0	1	0			
	silicon, multi-Si, casted, at plant	RER	0		kg	0	0	0	1			
technosphere	silicon, production mix, photovoltaics, at plant	CN	0		kg	1.00E+0	0	0	0	1	1.33	(2.4.4.2,1.5); Estimation
	silicon, production mix, photovoltaics, at plant	US	0		kg	0	1.00E+0	0	0	1	1.33	(2.4.4.2,1.5); Estimation
	silicon, production mix, photovoltaics, at plant	APAC	0		kg	0	0	1.00E+0	0	1	1.33	(2.4.4.2,1.5); Estimation
	silicon, production mix, photovoltaics, at plant	GLO	0		kg	0	0	0	1.00E+0	1	1.33	(2.4.4.2,1.5); Estimation
	argon, liquid, at plant	RER	0		kg	2.52E-1	2.52E-1	2.52E-1	2.52E-1	1	1.22	(1.2.4.1,1.3); de Wild-Scholten (2014) Life Cycle Assessment of Photovoltaics Status 2011, Part 1 Data Collection (table 12)
	helium, at plant	GLO	0		kg	7.76E-5	7.76E-5	7.76E-5	7.76E-5	1	1.22	(1.2.4.1,1.3); de Wild-Scholten (2014) Life Cycle Assessment of Photovoltaics Status 2011, Part 1 Data Collection (table 12)
	sodium hydroxide, 50% in H2O, production mix, at plant	RER	0		kg	5.00E-3	5.00E-3	5.00E-3	5.00E-3	1	1.58	(3.3.5.3,1.5); de Wild-Scholten (2014) Life Cycle Assessment of Photovoltaics Status 2011, Part 1 Data Collection (table 12)
	nitrogen, liquid, at plant	RER	0		kg	3.04E-2	3.04E-2	3.04E-2	3.04E-2	1	1.22	(1.2.4.1,1.3); de Wild-Scholten (2014) Life Cycle Assessment of Photovoltaics Status 2011, Part 1 Data Collection (table 12)
	ceramic tiles, at regional storage	CH	0		kg	2.14E-1	2.14E-1	2.14E-1	2.14E-1	1	1.22	(1.2.4.1,1.3); de Wild-Scholten (2014) Life Cycle Assessment of Photovoltaics Status 2011, Part 1 Data Collection (table 12)
	electricity, medium voltage, at grid	CN	0		kWh	7.00E+0	0	0	0	1	1.22	(2.2,1.2,1.5); ITRPV2020, Fig. 6, p.9
	electricity, medium voltage, at grid	US	0		kWh	0	7.00E+0	0	0	1	1.22	(2.2,1.2,1.5); ITRPV2020, Fig. 6, p.9
	electricity, medium voltage, at grid	KR	0		kWh	0	0	7.00E+0	0	1	1.22	(2.2,1.2,1.5); ITRPV2020, Fig. 6, p.9
	electricity, medium voltage, production ENTSO, at grid	ENTSO	0		kWh	0	0	0	7.00E+0	1	1.22	(2.2,1.2,1.5); ITRPV2020, Fig. 6, p.9
resource, in water	Water, cooling, unspecified natural origin, CN	-	-		m3	9.43E-1	0	0	0	1	1.60	(3.4.5.3,1.5); de Wild-Scholten (2014) Life Cycle Assessment of Photovoltaics Status 2011, Part 1 Data Collection (table 12)
	Water, cooling, unspecified natural origin, US	-	-		m3	0	9.43E-1	0	0	1	1.34	(3.4.4.3,1.5); de Wild-Scholten (2014) Life Cycle Assessment of Photovoltaics Status 2011, Part 1 Data Collection (table 12)
	Water, cooling, unspecified natural origin, KR	-	-		m3	0	0	9.43E-1	0	1	1.34	(3.4.4.3,1.5); de Wild-Scholten (2014) Life Cycle Assessment of Photovoltaics Status 2011, Part 1 Data Collection (table 12)
	Water, cooling, unspecified natural origin, RER	-	-		m3	0	0	0	9.43E-1	1	1.34	(3.4.4.3,1.5); de Wild-Scholten (2014) Life Cycle Assessment of Photovoltaics Status 2011, Part 1 Data Collection (table 12)
transport	transport, freight, lorry, fleet average	RER	0		tkm	1.05E+0	1.05E+0	1.05E+0	1.05E+0	1	2.09	(4.5,na,na,na,na); Transport distance: 100km; silicon: 1000kg
	transport, freight, rail	RER	0		tkm	2.00E-1	2.00E-1	2.00E-1	2.00E-1	1	2.09	(4.5,na,na,na,na); Standard distances 100km
infrastructure	silicone plant	RER	1		unit	1.00E-11	1.00E-11	1.00E-11	1.00E-11	1	3.09	(1.2.4,1,3,3); Estimation
disposal	treatment, sewage, to wastewater treatment, class 2	CH	0		m3	8.96E-1	8.96E-1	8.96E-1	8.96E-1	1	1.63	(4.3.5.3,1.5); Calculation based on water withdrawal and water emissions
emission air	Heat, waste	-	-		MJ	2.52E+1	2.52E+1	2.52E+1	2.52E+1	1	1.58	(3.3.5.3,1.5); Calculation
	Water, CN	-	-		kg	4.72E+1	0	0	0	1	1.88	(4.3.5.3,1.5); Assumption: 5% evaporation of cooling water; Frischknecht & Büsser Knöpfel (2013)
	Water, US	-	-		kg	0	4.72E+1	0	0	1	1.88	(4.3.5.3,1.5); Assumption: 5% evaporation of cooling water; Frischknecht & Büsser Knöpfel (2013)
	Water, KR	-	-		kg	0	0	4.72E+1	0	1	1.88	(4.3.5.3,1.5); Assumption: 5% evaporation of cooling water; Frischknecht & Büsser Knöpfel (2013)
	Water, RER	-	-		kg	0	0	0	4.72E+1	1	1.88	(4.3.5.3,1.5); Assumption: 5% evaporation of cooling water; Frischknecht & Büsser Knöpfel (2013)

B INVENTORY LIST

Table 12: Unit process LCI data of the single- and multi-crystalline silicon wafer production in China (CN) and North America (US)

product	Name	Location	Infrastructure	Process	Unit	single-Si wafer, photovoltaics, at plant				Uncertainty Type	Standard/Deviation/95%	GeneralComment
						CN		US				
						kg	m2	kg	m2			
	Location					CN	CN	US	US			
	InfrastructureProcess					0	0	0	0			
	Unit					m2	m2	m2	m2			
	single-Si wafer, photovoltaics, at plant	CN	0	m2		1	0	0	0			
	multi-Si wafer, at plant	CN	0	m2		0	1	0	0			
	single-Si wafer, photovoltaics, at plant	US	0	m2		0	0	1	0			
	multi-Si wafer, at plant	US	0	m2		0	0	0	1			
	single-Si wafer, photovoltaics, at plant	APAC	0	m2		0	0	0	0			
	multi-Si wafer, at plant	APAC	0	m2		0	0	0	0			
	single-Si wafer, photovoltaics, at plant	RER	0	m2		0	0	0	0			
	multi-Si wafer, at plant	RER	0	m2		0	0	0	0			
technosphere	CZ single crystalline silicon, photovoltaics, at plant	CN	0	kg		5.95E-1	0	0	0	1	1.22	(2.2,1.2,1.5); Wafer thickness: 170 um, kerfloss: 65 um, additional losses: 20.5 um; silicon density: 2330 kg/m3; ITRPV2020; Woodhouse et al. (2019); c-Si PV Manufacturing Costs 2018
	silicon, multi-Si, casted, at plant	CN	0	kg		0	6.35E-1	0	0	1	1.22	(2.2,1.2,1.5); Wafer thickness: 180 um, kerfloss: 65 um, additional losses: 27.5 um; silicon density: 2330 kg/m3; ITRPV2020; Woodhouse et al. (2019); c-Si PV Manufacturing Costs 2018
	CZ single crystalline silicon, photovoltaics, at plant	US	0	kg		0	0	5.95E-1	0	1	1.22	(2.2,1.2,1.5); Wafer thickness: 170 um, kerfloss: 65 um, additional losses: 20.5 um; silicon density: 2330 kg/m3; ITRPV2020; Woodhouse et al. (2019); c-Si PV Manufacturing Costs 2018
	silicon, multi-Si, casted, at plant	US	0	kg		0	0	0	6.35E-1	1	1.22	(2.2,1.2,1.5); Wafer thickness: 180 um, kerfloss: 65 um, additional losses: 27.5 um; silicon density: 2330 kg/m3; ITRPV2020; Woodhouse et al. (2019); c-Si PV Manufacturing Costs 2018
	CZ single crystalline silicon, photovoltaics, at plant	APAC	0	kg		0	0	0	0	1	1.22	(2.2,1.2,1.5); Wafer thickness: 170 um, kerfloss: 65 um, additional losses: 20.5 um; silicon density: 2330 kg/m3; ITRPV2020; Woodhouse et al. (2019); c-Si PV Manufacturing Costs 2018
	silicon, multi-Si, casted, at plant	APAC	0	kg		0	0	0	0	1	1.22	(2.2,1.2,1.5); Wafer thickness: 180 um, kerfloss: 65 um, additional losses: 27.5 um; silicon density: 2330 kg/m3; ITRPV2020; Woodhouse et al. (2019); c-Si PV Manufacturing Costs 2018
	CZ single crystalline silicon, photovoltaics, at plant	RER	0	kg		0	0	0	0	1	1.22	(2.2,1.2,1.5); Wafer thickness: 170 um, kerfloss: 65 um, additional losses: 20.5 um; silicon density: 2330 kg/m3; ITRPV2020; Woodhouse et al. (2019); c-Si PV Manufacturing Costs 2018
	silicon, multi-Si, casted, at plant	RER	0	kg		0	0	0	0	1	1.22	(2.2,1.2,1.5); Wafer thickness: 180 um, kerfloss: 65 um, additional losses: 27.5 um; silicon density: 2330 kg/m3; ITRPV2020; Woodhouse et al. (2019); c-Si PV Manufacturing Costs 2018
	flat glass, uncoated, at plant	RER	0	kg		9.99E-3	4.08E-2	9.99E-3	4.08E-2	1	1.26	(3.4,2.3,1.5); de Wild-Scholten (2014) Life Cycle Assessment of Photovoltaics Status 2011, Part 1 Data Collection (Table 19.25)
	sodium hydroxide, 50% in H2O, production mix, at plant	RER	0	kg		1.50E-2	1.50E-2	1.50E-2	1.50E-2	1	1.22	(1.2,4.1,1.3); de Wild-Scholten (2014) Life Cycle Assessment of Photovoltaics Status 2011, Part 1 Data Collection (Table 19.25)
	hydrochloric acid, 30% in H2O, at plant	RER	0	kg		2.70E-3	2.70E-3	2.70E-3	2.70E-3	1	1.22	(1.2,4.1,1.3); de Wild-Scholten (2014) Life Cycle Assessment of Photovoltaics Status 2011, Part 1 Data Collection (Table 19.25)
	acetic acid, 98% in H2O, at plant	RER	0	kg		3.90E-2	3.90E-2	3.90E-2	3.90E-2	1	1.22	(1.2,4.1,1.3); de Wild-Scholten (2014) Life Cycle Assessment of Photovoltaics Status 2011, Part 1 Data Collection (Table 19.25)
	dipropylene glycol monomethyl ether, at plant	RER	0	kg		3.00E-1	3.00E-1	3.00E-1	3.00E-1	1	1.22	(1.2,4.1,1.3); de Wild-Scholten (2014) Life Cycle Assessment of Photovoltaics Status 2011, Part 1 Data Collection (Table 19.25)
	alkylbenzene sulfonate, linear, petrochemical, at plant	RER	0	kg		2.40E-1	2.40E-1	2.40E-1	2.40E-1	1	1.22	(1.2,4.1,1.3); de Wild-Scholten (2014) Life Cycle Assessment of Photovoltaics Status 2011, Part 1 Data Collection (Table 19.25)
	acrylic binder, 34% in H2O, at plant	RER	0	kg		2.00E-3	3.85E-3	2.00E-3	3.85E-3	1	1.22	(1.2,4.1,1.3); de Wild-Scholten (2014) Life Cycle Assessment of Photovoltaics Status 2011, Part 1 Data Collection (Table 19.25)
	brass, at plant	CH	0	kg		7.44E-3	7.44E-3	7.44E-3	7.44E-3	1	1.22	(3.2,1.1,3.5); Proxy for diamond wire; Woodhouse et al. (2019); c-Si PV Manufacturing Costs 2018
	chromium steel 188, at plant	RER	0	kg		1.51E-3	1.51E-3	1.51E-3	1.51E-3	1	1.32	(3.2,1.1,3.5); de Wild-Scholten (2014) Life Cycle Assessment of Photovoltaics Status 2011, Part 1 Data Collection (Table 19.25)
	wire drawing, steel	RER	0	kg		8.95E-3	8.95E-3	8.95E-3	8.95E-3	1	1.32	(3.2,1.1,3.5); de Wild-Scholten (2014) Life Cycle Assessment of Photovoltaics Status 2011, Part 1 Data Collection (Table 19.25)
electricity, medium voltage, at grid	CN	0	kWh		4.76E+0	5.56E+0	0	0	1	2.05	(2.2,1.2,1.5); Woodhouse et al. (2019); c-Si PV Manufacturing Costs 2018	
electricity, medium voltage, at grid	US	0	kWh		0	0	4.76E+0	5.56E+0	1	2.05	(2.2,1.2,1.5); Woodhouse et al. (2019); c-Si PV Manufacturing Costs 2018	
electricity, medium voltage, at grid	KR	0	kWh		0	0	0	0	1	2.05	(2.2,1.2,1.5); Woodhouse et al. (2019); c-Si PV Manufacturing Costs 2018	
electricity, medium voltage, production ENTSO, at grid	ENTSO	0	kWh		0	0	0	0	1	2.05	(2.2,1.2,1.5); Woodhouse et al. (2019); c-Si PV Manufacturing Costs 2018	
natural gas, burned in industrial furnace low-NOx >100kW	RER	0	MJ		4.00E+0	4.00E+0	4.00E+0	4.00E+0	1	1.22	(1.2,4.1,1.3); de Wild-Scholten (2014) Life Cycle Assessment of Photovoltaics Status 2011, Part 1 Data Collection (Table 19.25)	
water, deionised, water balance according to MoeK 2013, at plant	CN	0	kg		5.56E+1	5.56E+1	0	0	1	1.26	(3.4,2.3,1.5); de Wild-Scholten (2014) Life Cycle Assessment of Photovoltaics Status 2011, Part 1 Data Collection (Table 19.25)	
water, deionised, water balance according to MoeK 2013, at plant	US	0	kg		0	0	5.56E+1	5.56E+1	1	1.26	(3.4,2.3,1.5); de Wild-Scholten (2014) Life Cycle Assessment of Photovoltaics Status 2011, Part 1 Data Collection (Table 19.25)	
water, deionised, water balance according to MoeK 2013, at plant	KR	0	kg		0	0	0	0	1	1.26	(3.4,2.3,1.5); de Wild-Scholten (2014) Life Cycle Assessment of Photovoltaics Status 2011, Part 1 Data Collection (Table 19.25)	
water, deionised, water balance according to MoeK 2013, at plant	RER	0	kg		0	0	0	0	1	1.26	(3.4,2.3,1.5); China photovoltaic cell industry cleaner production evaluation index system	
disposal	DE	0	kg		1.10E-1	1.70E-1	1.10E-1	1.70E-1	1	1.22	(1.2,4.1,1.3); de Wild-Scholten (2014) Life Cycle Assessment of Photovoltaics Status 2011, Part 1 Data Collection (Table 19.25)	
natural gas, burned in industrial furnace low-NOx >100kW	CH	0	m3		5.00E-2	5.00E-2	5.00E-2	5.00E-2	1	1.26	(3.4,2.3,1.5); Calculation based on water withdrawal and water emissions	
transport, freight, lorry, fleet average	RER	0	km		2.36E-1	2.77E-1	2.36E-1	2.77E-1	1	2.09	(4.5,na,na,na); Transport distance: 100km; silicon: 200km	
transport, freight, rail	RER	0	km		1.25E+0	1.27E+0	1.25E+0	1.27E+0	1	2.09	(4.5,na,na,na); Transport distance: 100-600km	
infrastructure	DE	1	unit		4.00E-6	4.00E-6	4.00E-6	4.00E-6	1	3.05	(1.2,4.1,1.3); de Wild-Scholten (2014) Life Cycle Assessment of Photovoltaics Status 2011, Part 1 Data Collection (Table 19.25)	
emission air	Heat, waste	-	-	MJ		1.71E+1	2.00E+1	1.71E+1	2.00E+1	1	1.34	(3.4,4.3,1.5); de Wild-Scholten (2014) Life Cycle Assessment of Photovoltaics Status 2011, Part 1 Data Collection (Table 19.25)
	Water, CN	-	-	kg		5.56E+0	5.56E+0	0	0	1	1.65	(3.4,4.3,1.5); de Wild-Scholten (2014) Life Cycle Assessment of Photovoltaics Status 2011, Part 1 Data Collection (Table 19.25)
	Water, US	-	-	kg		0	0	5.56E+0	5.56E+0	1	1.65	(3.4,4.3,1.5); de Wild-Scholten (2014) Life Cycle Assessment of Photovoltaics Status 2011, Part 1 Data Collection (Table 19.25)
	Water, KR	-	-	kg		0	0	0	0	1	1.65	(3.4,4.3,1.5); de Wild-Scholten (2014) Life Cycle Assessment of Photovoltaics Status 2011, Part 1 Data Collection (Table 19.25)
	Water, RER	-	-	kg		0	0	0	0	1	1.65	(3.4,4.3,1.5); de Wild-Scholten (2014) Life Cycle Assessment of Photovoltaics Status 2011, Part 1 Data Collection (Table 19.25)
emission water, river	COD, Chemical Oxygen Demand	-	-	kg		2.95E-2	2.95E-2	2.95E-2	2.95E-2	1	1.64	(2.4,4.3,1.5); de Wild-Scholten (2014) Life Cycle Assessment of Photovoltaics Status 2011, Part 1 Data Collection (Table 19.25)
	BOD5, Biological Oxygen Demand	-	-	kg		2.95E-2	2.95E-2	2.95E-2	2.95E-2	1	1.65	(3.4,5.3,1.5); de Wild-Scholten (2014) Life Cycle Assessment of Photovoltaics Status 2011, Part 1 Data Collection (Table 19.25)
	COD, Chemical Oxygen Demand	-	-	kg		1.11E-2	1.11E-2	1.11E-2	1.11E-2	1	1.85	(3.4,5.3,1.5); de Wild-Scholten (2014) Life Cycle Assessment of Photovoltaics Status 2011, Part 1 Data Collection (Table 19.25)
	TOC, Total Organic Carbon	-	-	kg		1.11E-2	1.11E-2	1.11E-2	1.11E-2	1	1.85	(3.4,5.3,1.5); de Wild-Scholten (2014) Life Cycle Assessment of Photovoltaics Status 2011, Part 1 Data Collection (Table 19.25)

B INVENTORY LIST

Table 19: Unit process LCI data of the photovoltaic laminate and panel production in China (CN)

product	Name	Location	InfrastructureProcess	Unit	photovoltaic panel, single-Si, at plant				Uncertainty Type	Standard/Revision/5%	GeneralComment
					photovoltaic panel, single-Si, at plant	photovoltaic panel, multi-Si, at plant	photovoltaic laminate, single-Si, at plant	photovoltaic laminate, multi-Si, at plant			
					CN	CN	CN	CN			
	Location InfrastructureProcess Unit				1	1	1	1			
	photovoltaic panel, single-Si, at plant	CN	1	m2	1	0	0	0			
	photovoltaic panel, multi-Si, at plant	CN	1	m2	0	1	0	0			
	photovoltaic laminate, single-Si, at plant	CN	1	m2	0	0	1	0			
	photovoltaic laminate, multi-Si, at plant	CN	1	m2	0	0	0	1			
	photovoltaic panel, single-Si, at plant	US	1	m2	0	0	0	0			
	photovoltaic panel, multi-Si, at plant	US	1	m2	0	0	0	0			
	photovoltaic laminate, single-Si, at plant	US	1	m2	0	0	0	0			
	photovoltaic laminate, multi-Si, at plant	US	1	m2	0	0	0	0			
	photovoltaic panel, single-Si, at plant	APAC	1	m2	0	0	0	0			
	photovoltaic panel, multi-Si, at plant	APAC	1	m2	0	0	0	0			
	photovoltaic laminate, single-Si, at plant	APAC	1	m2	0	0	0	0			
	photovoltaic laminate, multi-Si, at plant	APAC	1	m2	0	0	0	0			
	photovoltaic panel, single-Si, at plant	RER	1	m2	0	0	0	0			
	photovoltaic panel, multi-Si, at plant	RER	1	m2	0	0	0	0			
	photovoltaic laminate, single-Si, at plant	RER	1	m2	0	0	0	0			
	photovoltaic laminate, multi-Si, at plant	RER	1	m2	0	0	0	0			
materials	photovoltaic cell, single-Si, at plant	CN	0	m2	9.35E-1	0	0	9.35E-1	1	1.24	(1.4.4.3.1.3) de Wild-Scholten (2014) Life Cycle Assessment of Photovoltaics Status 2011, Part 1 Data Collection (Table 37)
	photovoltaic cell, multi-Si, at plant	CN	0	m2	0	9.35E-1	0	9.35E-1	1	1.24	(1.4.4.3.1.3) de Wild-Scholten (2014) Life Cycle Assessment of Photovoltaics Status 2011, Part 1 Data Collection (Table 37)
	photovoltaic cell, single-Si, at regional storage	US	0	m2	0	0	0	0	1	3.06	(1.4.4.3.1.3) de Wild-Scholten (2014) Life Cycle Assessment of Photovoltaics Status 2011, Part 1 Data Collection (Table 37)
	photovoltaic cell, multi-Si, at regional storage	US	0	m2	0	0	0	0	1	3.06	(1.4.4.3.1.3) de Wild-Scholten (2014) Life Cycle Assessment of Photovoltaics Status 2011, Part 1 Data Collection (Table 37)
	photovoltaic cell, single-Si, at plant	APAC	0	m2	0	0	0	0	1	1.24	(1.4.4.3.1.3) de Wild-Scholten (2014) Life Cycle Assessment of Photovoltaics Status 2011, Part 1 Data Collection (Table 37)
	photovoltaic cell, multi-Si, at plant	APAC	0	m2	0	0	0	0	1	1.24	(1.4.4.3.1.3) de Wild-Scholten (2014) Life Cycle Assessment of Photovoltaics Status 2011, Part 1 Data Collection (Table 37)
	photovoltaic cell, single-Si, at regional storage	RER	0	m2	0	0	0	0	1	3.06	(1.4.4.3.1.3) de Wild-Scholten (2014) Life Cycle Assessment of Photovoltaics Status 2011, Part 1 Data Collection (Table 37)
	photovoltaic cell, multi-Si, at regional storage	RER	0	m2	0	0	0	0	1	3.06	(1.4.4.3.1.3) de Wild-Scholten (2014) Life Cycle Assessment of Photovoltaics Status 2011, Part 1 Data Collection (Table 37)
	aluminium alloy, AlMg3, at plant	RER	0	kg	2.13E+0	2.13E+0	0	0	1	1.24	(1.4.4.3.1.3) de Wild-Scholten (2014) Life Cycle Assessment of Photovoltaics Status 2011, Part 1 Data Collection (Table 37)
	copper, at regional storage	RER	0	kg	1.03E-1	1.03E-1	1.03E-1	1.03E-1	1	1.24	(1.4.4.3.1.3) de Wild-Scholten (2014) Life Cycle Assessment of Photovoltaics Status 2011, Part 1 Data Collection (Table 37)
	wire drawing, copper	RER	0	kg	1.03E-1	1.03E-1	1.03E-1	1.03E-1	1	1.24	(1.4.4.3.1.3) de Wild-Scholten (2014) Life Cycle Assessment of Photovoltaics Status 2011, Part 1 Data Collection (Table 37)
	diode, unspecified, at plant	GLO	0	kg	2.81E-3	2.81E-3	2.81E-3	2.81E-3	1	1.34	(3.4.4.3.1.5) de Wild-Scholten (2014) Life Cycle Assessment of Photovoltaics Status 2011, Part 1 Data Collection (Table 37)
	silicone product, at plant	RER	0	kg	1.22E-1	1.22E-1	1.22E-1	1.22E-1	1	1.24	(1.4.4.3.1.3) de Wild-Scholten (2014) Life Cycle Assessment of Photovoltaics Status 2011, Part 1 Data Collection (Table 37)
	tin, at regional storage	RER	0	kg	1.29E-2	1.29E-2	1.29E-2	1.29E-2	1	1.34	(3.4.4.3.1.5) de Wild-Scholten (2014) Life Cycle Assessment of Photovoltaics Status 2011, Part 1 Data Collection (Table 37)
	lead, at regional storage	RER	0	kg	7.25E-4	7.25E-4	7.25E-4	7.25E-4	1	1.34	(1.4.4.3.1.3) de Wild-Scholten (2014) Life Cycle Assessment of Photovoltaics Status 2011, Part 1 Data Collection (Table 37)
	solar glass, low-iron, at regional storage	RER	0	kg	8.81E+0	8.81E+0	8.81E+0	8.81E+0	1	1.33	(1.4.4.3.3.3) de Wild-Scholten (2014) Life Cycle Assessment of Photovoltaics Status 2011, Part 1 Data Collection (Table 37)
	tempering, flat glass	RER	0	kg	8.81E+0	8.81E+0	8.81E+0	8.81E+0	1	1.24	(1.4.4.3.1.3) de Wild-Scholten (2014) Life Cycle Assessment of Photovoltaics Status 2011, Part 1 Data Collection (Table 37)
	glass fibre reinforced plastic, polyamide, injection moulding, at plant	RER	0	kg	2.95E-1	2.95E-1	2.95E-1	2.95E-1	1	1.24	(1.4.4.3.1.3) de Wild-Scholten (2014) Life Cycle Assessment of Photovoltaics Status 2011, Part 1 Data Collection (Table 37)
	polyethylene terephthalate, granulate, amorphous, at plant	RER	0	kg	3.46E-1	3.46E-1	3.46E-1	3.46E-1	1	1.24	(1.4.4.3.1.3) de Wild-Scholten (2014) Life Cycle Assessment of Photovoltaics Status 2011, Part 1 Data Collection (Table 37)
	polyethylene, HDPE, granulate, at plant	RER	0	kg	2.38E-2	2.38E-2	2.38E-2	2.38E-2	1	1.34	(3.4.4.3.1.5) de Wild-Scholten (2014) Life Cycle Assessment of Photovoltaics Status 2011, Part 1 Data Collection (Table 37)
	ethylvinylacetate, foil, at plant	RER	0	kg	8.75E-1	8.75E-1	8.75E-1	8.75E-1	1	1.24	(1.4.4.3.1.3) de Wild-Scholten (2014) Life Cycle Assessment of Photovoltaics Status 2011, Part 1 Data Collection (Table 37)
	polyvinylfluoride film, at plant	US	0	kg	1.12E-1	1.12E-1	1.12E-1	1.12E-1	1	1.24	(1.4.4.3.1.3) de Wild-Scholten (2014) Life Cycle Assessment of Photovoltaics Status 2011, Part 1 Data Collection (Table 37)
auxiliaries	tap water, water balance according to MbeK 2013, at user	CN	0	kg	5.03E+0	5.03E+0	5.03E+0	5.03E+0	1	1.24	(1.4.4.3.1.3) de Wild-Scholten (2014) Life Cycle Assessment of Photovoltaics Status 2011, Part 1 Data Collection (Table 37)
	tap water, water balance according to MbeK 2013, at user	US	0	kg	0	0	0	0	1	1.24	(1.4.4.3.1.3) de Wild-Scholten (2014) Life Cycle Assessment of Photovoltaics Status 2011, Part 1 Data Collection (Table 37)
	tap water, water balance according to MbeK 2013, at user	KR	0	kg	0	0	0	0	1	1.24	(1.4.4.3.1.3) de Wild-Scholten (2014) Life Cycle Assessment of Photovoltaics Status 2011, Part 1 Data Collection (Table 37)
	tap water, water balance according to MbeK 2013, at user	RER	0	kg	0	0	0	0	1	1.24	(1.4.4.3.1.3) de Wild-Scholten (2014) Life Cycle Assessment of Photovoltaics Status 2011, Part 1 Data Collection (Table 37)
	hydrogen fluoride, at plant	GLO	0	kg	6.24E-2	6.24E-2	6.24E-2	6.24E-2	1	1.34	(3.4.4.3.1.5) de Wild-Scholten (2014) Life Cycle Assessment of Photovoltaics Status 2011, Part 1 Data Collection (Table 37)
	1-propanol, at plant	RER	0	kg	1.59E-2	1.59E-2	1.59E-2	1.59E-2	1	1.24	(1.4.4.3.1.3) de Wild-Scholten (2014) Life Cycle Assessment of Photovoltaics Status 2011, Part 1 Data Collection (Table 37)
	isopropanol, at plant	RER	0	kg	1.47E-4	1.47E-4	1.47E-4	1.47E-4	1	1.34	(3.4.4.3.1.5) de Wild-Scholten (2014) Life Cycle Assessment of Photovoltaics Status 2011, Part 1 Data Collection (Table 37)
	potassium hydroxide, at regional storage	RER	0	kg	5.14E-2	5.14E-2	5.14E-2	5.14E-2	1	1.34	(3.4.4.3.1.5) de Wild-Scholten (2014) Life Cycle Assessment of Photovoltaics Status 2011, Part 1 Data Collection (Table 37)
	soap, at plant	RER	0	kg	1.16E-2	1.16E-2	1.16E-2	1.16E-2	1	1.34	(3.4.4.3.1.5) de Wild-Scholten (2014) Life Cycle Assessment of Photovoltaics Status 2011, Part 1 Data Collection (Table 37)
	corrugated board, mixed fibre, single wall, at plant	RER	0	kg	7.63E-1	7.63E-1	7.63E-1	7.63E-1	1	1.24	(1.4.4.3.1.3) de Wild-Scholten (2014) Life Cycle Assessment of Photovoltaics Status 2011, Part 1 Data Collection (Table 37)
	EUR-flat pallet	RER	0	unit	5.00E-2	5.00E-2	5.00E-2	5.00E-2	1	1.34	(3.4.4.3.1.5) de Wild-Scholten (2014) Life Cycle Assessment of Photovoltaics Status 2011, Part 1 Data Collection (Table 37)
energy	electricity, medium voltage, at grid	CN	0	kWh	1.40E+1	1.40E+1	1.40E+1	1.40E+1	1	1.09	(2.2.1.1.3) Woodhouse et al. (2019): c-Si PV Manufacturing Costs 2018
	electricity, medium voltage, at grid	US	0	kWh	0	0	0	0	1	1.09	(2.2.1.1.3) Woodhouse et al. (2019): c-Si PV Manufacturing Costs 2018
	electricity, medium voltage, at grid	KR	0	kWh	0	0	0	0	1	1.09	(2.2.1.1.3) Woodhouse et al. (2019): c-Si PV Manufacturing Costs 2018
	electricity, medium voltage, production ENTSO, at grid	ENTSO	0	kWh	0	0	0	0	1	1.09	(2.2.1.1.3) Woodhouse et al. (2019): c-Si PV Manufacturing Costs 2018
	diesel, burned in building machine, average	CH	0	MJ	8.75E-3	8.75E-3	8.75E-3	8.75E-3	1	2.12	(3.4.4.3.1.5) de Wild-Scholten (2014) Life Cycle Assessment of Photovoltaics Status 2011, Part 1 Data Collection (Table 37)
infrastructure	photovoltaic panel factory	GLO	1	unit	4.00E-6	4.00E-6	4.00E-6	4.00E-6	1	3.06	(1.4.4.3.1.3) de Wild-Scholten (2014) Life Cycle Assessment of Photovoltaics Status 2011, Part 1 Data Collection (Table 37)
transport	transport, freight, lorry, fleet average	RER	0	tkm	2.77E+0	3.01E+0	2.56E+0	2.79E+0	1	2.09	(4.5.na.na.na.na): Standard distance 100km, cells 500km
	transport, freight, rail	RER	0	tkm	1.66E-1	1.66E-1	1.54E-1	1.54E-1	1	2.09	(4.5.na.na.na.na): Standard distance 600km
disposal	disposal, municipal solid waste, 22.9% water, to municipal incineration	CH	0	kg	3.00E-2	3.00E-2	3.00E-2	3.00E-2	1	1.24	(1.4.4.3.1.3) Asema (personal communication) 2007, production waste
	disposal, polyvinylfluoride, 0.2% water, to municipal incineration	CH	0	kg	4.29E-3	4.29E-3	4.29E-3	4.29E-3	1	1.24	(1.4.4.3.1.3) de Wild-Scholten (2014) Life Cycle Assessment of Photovoltaics Status 2011, Part 1 Data Collection (Table 37)
	disposal, plastics, mixture, 15.3% water, to municipal incineration	CH	0	kg	2.81E-2	2.81E-2	2.81E-2	2.81E-2	1	1.24	(1.4.4.3.1.3) de Wild-Scholten (2014) Life Cycle Assessment of Photovoltaics Status 2011, Part 1 Data Collection (Table 37)
	disposal, used mineral oil, 10% water, to hazardous waste incineration	CH	0	kg	1.61E-3	1.61E-3	1.61E-3	1.61E-3	1	1.24	(1.4.4.3.1.3) de Wild-Scholten (2014) Life Cycle Assessment of Photovoltaics Status 2011, Part 1 Data Collection (Table 37)
	treatment, sewage, from residence, to wastewater treatment, class 2	CH	0	m3	4.53E-3	4.53E-3	4.53E-3	4.53E-3	1	1.24	(1.4.4.3.1.3) Calculation, water use
emissions air	Heat, waste	-	-	MJ	5.03E+1	5.03E+1	5.03E+1	5.03E+1	1	1.60	(3.4.5.3.1.5) Calculation, electrolyse
	NM VOC, non-methane volatile organic compounds, unspecified origin	-	-	kg	8.06E-3	8.06E-3	8.06E-3	8.06E-3	1	1.85	(3.4.5.3.1.5) de Wild-Scholten (2014) Life Cycle Assessment of Photovoltaics Status 2011, Part 1 Data Collection (Table 37)
	Carbon dioxide, fossil	-	-	kg	2.18E-2	2.18E-2	2.18E-2	2.18E-2	1	1.60	(3.4.5.3.1.5) de Wild-Scholten (2014) Life Cycle Assessment of Photovoltaics Status 2011, Part 1 Data Collection (Table 37)
	Water, CN	-	-	kg	5.03E-1	5.03E-1	5.03E-1	5.03E-1	1	1.85	(3.4.5.3.1.5) de Wild-Scholten (2014) Life Cycle Assessment of Photovoltaics Status 2011, Part 1 Data Collection (Table 37)
	Water, US	-	-	kg	0	0	0	0	1	1.85	(3.4.5.3.1.5) de Wild-Scholten (2014) Life Cycle Assessment of Photovoltaics Status 2011, Part 1 Data Collection (Table 37)
	Water, KR	-	-	kg	0	0	0	0	1	1.85	(3.4.5.3.1.5) de Wild-Scholten (2014) Life Cycle Assessment of Photovoltaics Status 2011, Part 1 Data Collection (Table 37)
	Water, RER	-	-	kg	0	0	0	0	1	1.85	(3.4.5.3.1.5) de Wild-Scholten (2014) Life Cycle Assessment of Photovoltaics Status 2011, Part 1 Data Collection (Table 37)

B INVENTORY LIST

Table 29: Unit process LCI data of the treatment of used c-Si PV modules in a first generation recycling process and of the recovered materials according to the cut-off approach

	Name	Location	InfrastructureProcess	Unit	treatment, c-Si PV module	glass cullets, recovered from c-Si PV module treatment	aluminium scrap, recovered from c-Si PV module treatment	copper scrap, recovered from c-Si PV module treatment	UncertaintyType	StandardDeviation95%	GeneralComment
					RER	RER	RER	RER			
product	treatment, c-Si PV module	RER	0	kg	1	0	0	0			
	glass cullets, recovered from c-Si PV module treatment	RER	0	kg	0	1	0	0			
	aluminium scrap, recovered from c-Si PV module treatment	RER	0	kg	0	0	1	0			
	copper scrap, recovered from c-Si PV module treatment	RER	0	kg	0	0	0	1			
	electricity, medium voltage, production ENTSO, at grid	ENTSO	0	kWh	5.56E-2	4.05E-3	1.42E-1	8.09E-1	1	1.25	(2,3,1,1,3,4,BU:1.05); Weighted average of data from recyclers; Economic allocation;
technosphere	diesel, burned in building machine, average	CH	0	MJ	3.24E-2	2.36E-3	8.25E-2	4.71E-1	1	2.07	(2,3,1,1,3,4,BU:2); Weighted average of data from recyclers; Economic allocation;
	disposal, plastics, mixture, 15.3% water, to municipal incineration	CH	0	kg	7.34E-2	5.34E-3	1.87E-1	1.07E+0	1	1.25	(2,3,1,1,3,4,BU:1.05); Weighted average of data from recyclers; Economic allocation;
	disposal, plastics, mixture, 15.3% water, to sanitary landfill	CH	0	kg	1.28E-2	9.33E-4	3.26E-2	1.87E-1	1	1.25	(2,3,1,1,3,4,BU:1.05); Weighted average of data from recyclers; Economic allocation;
	transport, freight, lorry 3.5-7.5 metric ton, EURO 5	RER	0	tkm	5.00E-2	3.64E-3	1.27E-1	7.27E-1	1	2.09	(4,5,na,na,na,na,BU:2); Assumed transport distance to collection point: 100 km; Economic allocation; Latunussa et al. 2016
	transport, freight, lorry, fleet average	RER	0	tkm	2.00E-1	1.45E-2	5.09E-1	2.91E+0	1	2.09	(4,5,na,na,na,na,BU:2); Assumed transport distance to recycling site: 400 km; Economic allocation; Latunussa et al. 2016

Table 36: Unit process LCI data of ground-mount PV mounting systems

	Name	Location	InfrastructureProcess	Unit	open ground construction, on ground, Mont Soleil	UncertaintyType	StandardDeviation95%	GeneralComment
					CH			
product materials	open ground construction, on ground, Mont Soleil	CH	1	m2	1			
	gravel, round, at mine	CH	0	kg	350	1	1.89	(2,1,5,1,1,5); gravel for access route
	excavation, hydraulic digger, average	CH	0	m3	0	1	3.21	(2,1,5,1,1,5); for access route
	zinc, primary, at regional storage	RER	0	kg	3	1	1.89	(2,1,5,1,1,5);
	concrete, normal, at plant	CH	0	m3	2.05E-2	1	1.89	(2,1,5,1,1,5); foundation and building
	reinforcing steel, at plant	RER	0	kg	3.95E+1	1	1.89	(2,1,5,1,1,5); for foundation
	steel, low-alloyed, at plant	RER	0	kg	2.51E+0	1	1.89	(2,1,5,1,1,5); for fence and building
	particleboard, average glue mix, uncoated, at plant	RER	0	m3	9.98E-4	1	1.89	(2,1,5,1,1,5); for building
	roof tile, at plant	RER	0	kg	5.41E-1	1	1.89	(2,1,5,1,1,5); for building
	polyurethane, flexible foam, at plant	RER	0	kg	9.94E-2	1	1.89	(2,1,5,1,1,5); for building insulation
	zinc coating, coils	RER	0	m2	1.83E-1	1	1.89	(2,1,5,1,1,5); coating of fence and building steel
	polyethylene, HDPE, granulate, at plant	RER	0	kg	4.17E-2	1	1.89	(2,1,5,1,1,5); for building
	acetone, liquid, at plant	RER	0	kg	4.57E-2	1	1.89	(2,1,5,1,1,5); for cleaning of profiles
	polyvinylchloride, at regional storage	RER	0	kg	1.11E-2	1	1.89	(2,1,5,1,1,5); for building
	bitumen, at refinery	CH	0	kg	2.03E-2	1	1.89	(2,1,5,1,1,5); for building
	rock wool, packed, at plant	CH	0	kg	1.92E-2	1	1.89	(2,1,5,1,1,5); for building
	flat glass, coated, at plant	RER	0	kg	7.21E-3	1	1.89	(2,1,5,1,1,5); for building
	acrylic binder, 34% in H2O, at plant	RER	0	kg	5.20E-3	1	1.89	(2,1,5,1,1,5); assumed for acryl tape
	silicone product, at plant	RER	0	kg	4.79E-2	1	1.89	(2,1,5,1,1,5); silicone glue
	transport	transport, freight, lorry 7.5-16 metric ton, fleet average	CH	0	tkm	9.45E+0	1	2.85
transport, freight, lorry 16-32 metric ton, fleet average		CH	0	tkm	2.95E+0	1	2.85	(4,5,na,na,na,na); Literature
disposal	disposal, concrete, 5% water, to inert material landfill	CH	0	kg	4.87E+1	1	1.91	(3,1,5,1,1,5); Literature and own estimations
	disposal, building, reinforcement steel, to sorting plant	CH	0	kg	3.95E+1	1	1.91	(3,1,5,1,1,5); Literature and own estimations
	disposal, building, fibre board, to final disposal	CH	0	kg	6.79E-1	1	1.91	(3,1,5,1,1,5); Literature and own estimations
	disposal, building, polyurethane foam, to final disposal	CH	0	kg	9.94E-2	1	1.91	(3,1,5,1,1,5); Literature and own estimations
	disposal, building, polyethylene/polypropylene products, to final disposal	CH	0	kg	4.17E-2	1	1.91	(3,1,5,1,1,5); Literature and own estimations
	disposal, building, polyethylene/polypropylene products, to final disposal	CH	0	kg	1.11E-2	1	1.91	(3,1,5,1,1,5); Literature and own estimations
	disposal, building, polyvinylchloride products, to final disposal	CH	0	kg	1.11E-2	1	1.91	(3,1,5,1,1,5); Literature and own estimations
	disposal, building, mineral wool, to sorting plant	CH	0	kg	1.92E-2	1	1.91	(3,1,5,1,1,5); Literature and own estimations
	disposal, building, glass pane (in burnable frame), to sorting plant	CH	0	kg	7.21E-3	1	1.91	(3,1,5,1,1,5); Literature and own estimations
	resources	Transformation, from pasture and meadow	-	-	m2	4.72E+0	1	2.00
Transformation, to industrial area, built up		-	-	m2	1.50E+0	1	3.23	(3,1,5,1,1,5); Literature and own estimations
Transformation, to industrial area, vegetation		-	-	m2	3.22E+0	1	1.91	(3,1,5,1,1,5); Literature and own estimations
emission	Occupation, industrial area, built up	-	-	m2a	4.50E+1	1	5.37	(3,1,5,1,1,5); Assumed life time: 30 a
	Occupation, industrial area, vegetation	-	-	m2a	9.67E+1	1	2.37	(3,1,5,1,1,5); Assumed life time: 30 a
	Acetone	-	-	kg	4.57E-2	1	1.89	(2,1,5,1,1,5); Assumed life time: 30 a

C Emissions from Recycling

```

area = 2.278*1.134 % m2 per panel
mass = 31.8 % kg per panel

% Values from the IEA PVPS rapport
copper_m2 = 1.03*10^-1 % kg per m2
alum_m2 = 46.2*10^-3 % kg per m2
glass_m2 = 8.81*2*2 % kg per m2

copper_panel = area*copper_m2 % m2 * kg/m2 = kg copper per panel
alum_panel = area*alum_m2 % kg aluminum per panel
glass_panel = area*glass_m2 % kg glass per panel

copper_co2_1kg = 3.74 % kg co2-eq per 1 kg copper
alum_co2_1kg = 0.654 % kg co2-eq per 1 kg aluminium
glass_co2_1kg = 0.158 % kg co2-eq per 1 kg glass
Treatment_co2_1kg = 0.459 % kg co2-eq per 1 kg modul

copper_co2_panel = copper_co2_1kg*copper_panel % kg co2-eq per
panel
alum_co2_panel = alum_co2_1kg*alum_panel % kg co2_eq per panel
glass_co2_panel = glass_co2_1kg*glass_panel % kg co2-eq per
panel
Treatment_co2_panel = mass*Treatment_co2_1kg % kg co2-eq per
panel

co2_panel = copper_co2_panel+alum_co2_panel+glass_co2_panel+
Treatment_co2_panel % kg co2-eq per panel
  
```

D LAND-USE CHANGE CALCULATIONS

D Land-Use Change Calculations

	A	B	C	D	E
1	Land use changes				
2					
3		Analysis period (years):	30		
4		Type of soil:	Mineral soil		
5		Type of forest:	Coniferous forest		
6					
7		<i>ton CO₂-eq/hectare/year</i>			
8	EMISSION FACTORS	Low site productivity	High site productivity		
9	No land-use change	-3,3	-3,7		
10	For the first year of the land-use change	39,78	57,66		
11	Per year the next 19 years	14,19	14,19		
12	For the area after the transition phase of 20 years	1,3	1,3		
13					
14	Low site productivity				
15		CO ₂	CH ₄	N ₂ O	Total (CO ₂ -eqv)
16	Emission / absorption from the area without land-use change	-3793,2	767,7	57,6	-2967,9
17	Emission / absorption if there is a land-use change	9680,8	0,0	0,0	9680,8
18	Total climate effect of the land-use change	13474,0	-767,7	-57,6	12648,7
19					
20	High site productivity				
21		CO ₂	CH ₄	N ₂ O	Total (CO ₂ -eqv)
22	Emission / absorption from the area without land-use change	-4154,6	767,7	57,6	-3329,3
23	Emission / absorption if there is a land-use change	10217,0	0,0	0,0	10217
24	Total climate effect of the land-use change	14371,6	-767,7	-57,6	13546,3
25					
26	Constructed area				
27		CO ₂	CH ₄	N ₂ O	Total (CO ₂ -eqv)
28	Emission / absorption from the area without land-use change	0,0	0,0	0,0	0,0
29	Emission / absorption if there is a land-use change	0,0	0,0	0,0	0,0
30	Total climate effect of the land-use change	0,0	0,0	0,0	0,0

Figure D.1: Land use change calculations in Excel

	A	B	C	D	E
1	Land use changes				
2					
3		Analysis period (years):	30		
4		Type of soil:	Mineral soil		
5		Type of forest:	Coniferous forest		
6					
7		<i>ton CO₂-eq/hectare/year</i>			
8	EMISSION FACTORS	Low site productivity	High site productivity		
9	No land-use change	-3,3	-3,7		
10	For the first year of the land-use change	39,78	57,66		
11	Per year the next 19 years	14,19	14,19		
12	For the area after the transition phase of 20 years	1,33	1,33		
13					
14	Low site productivity				
15		CO ₂	CH ₄	N ₂ O	Total (CO ₂ -eqv)
16	Emission / absorption from the area without land-use change	=-2528,8/20*C3	=511,8/20*C3	=38,4/20*C3	=B16+C16+D16
17	Emission / absorption if there is a land-use change	=9281,8+M22*B12*(C3-20)	0	0	=B17+C17+D17
18	Total climate effect of the land-use change	=B17-B16	=C17-C16	=D17-D16	=E17-E16
19					
20	High site productivity				
21		CO ₂	CH ₄	N ₂ O	Total (CO ₂ -eqv)
22	Emission / absorption from the area without land-use change	=-2769,7/20*C3	=511,8/20*C3	=38,4/20*C3	=B22+C22+D22
23	Emission / absorption if there is a land-use change	=N23	0	0	=B23+C23+D23
24	Total climate effect of the land-use change	=B23-B22	=C23-C22	=D23-D22	=B24+C24+D24
25					
26	Constructed area				
27		CO ₂	CH ₄	N ₂ O	Total (CO ₂ -eqv)
28	Emission / absorption from the area without land-use change	0	0	0	=B28+C28+D28
29	Emission / absorption if there is a land-use change	0	0	0	=B29+C29+D29
30	Total climate effect of the land-use change	=B29-B28	=C29-C28	=D29-D28	=B30+C30+D30

Figure D.2: Land use change calculations in Excel with formulas

E Snow Cover Calculations

E.1 Snow Data from the Norwegian Climate Service Center

Navn	Stasjon	Tid(norsk normaltid)	Gjennomsnittlig snødekke (mnd)
Halden	SN1230	jun.17	0
Halden	SN1230	jul.17	0
Halden	SN1230	aug.17	0
Halden	SN1230	sep.17	0
Halden	SN1230	okt.17	0
Halden	SN1230	nov.17	0
Halden	SN1230	des.17	1
Halden	SN1230	jan.18	2
Halden	SN1230	feb.18	2
Halden	SN1230	mar.18	1
Halden	SN1230	apr.18	0
Halden	SN1230	mai.18	0
Halden	SN1230	jun.18	0
Halden	SN1230	jul.18	0
Halden	SN1230	aug.18	0
Halden	SN1230	sep.18	0
Halden	SN1230	okt.18	0
Halden	SN1230	nov.18	0
Halden	SN1230	des.18	1
Halden	SN1230	jan.19	2
Halden	SN1230	feb.19	1
Halden	SN1230	mar.19	0
Halden	SN1230	apr.19	0
Halden	SN1230	mai.19	0
Halden	SN1230	jun.19	0
Halden	SN1230	jul.19	0
Halden	SN1230	aug.19	0
Halden	SN1230	sep.19	0
Halden	SN1230	okt.19	0
Halden	SN1230	nov.19	0
Halden	SN1230	des.19	0
Halden	SN1230	jan.20	0
Halden	SN1230	feb.20	0
Halden	SN1230	mar.20	0
Halden	SN1230	apr.20	0
Halden	SN1230	mai.20	0
Halden	SN1230	jun.20	0
Halden	SN1230	jul.20	0
Halden	SN1230	aug.20	0
Halden	SN1230	sep.20	0
Halden	SN1230	okt.20	0
Halden	SN1230	nov.20	0
Halden	SN1230	des.20	0
Halden	SN1230	jan.21	0
Halden	SN1230	feb.21	3
Halden	SN1230	mar.21	1
Halden	SN1230	apr.21	0
Halden	SN1230	mai.21	0
Halden	SN1230	jun.21	0
Halden	SN1230	jul.21	0
Halden	SN1230	aug.21	0
Halden	SN1230	sep.21	0
Halden	SN1230	okt.21	0
Halden	SN1230	nov.21	0
Halden	SN1230	feb.22	1
Halden	SN1230	mar.22	0
Halden	SN1230	apr.22	0
Halden	SN1230	mai.22	0
Halden	SN1230	jul.22	0
Halden	SN1230	aug.22	0
Halden	SN1230	sep.22	0
Halden	SN1230	okt.22	0
Halden	SN1230	nov.22	0

Data er gyldig per 13.04.2023 (CC BY 4.0), Meteorologisk institutt (MET)

E.2 MATLAB-script

```

sno_data = uiimport('-file'); % imports CSV file with snow data
    for Halden
sno = sno_data.data(1:63,2);

Sno=sno(8:63);

data_2017=sno(1:7); % June to December 2017
data_2018 = sno(8:19); % January to December 2018
data_2019 = sno(20:31); % January to December 2019
data_2020 = sno(32:43); % Januar to December 2020
data_2021 = sno(44:54); % Januar to November 2021
data_2022 = sno(55:63); % Frebruary to November 2022

% Find the average value for the different months
January = (data_2018(1)+data_2019(1)+data_2020(1)+data_2021(1))/4

Frebruary = (data_2018(2)+data_2019(2)+data_2020(2)+data_2021(2)+
    data_2022(1))/5

March = (data_2018(3)+data_2019(3)+data_2020(3)+data_2021(3)+
    data_2022(2))/5

April = (data_2018(4)+data_2019(4)+data_2020(4)+data_2021(4)+
    data_2022(3))/5

May = (data_2018(5)+data_2019(5)+data_2020(5)+data_2021(5)+
    data_2022(4))/5

June = (data_2018(6)+data_2019(6)+data_2020(6)+data_2021(6)+
    data_2022(5)+data_2017(1))/6

July = (data_2018(7)+data_2019(7)+data_2020(7)+data_2021(7)+
    data_2022(6)+data_2017(2))/6

August=(data_2018(8)+data_2019(8)+data_2020(8)+data_2021(8)+
    data_2022(7)+data_2017(3))/6

September = (data_2018(9)+data_2019(9)+data_2020(9)+data_2021(9)+
    data_2022(8)+data_2017(4))/6

October = (data_2018(10)+data_2019(10)+data_2020(10)+data_2021
    (10)+data_2022(9)+data_2017(5))/6

November = (data_2018(11)+data_2019(11)+data_2020(11)+data_2021
    (11)+data_2022(9)+data_2017(6))/6

```


E SNOW COVER CALCULATIONS

```
December = (data_2018(12)+data_2019(12)+data_2020(12)+data_2017  
(7))/4
```

F Ratio between Production and Emission Calculations

	A	B	C	D	E	F	G	H	I	J	K	L	M	N	O	P
1																
2																
3																
4		Quantity	kg CO2-eq pr. quantity	8 meters [ton CO2-eq]	9 meters [ton CO2-eq]	10 meters [ton CO2-eq]	11 meters [ton CO2-eq]	12 meters [ton CO2-eq]	13 meters [ton CO2-eq]	14 meters [ton CO2-eq]	15 meters [ton CO2-eq]					
5	Production	1 m2	122	20 150	17 971	16 065	14 701	13 615	12 526	11 709	10 892			Type of area	Emission [ton CO2-eq]	
6	Mounting	1 m2	91,9	15 178	13 538	12 102	11 074	10 256	9 435	8 820	8 205			Forest	Low site prod	12648,7
7	Transportation	All panels	220	0,220	0,220	0,220	0,220	0,220	0,220	0,220	0,220				High site prod	13 546,3
8	Recycling	1 panel	30,053	1 921	1 714	1 532	1 402	1 298	1 194	1 117	1 039			Constructed area		0
9				37 250	33 223	29 699	27 177	25 169	23 155	21 645	20 135					
10																
11																
12																
13																
14		JA-solar panel				Production per 30 years [MWh]		Production [MWh/year]		Total emissions [tonn CO2-eq]			kg CO2-eq per MWh			
15		Hight [m]	2,278	Pitch	Number of panels	Constructed area	Forest	Constructed area	forest	Constructed area	High site productivity	Low site productivity	Constructed area	High site productivity	Low site productivity	
16		Width [m]	1,134	8	63936	957 592	954 414	34 051	33 938	37 250	50 796	49 899	38,8997	53,2225	52,2821	
17		Area [m2]	2,583252	9	57024	882 196	878 877	31 370	31 252	33 223	46 769	45 872	37,6594	53,2148	52,1935	
18		Mass [kg]	31,8	10	50976	804 606	801 288	28 611	28 493	29 699	43 246	42 348	36,9117	53,9702	52,8500	
19				11	46646	746 506	744 003	26 545	26 456	27 177	40 723	39 825	36,4052	54,7350	53,5285	
20		Loss calculations		12	43200	698 754	695 520	24 847	24 732	25 169	38 715	37 818	36,0198	55,6638	54,3733	
21		n	30	13	39744	647 881	644 759	23 038	22 927	23 155	36 702	35 804	35,7404	56,9232	55,5311	
22		k	0,9955	14	37152	609 944	606 907	21 689	21 581	21 645	35 192	34 294	35,4875	57,9853	56,5063	
23				15	34560	570 348	567 451	20 281	20 178	20 135	33 682	32 784	35,3034	59,3558	57,7740	

Figure F.1: Ratio between Production and Emission calculations in Excel

	A	B	C	D	E	F	G	H	I	J	K	L	M	N	O	P
1																
2																
3																
4			Quantity	kg CO2-eq pr. quantity	8 meters [ton CO2-eq]	9 meters [ton CO2-eq]	10 meters [ton CO2-eq]	11 meters [ton CO2-eq]	12 meters [ton CO2-eq]	13 meters [ton CO2-eq]	14 meters [ton CO2-eq]	15 meters [ton CO2-eq]				
5	Production	1 m2	122	=D55*\$C\$17*\$F516*0,001	=D55*\$C\$17*\$F17*0,001	=D55*\$C\$17*\$F18*0,001	=D55*\$C\$17*\$F19*0,001	=D55*\$C\$17*\$F20*0,001	=D55*\$C\$17*\$F21*0,001	=D55*\$C\$17*\$F22*0,001	=D55*\$C\$17*\$F23*0,001					
6	Mounting	1 m2	91,9	=D56*\$C\$17*\$F516*0,001	=D56*\$C\$17*\$F17*0,001	=D56*\$C\$17*\$F18*0,001	=D56*\$C\$17*\$F19*0,001	=D56*\$C\$17*\$F20*0,001	=D56*\$C\$17*\$F21*0,001	=D56*\$C\$17*\$F22*0,001	=D56*\$C\$17*\$F23*0,001					
7	Transportation	All panels	220	=D57*0,001	=D57*0,001	=D57*0,001	=D57*0,001	=D57*0,001	=D57*0,001	=D57*0,001	=D57*0,001			Forest	Low site productivity	12648,7
8	Recycling	1 panel	30,053	=D58*\$F516*0,001	=D58*\$F17*0,001	=D58*\$F18*0,001	=D58*\$F19*0,001	=D58*\$F20*0,001	=D58*\$F21*0,001	=D58*\$F22*0,001	=D58*\$F23*0,001			Constructed area	High site productivity	13546,3
9				=SUMMER(E5:E8)	=SUMMER(F5:F8)	=SUMMER(G5:G8)	=SUMMER(H5:H8)	=SUMMER(I5:I8)	=SUMMER(J5:J8)	=SUMMER(K5:K8)	=SUMMER(L5:L8)					0
10																
11																
12																
13																
14		JA-solar panel					Production per 30 years [MWh]		Production [MWh/year]		Total emissions [tonn CO2-eq]			kg CO2-eq per MWh		
15		Height [m]	2,278		Pitch	Number of panels	Constructed area	Forest	Constructed area	forest	Constructed area	High site productivity	Low site productivity	Constructed area	High site productivity	Low site productivity
16		Width [m]	1,134		8	63936	=I16*(((\$C\$22*\$C\$21-1))/(\$C\$22-1))	=I16*(((\$C\$22*\$C\$21-1))/(\$C\$22-1))	34051	33938	=E9+P8	=E9+P7	=E9+P6	=K16/(G16)*1000	=L16/(H16)*1000	=M16/(I16)*1000
17		Area [m2]	=C15*C16		9	57024	=I17*(((\$C\$22*\$C\$21-1))/(\$C\$22-1))	=I17*(((\$C\$22*\$C\$21-1))/(\$C\$22-1))	31370	31252	=F9+P8	=F9+P7	=F9+P6	=K17/(G17)*1000	=L17/(H17)*1000	=M17/(I17)*1000
18		Mass [kg]	31,8		10	50976	=I18*(((\$C\$22*\$C\$21-1))/(\$C\$22-1))	=I18*(((\$C\$22*\$C\$21-1))/(\$C\$22-1))	28611	28493	=G9+P8	=G9+P7	=G9+P6	=K18/(G18)*1000	=L18/(H18)*1000	=M18/(I18)*1000
19					11	46646	=I19*(((\$C\$22*\$C\$21-1))/(\$C\$22-1))	=I19*(((\$C\$22*\$C\$21-1))/(\$C\$22-1))	26545	26456	=H9+P8	=H9+P7	=H9+P6	=K19/(G19)*1000	=L19/(H19)*1000	=M19/(I19)*1000
20		Loss calculations			12	43200	=I20*(((\$C\$22*\$C\$21-1))/(\$C\$22-1))	=I20*(((\$C\$22*\$C\$21-1))/(\$C\$22-1))	24847	24732	=I9+P8	=I9+P7	=I9+P6	=K20/(G20)*1000	=L20/(H20)*1000	=M20/(I20)*1000
21		n	30		13	39744	=I21*(((\$C\$22*\$C\$21-1))/(\$C\$22-1))	=I21*(((\$C\$22*\$C\$21-1))/(\$C\$22-1))	23038	22927	=J9+P8	=J9+P7	=J9+P6	=K21/(G21)*1000	=L21/(H21)*1000	=M21/(I21)*1000
22		k	=(1-0,45%)		14	37152	=I22*(((\$C\$22*\$C\$21-1))/(\$C\$22-1))	=I22*(((\$C\$22*\$C\$21-1))/(\$C\$22-1))	21689	21581	=K9+P8	=K9+P7	=K9+P6	=K22/(G22)*1000	=L22/(H22)*1000	=M22/(I22)*1000
23					15	34560	=I23*(((\$C\$22*\$C\$21-1))/(\$C\$22-1))	=I23*(((\$C\$22*\$C\$21-1))/(\$C\$22-1))	20281	20178	=L9+P8	=L9+P7	=L9+P6	=K23/(G23)*1000	=L23/(H23)*1000	=M23/(I23)*1000

Figure F.2: Ratio between Production and Emission calculations in Excel with formulas



 **NTNU**

Norwegian University of
Science and Technology